Design of Overhead Transmission Lines Subject to Localized High Intensity Wind

by

Sébastien Langlois

January 2007

Department of Civil Engineering and Applied Mechanics

McGill University, Montréal

A Thesis submitted to the Graduate and Postdoctoral Studies Office in partial fulfillment of the requirements of the degree of Master of Engineering

Your file Votre référence
ISBN: 978-0-494-32603-9
Our file Notre référence
ISBN: 978-0-494-32603-9

Abstract

Wind loading considered in the design of overhead transmission lines is based on extreme values of synoptic wind, i.e. boundary layer wind originating from large-scale meteorological pressure systems. Localized high intensity wind (HIW) storms such as tornadoes and downbursts are a different type of extreme wind frequently causing failures of overhead lines. This thesis covers the design aspects of overhead transmission lines when subject to localized HIW storms. A comprehensive review of the literature is included on the effects of such wind storms on lines and on mitigation measures. Furthermore, several options for the design of self-supporting transmission towers against localized HIW are discussed based on numerical simulations of several simple load cases on four examples of lattice structures.

Sommaire

Les charges de vent considérées pour la conception des lignes aériennes de transport d'énergie sont basées sur des vents synoptiques, i.e. des vents en accord avec la théorie de la couche limite provenant de systèmes météorologiques à grande échelle. Les vents localisés de forte intensité comme les tornades ou les rafales descendantes représentent un type distinct de vent qui cause souvent des dommages structuraux sur les lignes aériennes. L'auteur analyse différents aspects de la conception de lignes reliés aux vents localisés de forte intensité. Il présente d'abord une revue bibliographique sur les effets de ce type de vent sur les lignes et sur les mesures correctives suggérées. Par la suite, plusieurs options de calcul pour la conception des pylônes autoporteurs sont évaluées par simulation numérique avec divers cas de charges simplifiés sur quatre exemples de structures classiques en treillis.

Acknowledgements

I would like to acknowledge the following individuals and organizations for their support in this project:

NSERC for its financial support;

My supervisor, Ghyslaine McClure for involving me in that project, and for her guidance and support;

Svein Fikke and H. Brian White for their input concerning respectively the meteorological and the design aspects of my thesis;

Alan B. Peabody and Hydro-Québec for sharing information on the transmission towers studied;

All members of CIGRÉ Working Group B2.06, as well as John D. Holmes and Eric Savory for their comments;

Colin Rogers and Asim Haldar for their constructive comments.

Table of Contents

List of Figures

List of Tables

List of Symbols

A	=	exposed area of a tower section, m^2
A_c	=	wind force on conductors, N
A_t	=	wind force on a tower panel, N
BLX	=	longitudinal diagonal bracing members below the waist
BTX	=	transversal diagonal bracing members below the waist
CB0	=	Canadian Bridge 0° tower
CB15	=	Canadian Bridge 15° tower
CD_C	=	drag coefficient for conductors (PLS-CADD)
CD_S	=	drag coefficient for structures (PLS-CADD)
C_{XC}	=	drag coefficient for conductors (IEC)
C_{xt1}, C_{xt2}	=	drag coefficient of a tower panel (faces 1 and 2) (IEC)
D	=	diameter of the conductor (PLS-CADD)
G_C	=	combined factor for conductors
G_L	=	span factor
GRF_C	=	gust response factor for conductors
GRF_S	=	gust response factor for structures
G_t	=	combined factor for supports
HL	=	longitudinal horizontal members
HT	=	transversal horizontal members
HX	=	horizontal bracing members
K_R	=	terrain roughness factor
L	=	wind span, m

LFW	=	load factor for wind
LL	=	main leg members below the waist
LR	=	line reliability level
P	=	members of the ground-wire peak and the crossarms
PB	=	Peabody tower
Q	=	air density factor, kg/m^3 (PLS-CADD)
Q_c	=	distributed wind force on conductors, kN/m
Q_t	=	wind pressure on tower, kN/m^2
R	=	radial velocity, m/s
RP	=	microburst return period, years
S_{t1}, S_{t2}	=	total vertically projected areas of a tower panel (faces 1 and 2), m^2
T	=	tangential velocity, m/s
TC	=	upper and lower chord members in the tower truss
TX	=	members in the tower truss that are not TC members
UH	=	conductor wind load per unit length, N/m
UL	=	main leg members above the waist
V	=	horizontal wind speed, m/s
V(z)	=	wind velocity at height z above ground, m/s
V_1	=	wind velocity at reference height z_1, m/s
V_{max}	=	maximum horizontal wind speed, m/s
V_R	=	reference wind speed, m/s
W	=	vertical velocity, m/s
W_G	=	width of gust, m

WA	=	incidence between wind direction and transverse axis, degree (PLS-CADD)
WF	=	wind force on a tower section, N
WI	=	Wisconsin tower
WLF	=	weather load factor
WLX	=	longitudinal diagonal bracing members above the waist
WTX	=	transversal diagonal bracing members above the waist
W_Z	=	design wind speed at height z, m (PLS-CADD)
d	=	diameter of the conductor, m (IEC)
h_1, h_2	=	height of the projected intersection of the main legs
q_0	=	dynamic reference wind pressure, Pa
r	=	radius, m
r_{max}	=	radius of maximum horizontal wind speed, m
t_Z	=	ice thickness, m
z	=	height above ground, m
$z_{0.5*Vmax}$	=	height where wind speed is half its maximum value, m
z_1	=	reference height above ground, m
Ω	=	incidence between the wind direction and the conductor, degree
α	=	wind power law exponent
χ	=	solidity ratio of tower panel
μ	=	air mass per unit volume, kg/m^3 (IEC)
θ	=	incidence between wind direction and transverse axis, degree (IEC)
τ	=	air density correction factor (IEC)

1 Introduction

The objective of this research is to discuss design aspects of overhead transmission lines related to localized high intensity wind (HIW) storms, namely tornadoes and downbursts. This Master of Engineering thesis includes a comprehensive review of the literature on the effects of such wind storms on lines. Furthermore, several options for the design of self-supporting transmission towers against localized HIW are discussed based on numerical simulations of several simple load cases using the commercial transmission line analysis software PLS-CADD (Power Line Systems Computer Aided Design and Drafting, 2006).

Loading models representing the effects of extreme wind on overhead lines are traditionally based on synoptic winds, which originate from large-scale meteorological pressure systems. Design wind velocities are selected based on the maximum velocities expected during the line's projected lifetime. Those design wind speeds are average values over a duration varying from 3 seconds to 10 minutes. The design wind speed is then converted to a static pressure through Bernouilli's equation where the pressure is proportional to the air density and the square of the wind speed. A vertical profile of static wind pressures is calculated according to the boundary layer wind theory and applied to all the components of the line (supports, conductors, insulator strings) according to the theory of gust response factors: this is the approach proposed by Davenport (1967, 1979) in his early work. In this approach, various line components have different gust response factors. This relatively complex synoptic wind loading model is not necessarily applicable to localized wind storms such as tornadoes or downbursts.

Localized HIW storms cover such a small footprint that they are very rarely recorded by meteorological stations. Due to their elongated geometry, transmission line systems are prone to suffer the effects of those wind events. In fact, transmission lines are thought to be the most effective human constructions in intercepting and recording those storms (Dempsey & White, 1996). Following the observation of a significant number of line failures due to non-synoptic winds, a few authors have proposed simple loadings or design recommendations to account for the effects of tornadoes and downbursts on overhead power lines (American Society of Civil Engineers [ASCE], 1991, 2005; Behncke & White, 1984; Behncke, White & Milford, 1994; Energy Networks Association [ENA], 2006; Ishac & White, 1995).

Section 2 of the thesis presents background information on overhead transmission line systems and on the traditional design method for wind loading. A literature review on localized HIW storms and line systems is found in Section 3. Sections 4 and 5 present respectively, the modeling assumptions, and the results and discussion of the numerically simulated wind load cases on four self-supporting lattice towers.

2 Overhead Line Systems and Wind Loading Method

2.1 Overhead Transmission Line Systems

Power lines serve the purpose of carrying electric power from generating stations to customers. It is often convenient to distinguish between transmission lines, which carry power at high voltage, and distribution lines, which bring power to small customers through low voltage networks. The present work focuses only on the effects of localized HIW storms on overhead transmission lines. Overhead distribution lines are also very vulnerable to localized wind storms. However, such small-scale storms usually have a limited overall impact considering the high redundancy of most distribution networks. Furthermore, failures of distribution lines during tornadoes and downbursts are likely to be caused directly by projectiles hitting line components rather than by excessive wind pressures on the conductors and their supports. Projectiles are very difficult, if not impossible, to account for in the design of overhead lines.

This study is linked to the activities of Working Group B2.06 from CIGRÉ (*Conseil International des Grands Réseaux Électriques* – International Council on Large Electric Systems) and most definitions used herein match those used by the International Electrotechnical Commission (IEC) and its standards on the design of overhead transmission lines (IEC, 2003). Transmission lines, in agreement with this IEC document, refer to lines with voltages of 45 kV and above.

The design approach for overhead transmission lines (Figure 1) assumes that a line is a system made of several components where failure/unserviceability of one component can lead to the failure/unserviceability of the whole system. The main line components are the supports, foundations, conductors, and insulator strings. In this document, the term conductor refers to all the suspended cables including ground wires. Each component comprises several mechanical elements; for example, lattice steel supports are composed of steel shapes, connecting plates, and bolts.

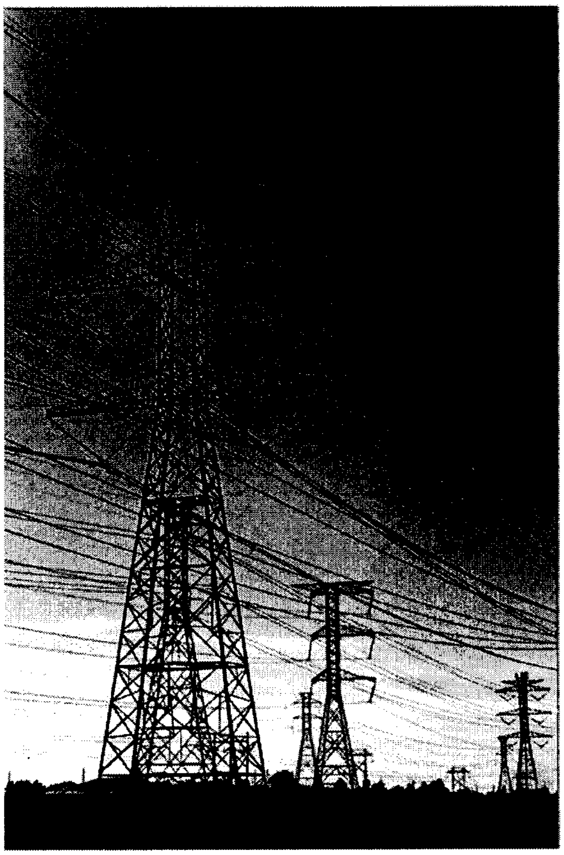

Figure 1: Overhead transmission lines

The first steps towards the design of overhead transmission lines are the selection of the electrical properties, and the determination of the line route. The geometry of the supports and the type of foundations selected are highly dependent on the conductor properties, electrical clearance requirements, and terrain properties. Then, detailed design of the system and its components to resist anticipated loads can be performed. IEC 60826 Standard (2003) recommends reliability-based design methods (RBD) for the design of overhead transmission lines against climatic loads. Lines can be designed for different reliability levels based on the probabilistic evaluation of weather-related loads and strength of components. Climatic loads governing the reliability of lines are divided in three categories: wind loads, ice loads without wind, and combined ice and wind loads. Sections 2.2 and 2.3 describe the method used for the calculation of wind loads. The IEC standard (2003) recognizes that: "other conditions, not dealt with in the design process, can occur and lead to line failure such as impact of objects, defects in material, etc" (p. 29). To account for those, security requirements are proposed to reduce damage and limit risks of propagation of failures through cascading effects. A third type of design criteria are the safety requirements which consist of special loads ensuring safety of people during construction and maintenance.

There are many structural types of line supports: steel lattice towers, poles, and frame structures to name the main categories (Hydro-Québec, 1982). Lattice towers are further divided into classical self-supporting and guyed structures. Figure 2 illustrates some typical supports. An important distinction must be made between suspension structures and dead-end structures (see Figure 3). Suspension structures are designed for straight sections of lines. Dead-end structures can be used where there is a significant change in line orientation or in the vertical line profile: their conductors are linked to horizontal insulators through which full cable tension loads are transmitted to the support independently for each of the two adjacent spans. The terminology related to self-supporting steel lattice towers is illustrated in Figure 4.

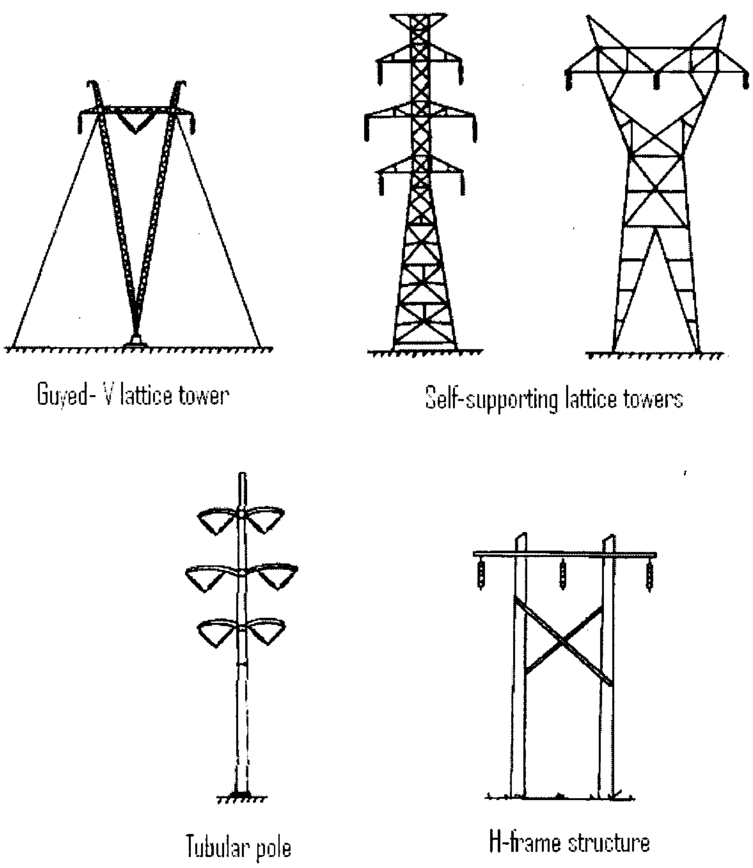

Figure 2: Common types of overhead line supports (Hydro-Québec, 1982)

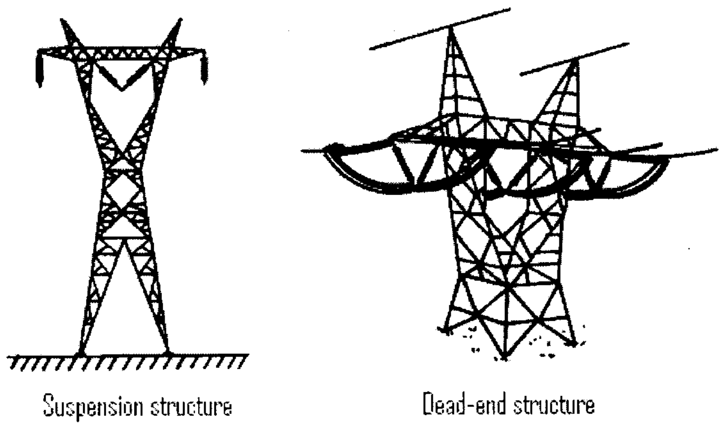

Figure 3: Suspension and dead-end structures (Hydro-Québec, 1982)

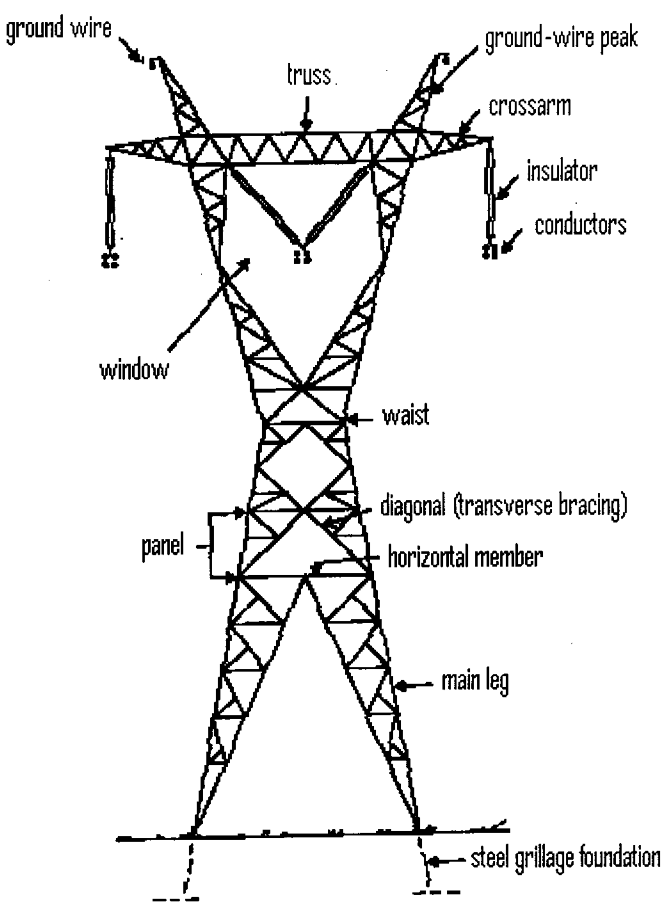

Figure 4: Classical suspension lattice tower and line components (Hydro-Québec, 1982)

2.2 Description of Synoptic Wind Method

In this study, the general methodology traditionally used to calculate wind pressures on overhead lines will be called "synoptic wind method", since its derivation is based on observation of winds originating from large-scale meteorological pressure systems. Wind loading is commonly applied only in the transverse direction (perpendicular to the line axis). A Hydro-Québec document by Lafrenière (2004) compares several overhead line design codes for the calculation of wind pressures on conductors, and identifies the various factors used in the methodology. These factors are described next.

Drag Factor

The drag factor is a coefficient used in the conversion of wind speeds to wind pressures. It varies with the shape and surface properties of the element hit by the wind. Values of drag factors on individual components or sub-systems can be derived from wind tunnel tests. In the case of lattice towers, the geometry of the structure affects the drag factor, and it is therefore difficult to evaluate. For simplicity, the solidity ratio, which is defined as the ratio of the projected area of members in a panel to the total panel area, is often used to approximate the drag factor to be used for a tower section. Drag factors for lattice towers range between 1.5 and 4.0, while they are usually close to 1.0 for bare conductors.

Gust Response Factor (GRF)

This factor is based on the theory developed by Davenport (1967, 1979) that takes into account the dynamic interaction of wind on structures. The dynamic properties of high boundary layer winds are represented in this factor, along with the dynamic response properties of conductors and line supports. This factor is related to the height above ground of elements and to terrain roughness. It generally varies between 1.2 and 2.0.

Height Adjustment Factor

This factor is meant to adjust wind pressure with height to match the vertical profile of horizontal wind speed described by the boundary layer wind theory. This profile is calculated by the following power law:

$$V(z) = V_1 * (z / z_1)^{\alpha} , \qquad \text{Equation 1}$$

where $V(z)$ is the wind velocity at height z above ground, V_1 is the horizontal wind velocity at reference height z_1 (usually measured at 10 m above ground in weather stations at airports), and α is the power law exponent mainly depending on terrain roughness. A value of $\alpha = 1/7$ is commonly used for terrains in open country with very few obstacles (Liu, 1991).

Span Factor

The span factor is a coefficient used to reduce the wind load on conductors. Its rationale is that the probability that a severe gust wind will affect simultaneously and uniformly all points of a conductor span is fairly low. Unlike most other wind calculation factors, the value of this factor is below 1.0, and it decreases with longer spans up to values around 0.6.

Terrain Roughness Factor

The terrain roughness factor is associated with a small number of general terrain categories, ranging from large water surfaces to surfaces with many large obstacles. This factor adjusts the wind speed according to the resistance encountered by the horizontal wind flow at low altitude. Those factors are usually calibrated such that they adjust reference wind speeds measured in the area to the local surface conditions. Terrain roughness factors range from 0.6 to 1.2.

Topographical Factor

This factor is also called sometimes "speed-up" factor as it accounts for increases in wind speed due to topographical features such as mountains, valleys, hills, canyons, etc. In Figure 5, the wind speed at the top of the hill could be twice as large as the surface wind speed at the bottom (Liu, 1991). This factor is not included in IEC 60826-2003, but is considered for example in ENA C(b)1-2006.

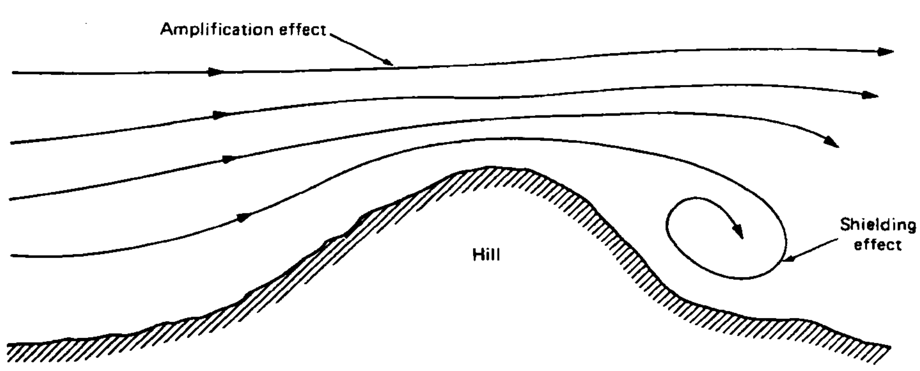

Figure 5: Effects of hill on surface wind velocity (Liu, 1991)

Temperature and Atmospheric Pressure Factor

In the calculation of wind pressures from wind speeds, a value for the air density is needed, which changes with temperature and atmospheric pressure. The factor is often calibrated such that a value of 1.0 refers to normal conditions of 15 °C and 101.3 kPa.

2.3 IEC 60826 Wind Loading Method

The International Standard IEC 60826 (IEC, 2003) will be used for comparison later in this work, and it is necessary here to summarize the methodology proposed to design overhead transmission lines against extreme synoptic winds.

The IEC method is limited to lines with span length between 200 m and 800 m, to supports with height less than 60 m, to areas at altitude less than 1300 m above the average level of the topographic environment, and finally to terrain without significant topographical features. Furthermore, localized wind storms such as tornadoes and downbursts are not covered in the standard.

The reference wind speed V_R (in m/s) is determined from statistical analysis of wind speed data measured at 10 m above ground with an averaging period of 10 minutes. If the data does not come from a category B terrain, it must be multiplied by a terrain roughness factor, K_R given in Table 1.

Table 1: Terrain roughness categories in IEC 60826 (2003)

Terrain category	Roughness characteristics	K_R
A	Large stretch of water upwind, flat coastal areas	1,08
B	Open country with very few obstacles, for example airports or cultivated fields with few trees or buildings	1,00
C	Terrain with numerous small obstacles of low height (hedges, trees and buildings)	0,85
D	Suburban areas or terrain with many tall trees	0,67

The dynamic reference wind pressure in Pa is calculated from the formula:

$q_0 = \frac{1}{2} \tau \mu V_R^2$, Equation 2

where the air mass per unit volume μ is equal to 1.225 kg/m^3 for a temperature of 15 °C and an atmospheric pressure of 101.3 kPa, and τ is a correction factor for the air density varying with temperature and altitude as shown in Table 2.

Table 2: Correction factor τ of dynamic reference wind pressure due to altitude and temperature (IEC, 2003)

Temperature °C	Altitude m			
	0	1 000	2 000	3 000
30	0,95	0,84	0,75	0,66
15	1,00	0,89	0,79	0,69
0	1,04	0,94	0,83	0,73
−15	1,12	0,99	0,88	0,77
−30	1,19	1,05	0,93	0,82
NOTE The reference value corresponds to 0 m altitude and a temperature of 15 °C.				

Wind Load on Conductors

The wind force on conductors, A_c (in N) is calculated from the dynamic reference wind pressure, q_0, using the formula:

$A_c = q_0 \, C_{XC} \, G_C \, G_L \, d \, L \sin^2 \Omega$, Equation 3

where

C_{XC} is the drag coefficient of the conductor usually taken as 1.0.

G_C is the combined wind factor for conductors given in Figure 6.

G_L is the span factor given in Figure 7.

d is the diameter of the conductor in m.

L is half the sum of the two adjacent spans lengths (called the wind span) in m.

Ω is the incidence between the wind direction and the conductor.

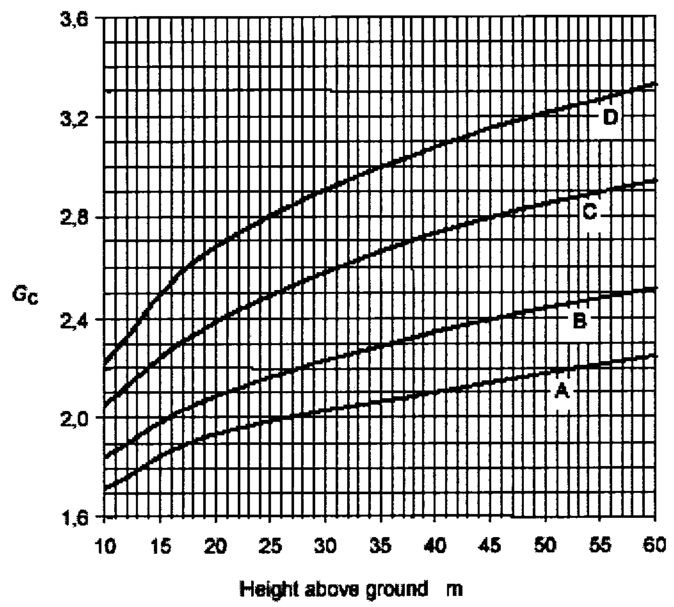

Figure 6: IEC 60826 (2003) combined wind factor G_C for conductors for various terrain categories and heights above ground

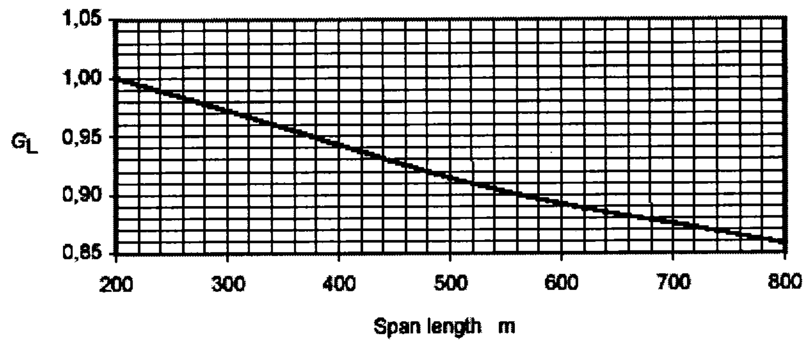

Figure 7: IEC 60826 (2003) span factor G_L

The combined wind factors in IEC 60826, G_C and G_t, combines the gust response factor and the height adjustment factor.

Wind Load on Supports

Two simplified formulas are available for wind on supports in the standard: one for lattice towers of rectangular cross-section and one for supports with cylindrical members. The latter will not be discussed here. The IEC standard also provides a formula for wind on insulator strings.

The wind force A_t (in N) applied on a windward lattice panel is given by:

$A_t = q_0 \,(1 + 0.2 \sin^2 2\theta) \,(S_{t1}\, C_{xt1} \cos^2 \theta + S_{t2}\, C_{xt2} \sin^2 \theta)\, G_t$ Equation 4

where

S_{t1} , S_{t2} are the total vertically projected areas of the panel of tower faces 1 and 2 (in m^2).

C_{xt1} , C_{xt2} are drag coefficients of the panel for faces 1 and 2 given in Figure 8 for corresponding solidity ratios χ.

χ	is the solidity ratio equal to the projected area of members divided by the total panel area.
θ	is the incidence of the horizontal wind with respect to the transverse tower axis.
G_t	is the combined wind factor for supports given in Figure 9.

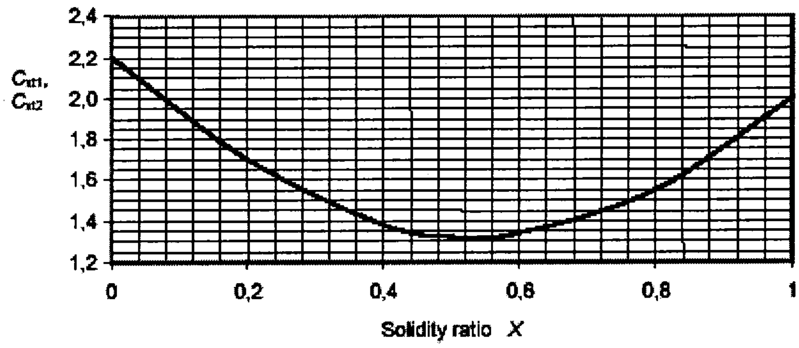

Figure 8: Drag coefficients for lattice towers in IEC 60826 (2003)

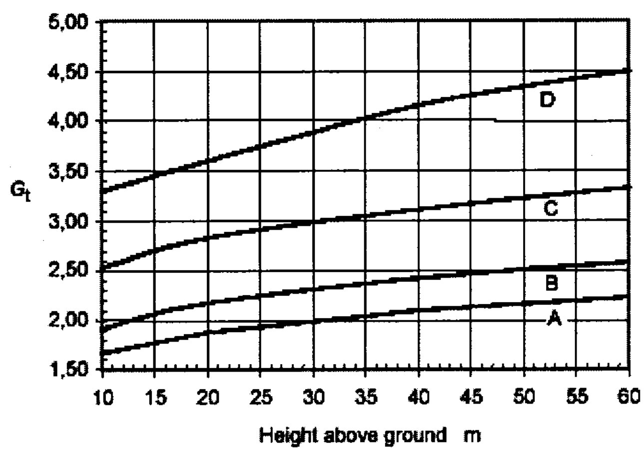

Figure 9: IEC 60826 (2003) combined wind factor G_t for supports and insulators strings for various terrain categories and heights above ground

3 Literature Review

This literature review is also available in a separate report (Langlois, 2006). The purpose of this review is to provide line designers with a summary of the research on localized HIW storms and to help them understand those phenomena. This section also discusses suggestions available to design overhead lines against such wind storms.

3.1 Definitions

3.1.1 High Intensity Wind (HIW)

There is a need to define the limits of the concept of "high intensity wind" as used in this report. Throughout the literature, several different definitions are found. There are basically two types of definitions: one that includes all winds over a threshold wind speed, and one that is limited to high winds due to localized storm effects.

The first type of definition is found in a recent review on design practices for overhead lines subjected to high intensity winds. It states: "high intensity winds are those having velocities exceeding 45 m/s or those likely to cause structural damage to property" (CIGRÉ WG B2.16, 2004, p. 4). With such a definition, all types of storms induced by thunderstorms can be included, as well as large-scale tropical and extratropical storms, such as hurricanes, cyclones, typhoons and gales. A study by Hoxey et al. (2003) identifies hurricanes, tornadoes and downbursts as being the three basic storm sources of high intensity winds.

However, their research focuses only on the last two types. The advantage of this definition is that the threshold wind speed parameter is a precise criterion for the identification of high intensity winds.

The ASCE Draft Revision of the Guidelines for Electrical Transmission Line Structural Loading (ASCE, 2005) treats only tornadoes, microbursts and downbursts in its section specifically titled "High Intensity Winds". Much attention is given to the narrow-fronted characteristic of those winds. Several authors, including Behncke et al. (1994), Dempsey and White (1996), and Savory et al. (2001), accept a similar definition.

The purpose of the study is to identify the effects of local storms and to assess how they are different from synoptic wind effects. Large-scale storms such as hurricanes are typically covered by codes and design practices in regions prone to such events. In this report, the expression "localized HIW" is used to refer specifically to severe winds resulting from localized thermal activity generally created in thunderstorms.

3.1.2 Thunderstorm

A thunderstorm covers only a small surface area. However, these storms frequently produce structural damage. A general understanding of the physical phenomenon is needed because most tornadoes and downbursts are created in thunderstorms.

The important process in the physics of thunderstorms is convection. The instability of the air, caused by cold air over a warm surface, generates a convection where warm moist air rises from the ground (updraft) and is substituted by dry colder air from aloft (downdraft). Due to adiabatic cooling the rising air becomes saturated and the water vapour condenses into the convective clouds. The updraft is usually strengthened due to the release of latent heat during condensation.

The thunderstorm process (illustrated in Figure 10) is divided into three stages: the cumulus stage, the mature stage, and the dissipating stage (Battan, 1984). During the cumulus stage, several cumuli clouds converge and combine, forming a large cell with precipitation particles. This formation is dominated by updrafts with moist air that can ascend up to several kilometres. As the air cools down and loses its buoyancy, a downdraft is initiated. This is the beginning of the mature stage during which both strong updrafts and downdrafts are present. The dissipating stage is characterized by a weak downdraft and the dissipation of the storm cell. Thunderstorms are generally accompanied by heavy rain or hail. "Severe storm" is another expression that sometimes replaces the term "thunderstorm" to describe more generally and probably more accurately the storms able to create damaging winds.

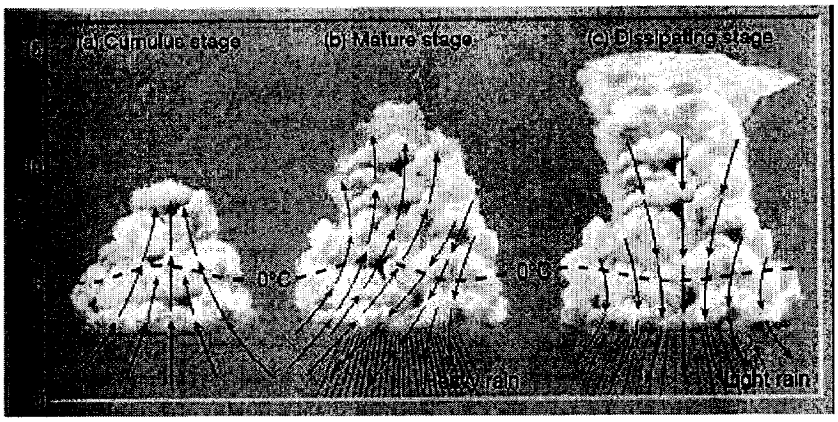

Figure 10: The three stages of a thunderstorm (Lutgens & Tarbuck, 2001)

Two types of storm cells are the ordinary cell and the supercell (CIGRÉ WG B2.16, 2004). The latter covers a larger area and can produce the most devastating of all thunderstorm wind events: the tornado. Tornadoes originate from the updraft part of the cell. The downdraft part can also produce high velocity winds as it reaches the ground and spreads outwards. When this mechanism is strong enough, it is called a downburst. Tornadoes, downbursts and their respective characteristics are further defined in Section 3.2. In general, severe storms have a 1-3 hours duration and the cell travels at 5-11 m/s. High winds rarely last more than 15 minutes at a particular location (Hawes & Dempsey, 1993).

Much is still to be learned from the wind flow field of thunderstorms. Letchford et al. (2002) summarize the extent of the research done on the subject prior to 2002, outline the most important characteristics of thunderstorm winds, and differentiate them from synoptic winds. The differences are: their non-stationary nature, their complex three-dimensional flow, their velocity profile with height, the lesser role of turbulence, and their smaller spatial and temporal extents.

3.1.3 Downburst

As defined by Fujita (1981), a downburst is a strong downdraft which induces an outburst of damaging winds on, or near the ground. The downdraft makes contact with the ground and then spreads outwards, causing severe winds at low altitudes. Downbursts can be further subdivided into microbursts and macrobursts. Microbursts have damaging winds extending up to four kilometres and macrobursts have damaging winds extending over four kilometres (Fujita, 1990). The lifetime of a downburst is generally between 5 and 30 minutes for a macroburst and between 5 to 10 minutes for a microburst (McCarthy & Melsness, 1996). Downbursts are often observed through damage to the vegetation. An example of a downburst damage pattern is provided in Figure 11. Damage often affects an elliptical footprint and is said to be divergent, as trees affected usually fall away from the centre of the damaged area.

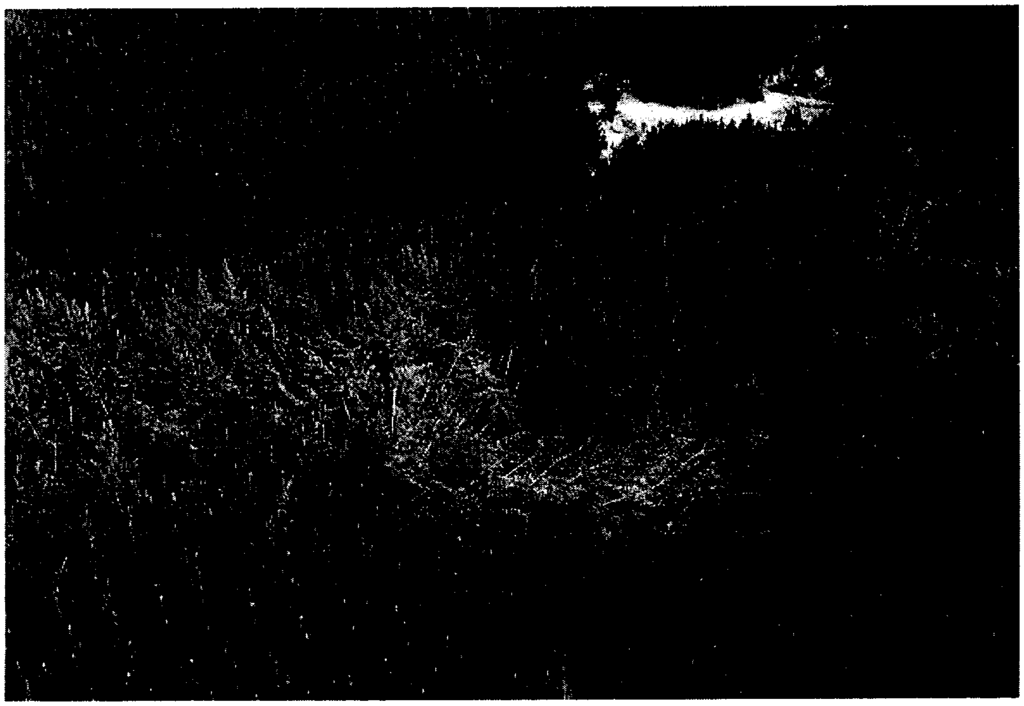

Figure 11: Effect of a small downburst on a pine forest (Reid & Revell, 2006)

3.1.4 Tornado

The most severe winds that can be produced by local storms occur through tornadoes. A tornado is a rotating column of air originating from a convective cloud (Twisdale, 1982). It takes the appearance of a narrow funnel, cylinder or rope that extends from the base of the thunderstorm cloud to the ground. The visible shape of the tornado is mostly due to the presence of water droplets. The path width of damaging winds in tornadoes, that covers a distance much larger than the funnel itself, is generally smaller than a few hundred metres, and rarely reaches one kilometre (Battan, 1984). Their path length varies according to their strength, and can exceed 50 kilometres (Holmes, 2001).

Even though they have been recorded more frequently in North America, tornadoes occur in all subtropical or temperate land masses. Some result from isolated storm cells, while others result from very complex storms that can cause damage over a relatively large area and create several tornadoes and downbursts. Large tropical storms can produce thunderstorms and tornadoes as well. For example, the remnants of Hurricane Danny in 1985 spawned over 20 tornadoes in Mississipi, U.S.A (McCaul, 1987). There also exist tornadoes, often called waterspouts, occurring over water.

The most widely used tornado intensity scale is called the Fujita-Pearson (FPP) scale (Fujita, 1973). The scale is defined in Table 3. Each tornado can be assigned a number between 0 and 5 for each of the following intensity indicators: maximum wind speed, path length (along the direction of propagation), and path width (perpendicular to the direction of propagation). For example, the smallest recorded tornado would be scaled FPP 000. Tornadoes exceeding the criteria for level 5 are possible but very unlikely. As explained in the ASCE Manual 74 (1991), it is common practice to characterize tornadoes based only on wind speed. They are therefore often scaled between F0 and F5. A large portion of the recorded tornadoes are relatively weak and described as F0 or F1.

Table 3: The FPP tornado scale (Fujita, 1973)

Scale	Max. wind speed (m/s)	Path length (km)	Path width (m)	Expected damage
0	less than 33	less than 1.6	less than 15	light
1	33-50	1.6-5.0	15-50	moderate
2	50-70	5-16	50-160	considerable
3	70-92	16-50	160-500	severe
4	92-116	50-159	500-1600	devastating
5	116-142	159-507	1600-5000	incredible

Damages from tornadoes might be similar to those induced by a downburst, and therefore, after-the-fact identification of the phenomenon based on observations of damage can be difficult. However, tornadoes generally show near straightline damage pattern and have highly convergent flows (CIGRÉ WG B2.16, 2004). A narrow path of damage is usually expected.

3.2 Research on Wind Characteristics

3.2.1 Extreme Wind Speeds

Estimations for the maximum wind speeds that can occur in downbursts or tornadoes are difficult to assess. Because of their relatively small horizontal extent, very few downbursts and tornadoes have actually been recorded. An anemograph of the famous downburst recorded on August 1st 1983 at the Andrews Air Force Base in the United States is presented in Figure 12. The peak gust recorded is 67 m/s (130 knots). This is the highest wind speed ever measured from a downburst and therefore, a fair estimation is that downburst winds could go as high as 75 m/s (Letchford et al., 2002).

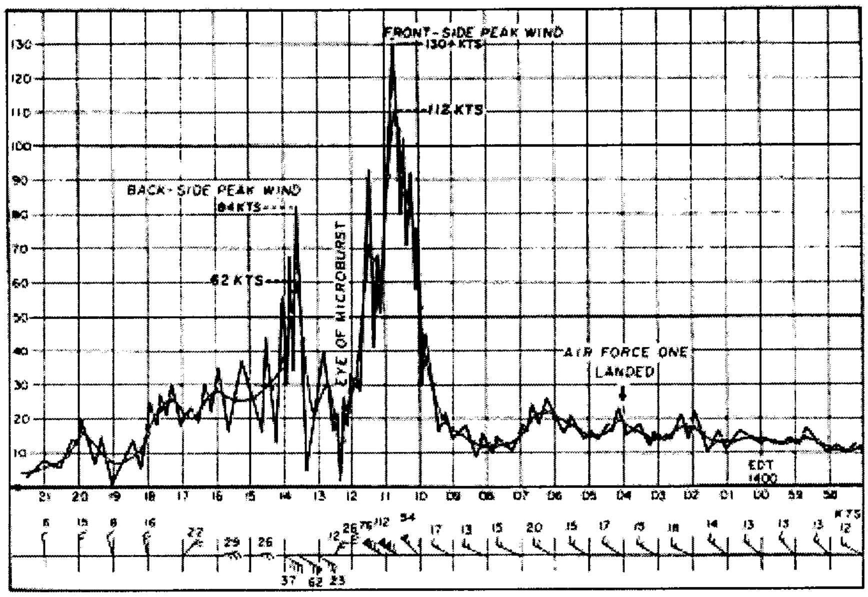

Figure 12: Recorded downburst at Andrews Air Force Base (Holmes & Oliver, 2000)

Tornadoes have been studied for a much longer period and many estimates were given for what is thought to be the ultimate wind speed. Since most measuring devices are unable to sustain such powerful winds, there remain only three ways to measure or estimate extreme wind speeds: photogrammetric analysis using videos of moving objects in tornadoes, research Doppler radar, or damage survey (McCarthy & Melsness, 1996). Traditionally, experts who study damage surveys from tornadoes have given very high evaluations of the maximum wind speed. Some even thought it could reach the speed of sound (340 m/s) (Battan, 1984). However, with new techniques to evaluate wind speed and a more objective approach towards damage surveys, specialists rarely state an ultimate value over 125 m/s. In the elaboration of his intensity scale, Fujita (1990) did not expect to ever record an F6 tornado, that is a wind speed over 142 m/s. In an extensive report, Minor et al. (1993) estimate the upper limit to be in the range 111-123 m/s.

3.2.2 Wind Field Characteristics

Localized high intensity winds being difficult to observe, they were often neglected compared to the well-studied, boundary layer winds. In their report, Letchford et al. (2002) argue that wind engineering must focus on the fundamental issue of analyzing the flow structure in the strongest winds encountered on earth. This section presents an overview of the research performed on the subject.

Downburst Wind Field

It was Fujita who first observed that thunderstorm downdrafts could produce highly damaging winds. He was able to correlate downburst winds to damage on the ground and aircraft accidents (Fujita, 1990). Before the 1970s, the existence of a downdraft in thunderstorms was known. However, it was believed that, since a current must necessarily slow down and stop before reaching the ground, downdraft winds near the ground were minimal. Based on his observations, Fujita described the phenomenon he called downburst and that he later subdivided into microbursts and macrobursts. Fujita (1990) defined the microburst as being "an anti-tornado storm, consisting of a slow-rotating column of descending air which, upon reaching the ground, bursts out violently" (p. 76).

Following Fujita's observations, three important projects were performed in the United States to accumulate specific data on downbursts. Those projects are: the

Northern Illinois Meteorological Research on Downbursts (NIMROD) in 1978, the Joint Airport Weather Studies (JAWS) in 1982, and the Microburst and Severe Thunderstorm (MIST) project in 1986. Instruments used during those projects include anemometers and Doppler radars. A conclusion of these observational projects is that "the shape of the profiles are mainly determined by the horizontal location in relation to the downdraft, and much less dependent on the underlying roughness of the ground surface" (Holmes, 1999, p. 1410).

Some important characteristics of the phenomenon were recognized due to the Andrews Air Force Base record (see Figure 12). For example, it was observed that the passage of a downburst generally creates two distinct peaks in the history of wind speed. In analogy to the calm region of a hurricane, Fujita named it the eye of the downburst (Letchford et al., 2002). Concretely, these two peaks suggest that the wind speed in the centre of the downburst is small and that it increases with radius up to a certain distance. Other characteristics that were revealed by this record are the short storm duration, and the rapid fluctuations in wind direction during the passage of the storm (Holmes, 2001).

Hjelmfelt (1988) presented an analysis of microbursts recorded during the JAWS project. He characterized the size of those events and concluded that the outflow was similar to the well-studied fluid flow model called "wall jet" model for both radial and vertical profiles of horizontal wind velocity. In this model, the flow field is compared to a jet of fluid impinging on a surface (see Figure 13). A more complex alternative to the wall jet model is the "ring vortex" model. A sketch is shown in Figure 14. This illustrates the formation of a vortex near the ground which indicates the presence of both horizontal and vertical winds.

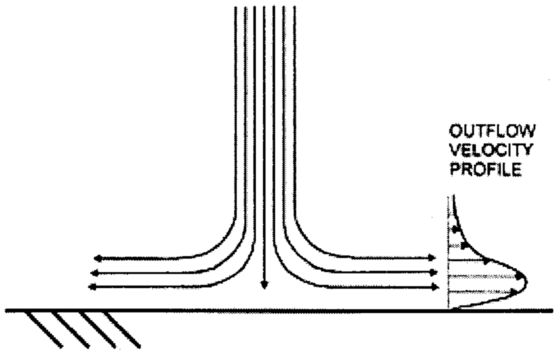

Figure 13: Wall jet model (Savory et al, 2001)

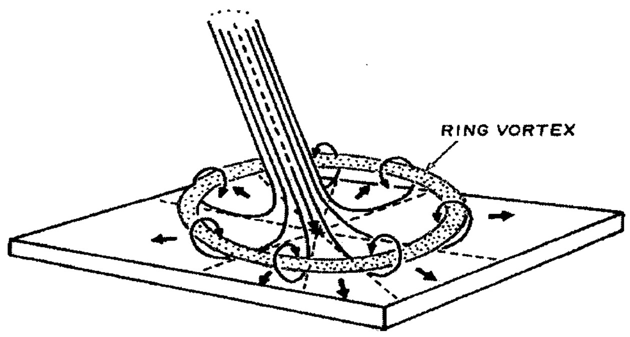

Figure 14: Ring vortex model (Letchford et al., 2002)

The first concern related to microburst winds was their effect on aviation, which explains why the aircraft industry is responsible for some of the early development on the knowledge of downbursts. An example of a model of the wind field adapted to this industry is given in Zhu and Etkin (1985). Performing early numerical simulations, meteorologists were often interested in the whole process of downburst, and did not focus on the distribution of high winds near the ground.

The first numerical simulation using the wall jet model that focused on low-altitude wind flow over objects was performed by Selvam and Holmes (1992). More recently, Holmes and Oliver (2000) developed a simplified empirical model of a downburst that addresses directly the problem of transmission line wind loading. Figure 15 is a schematic graph showing the variation of the magnitude of the horizontal radial component of the wind speed vector, V, as a function of the position r with respect to the centre of the storm. The variation is linear up to a point of maximum velocity (V_{max} at position r_{max}) and then decreases exponentially. In this model, the resultant wind velocity is obtained from the vector summation of the radial wind velocity and the translational velocity of the moving storm. An example of a downburst footprint as described in the model is shown in Figure 16. As observed in the different records, the translational component of velocity can represent a significant fraction of the peak wind speed measured.

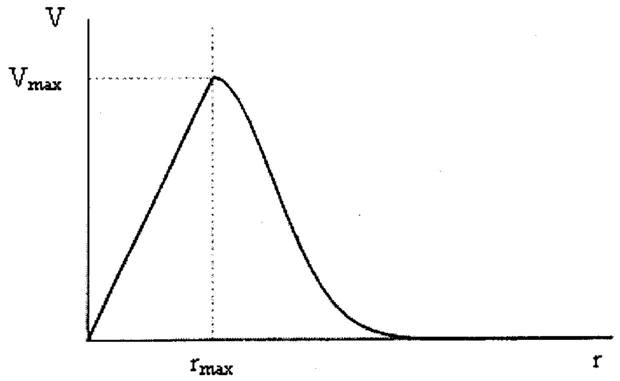

Figure 15: Horizontal radial profile of wind velocity in a downburst model by Holmes and Oliver (2000)

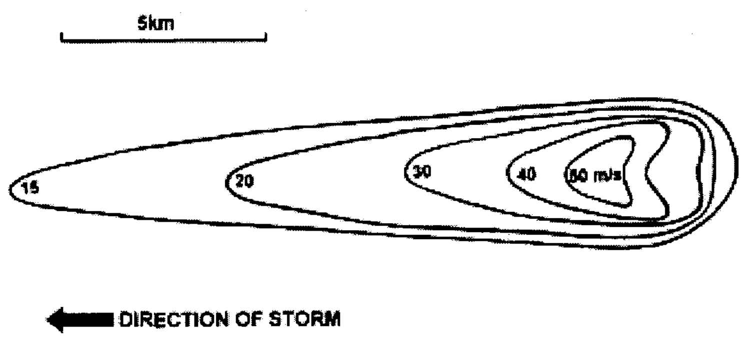

Figure 16: Footprint of a downburst (Holmes & Oliver, 2000)

As opposed to the boundary layer winds, downburst winds reach their maximum intensity at relatively low altitudes. In general, it is believed that the vertical profile shows a peak between 50 and 100 metres above ground (Holmes, 1999). Early observations by Fujita and Hjelmfelt during the 1980s are among the very small number of full-scale measurements available to verify the profiles of horizontal downburst wind. Work by Wood et al. (2001) gives an empirical formula to approximate the distribution of high winds with height. This formula and the specific parameters used in the numerical study reported in Sections 4 and 5 are given in Appendix A. Figure 17 shows the difference between this empirical formula and a typical boundary layer wind formula, along with other profiles resulting from numerical simulations of a downburst at different scales (1/20, 1/2,000, 1/20,000) performed by Hangan (2002). The graph is normalized with respect to the maximum wind speed (V_{max}) and the height where the wind speed is at one half of its maximum value ($z_{0.5*Vmax}$).

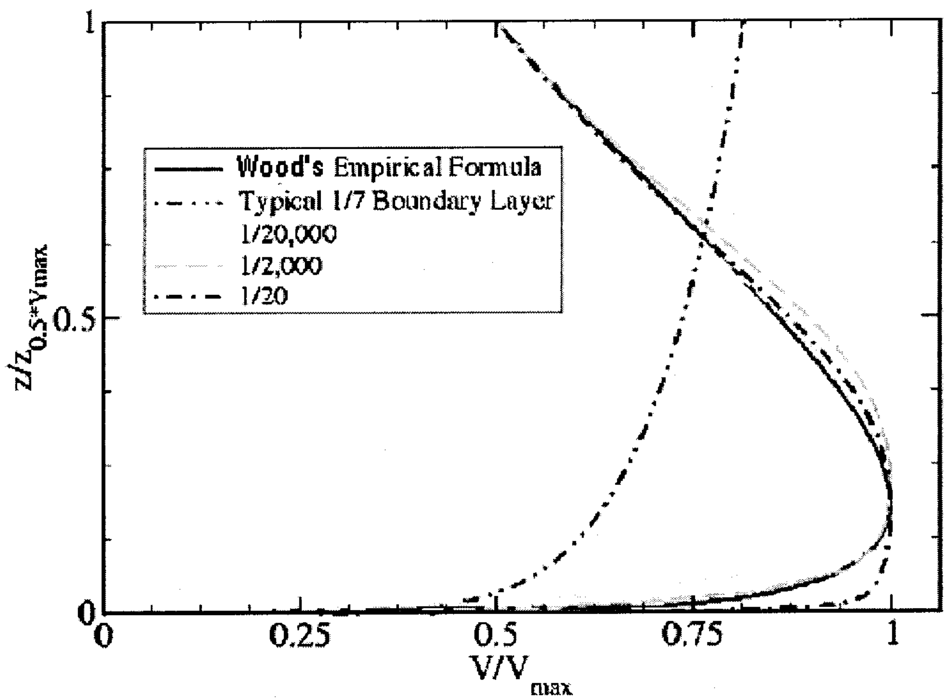

Figure 17: Downburst horizontal radial velocity profiles (Hangan, 2002)

With the development of computational fluid dynamics (CFD), numerical simulations now take into account many properties of downbursts. The challenge is to generate, from those simulations, wind loads applicable to structures. Chay et al. (2006) attacked this problem and attempted to develop "a comprehensive model of a downburst that is suitable for the generation of wind loads in a time domain structural dynamic analysis" (p. 240). The work by Hangan (2002) provides another numerical downburst model.

Along with numerical simulations, some laboratory simulations have been tried. The research is still very limited and does not compare to the well-developed boundary layer wind tunnel work. One way of simulating a downburst is to use an outlet jet from a wind tunnel impinging on a vertical board. This technique was used for example by Wood et al. (2001). The method represents well the velocity profiles but fails to demonstrate the transient characteristics of the flow (Holmes, 2001). One major problem is that the source, contrary to a real storm, is stationary. Recent progress includes the development of a moving jet method (Mason et al., 2005). The milestones of this development are explained by Letchford et al. (2002), and a large part of the work has been done by the same authors at the University of Queensland in Australia and Texas Tech University in the United States. There are also ongoing research developments on downburst simulations at the Boundary Layer Wind Tunnel Laboratory of the University of Western Ontario in Canada (Lin et al., 2006).

Tornado Wind Field

Tornadoes are more easily identified than downbursts due to their visible narrow funnel. The phenomenon has been studied for a long time and the general structure of the wind flow is well known. The flow field of tornadoes was studied through observations, numerical simulations, and physical simulations. Analyses from observations are useful, but limited by the rarity and unpredictability of events. Nowadays, research using computer modeling is dominant. However, a large part of the basic knowledge on tornadoes was revealed through laboratory simulations.

A complete review of the evolution of physical modeling of tornadoes is available in Letchford et al. (2002). The first serious modeling attempts were made during the 1960s and the 1970s. Davies-Jones (1976) reviewed the work in the field and concluded that the simulator developed by Ward (1972) was the most realistic. The Ward-type simulator was further developed by some authors including Church et al. (1979). Others used it to verify the effects of tornadoes on structures. For example, Jischke and Light (1983) studied the pressures on a rectangular model structure in a Ward-type simulator. Recent advances in tornado simulators include translation of the simulated storm and development of multiple vortices (Letchford et al., 2002).

The tornado is characterized by a vortex of high-speed air. Wind speeds are affected by a solid boundary: the ground. It is convenient to decompose the wind velocity into three components, namely the tangential (T), radial (R) and vertical (W) components, as shown in Figure 18. Velocity profiles are developed with respect to height (z) and radius (r). Note that the tangential velocity increases with radius up to a certain distance. Radial velocities have maxima at relatively low heights. Based on this representation, Wen (1975) developed a loading model that was later used by several authors (Council for Scientific and Industrial Research [CSIR], 1992; Savory et al., 2001). Wen's model is presented in Appendix B with the assumptions used to derive a profile for the numerical study reported in Sections 4 and 5.

As for a downburst, the direction and speed of the storm producing the tornado will affect the maximum wind velocities. ASCE Manual 74 (1991) provides a simplified diagram of the regions of higher winds within a tornado (Figure 19). It is assumed that the rotary and translational components sum up as vectors. That creates an area of high winds in the right-hand side of the tornado for a counterclockwise rotating wind field.

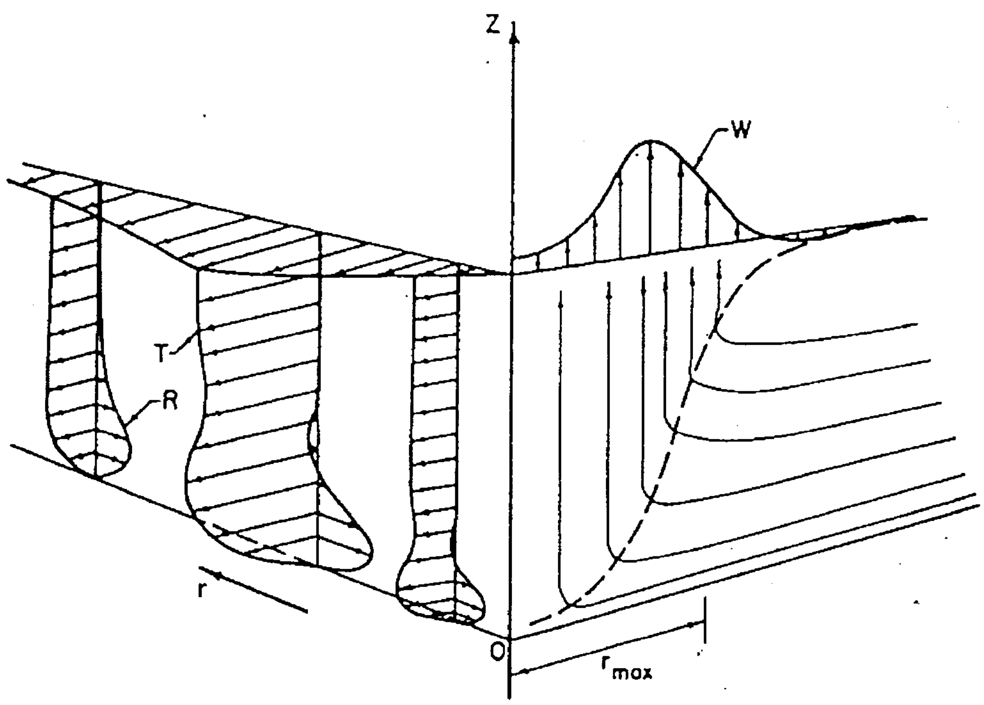

Figure 18: Schematic representation of the wind velocity components in a tornado vortex (Kuo, 1971; Wen, 1975)

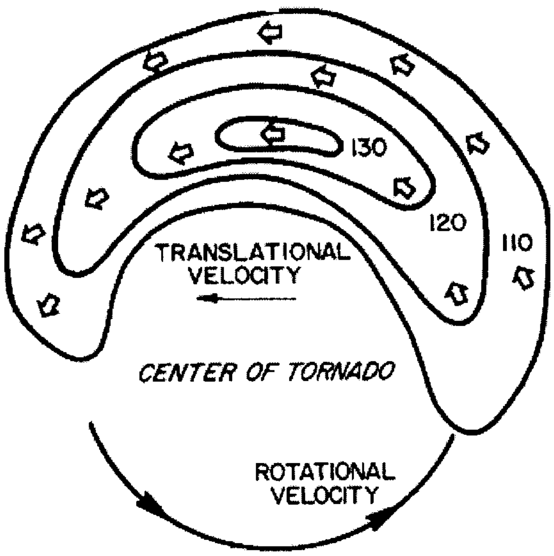

Figure 19: Hypothetical pattern of tornado wind velocities and directions (ASCE, 1991)

Another important feature of tornadoes is the presence of very low pressures near the centre due to extremely high wind speeds. The difference between pressures at the centre and outside the storm can be as high as 200 mbar (National Research Council [U.S.] - Committee on Atmospheric Sciences, 1973). This is not a major threat to transmission structures, but extremely low pressures can have devastating effects when they occur nearby buildings with closed doors and windows. Roof and walls can be blown out as large forces are created by the unequal pressures inside and outside the building.

As accounted for by recent laboratory simulations (see Letchford et al., 2002), large tornadoes can have more than one vortex. Those small-scale vortices were called suction vortices by Fujita (1981) and are represented in Figure 20. They explain the fact that damage is generally not homogeneous over a region. Suction vortices have diameters of about 10 m (Battan, 1984).

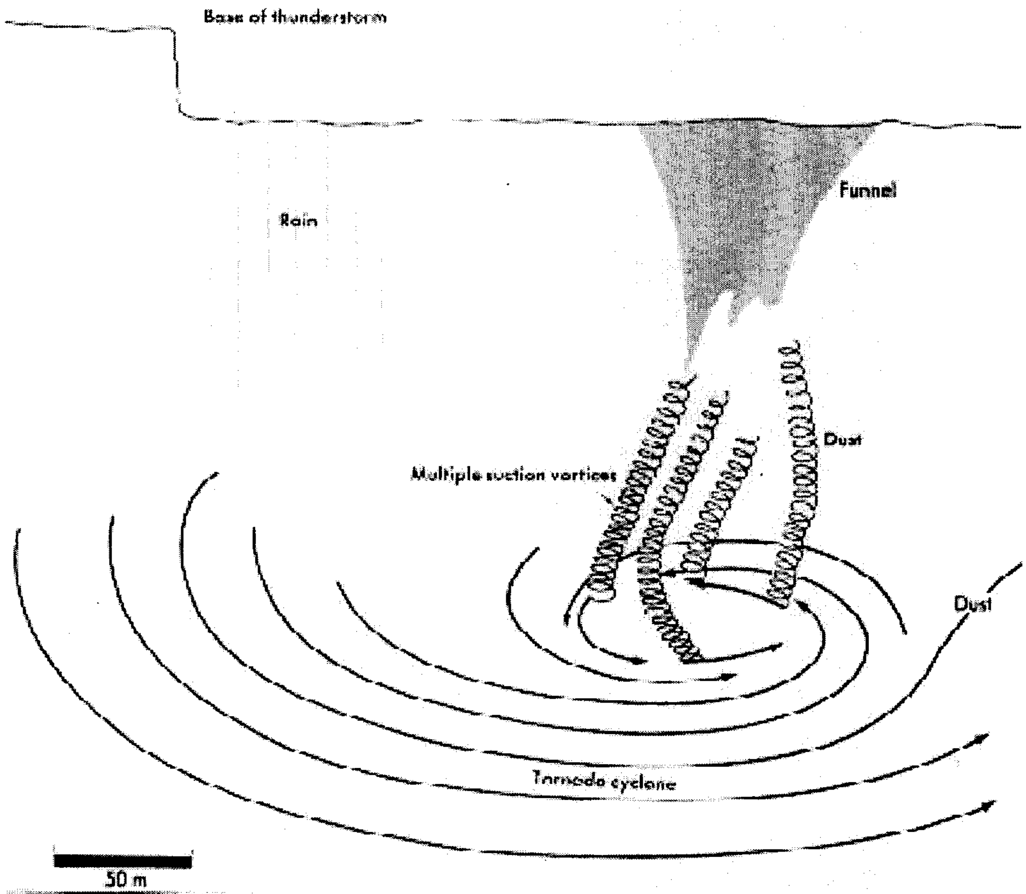

Figure 20: Schematic representation of tornado cyclone, funnel, and suction vortices (Battan, 1984)

3.3 Risk Assessment

To perform the design of transmission towers is to balance the costs of initial construction or reinforcement with the costs of power interruption and tower replacement. Twisdale (1982) expressed the opinion that for the United States, the risk of failure of transmission lines under tornado loads was generally too high. A survey by CIGRÉ Working Group B2.06 (Nolasco, 1996) revealed that among wind-related failures, many were due to tornadoes and thunderstorm winds. In response to these failures, one first step is to find when, where and how often localized HIW storms occur. Those questions have proven to be difficult to answer.

What makes overhead lines particularly vulnerable to localized high intensity winds is the line-like geometry of the system. The probability of a severe local wind event striking any point on a line is much higher than the probability of that wind striking a single point. Nevertheless, many challenges are encountered when assessing the risk of local severe wind events on transmission lines. The quality of tornado and downburst records is often insufficient to perform significant risk assessment. Firstly, localized HIW records are usually limited to a few decades. Downbursts, for example, were unknown before the 1960s. Secondly, tornadoes and downbursts affect such a small footprint area, that they are, even today, rarely properly recorded. Finally, localized HIW storms are difficult to classify because of their complexity. In fact, every severe storm has a different wind field and therefore, the exact prediction of wind loadings due to localized HIW is impossible. The only way to obtain useful data is to categorize wind events and to study common patterns in their wind field.

For developing a proper risk model, an adequate probability distribution must be chosen. Traditionally, the Type I Extreme-Value distribution, also called Gumbel distribution, is used to analyze annual extreme wind speeds. However, according to Holmes (1999), this distribution should not be used for winds originating from local storms which occur as discrete events. The distribution proposed is a Type III Extreme-Value distribution. According to Holmes, the latter is more realistic when return periods need to be extrapolated beyond the data limits.

The question of the choice of distribution also points out the problem of dealing properly with extreme wind data in climates where different types of severe wind events occur. Twisdale (1982) argues that: "the most accurate prediction of wind-loading risk is obtained from a separate analysis of each wind-producing phenomena" (p. 44). Separate analysis of wind gusts from thunderstorms in the region of Sydney, Australia was performed by Gomes and Vickery (1976). They later developed a technique to analyze separately the wind speeds from different storm types and combine them into a single design wind speed (Gomes & Vickery, 1978). The importance of thunderstorm winds was demonstrated when Twisdale and Vickery (1992) showed that those winds dominated the records of many weather stations in the United States. The fundamental issue is to statistically describe localized HIW as a distinct population of wind event: this is a first milestone towards the development of probabilistic methods to design against localized wind storms.

The distribution of localized HIW storms is not uniform over the planet: they are more common in large continental areas and their occurrence varies with latitude.

Severe thunderstorms are critical in sub-tropical regions, i.e. at latitudes between 25 and 40 degrees. In tropical regions located between latitudes 10 and 25 degrees, severe winds can occur due to both thunderstorms and occasional tropical cyclones (*Notes on meeting*, 1993). In the equatorial region (about 10 degrees North to 10 degrees South), most extreme winds occur in thunderstorms, but peak gusts are generally lower than in other regions (Holmes, 1999). In colder climates, wind is not the only weather-related threat, and failures in transmission line systems are often caused by ice accumulation or by a combination of wind and ice (Nolasco, 1996). Failures due to localized HIW have occurred in various climates where they have hit structures in off-design conditions, i.e. under loadings that were not specifically considered in design. In effect, most regions of the world should be concerned with the risk of localized HIW, while mitigation measures should be different from one climate to the other.

Several risk models have been developed for localized HIW and some of them are directly applied to transmission lines. Most of them consider only tornadoes, or only downbursts. A review of those models is presented next.

3.3.1 Downburst Risks

Downburst risk modeling is a new area of research. It is limited by the short period of data records. Only a few regions of the world, including the United States and Australia, have been studied for the probability of occurrence of downbursts. During the NIMROD and JAWS projects in the United States, tens of microbursts were recorded, and statistical analyses were performed. In Figure 21, the yearly probability of occurrence is plotted as a function of wind speed: it is seen that few observations are available for high wind speeds. Fujita (1990) notes that "because of higher frequencies and large individual area of a microburst, probabilities of structural damage by microbursts with 50 to 100 mph (22 to 45 m/s) range of windspeeds could be much higher than those of tornadoes" (p. 85).

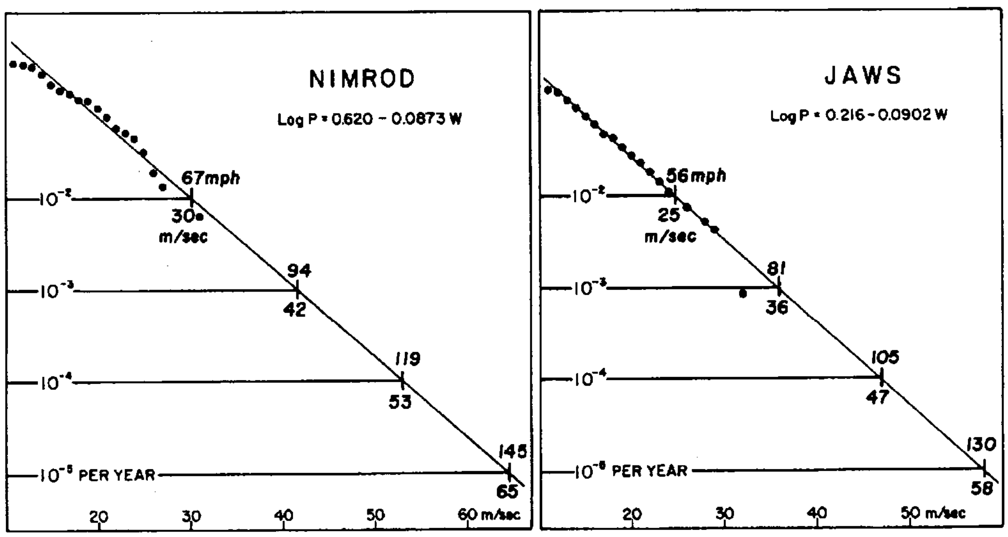

Figure 21: Microburst wind speeds in the NIMROD and JAWS projects plotted as functions of the occurrence probability per year (Fujita, 1990)

In Australia, downbursts and their resulting damages are observed frequently. Holmes and Oliver (2000), based on a ESAA (now ENA) report, evaluated that for the state of New South Wales, the yearly average occurrence of downbursts producing winds higher than 20.6 m/s at a recording station is 2.0. The peak gust recorded for such events was 42.2 m/s. Similarly, in Queensland, the average is 2.35 per annum with a maximum recorded wind velocity of 51.5 m/s. Hawes and Dempsey (1993) added that for New South Wales, the frequency of microbursts is similar to that found during the NIMROD and JAWS projects and that a return period of around 100 years per hundred kilometres of overhead line is expected for a wind speed of 45 m/s.

Based on their observations of downbursts, Australians have developed risk models for the intersection with transmission lines. A conceptual model is presented by Li and Holmes (1995) and Li (2000). A less complex and well-accepted model is the one by Oliver et al. (2000). The return period of a downburst event with wind speeds above a certain threshold on a line can be obtained from a limited number of parameters such as the yearly probability of downburst event in a region, the average width of downbursts, and the length of the line. In this formula, the return period is inversely proportional to the length of the line. This model, or more precisely an earlier version of it, is used in the works of Letchford (1998) to study a line that had failed twice under localized HIW. Using the same model, Letchford and Hawes (2000) assessed the risk of failure of the entire high voltage transmission line network due to downbursts in Queensland, Australia. The model generally predicts more failures due to downbursts than what is really observed. This is due to both a conservative design process and a conservative extreme wind speed analysis.

Some other risk models were developed in other countries. For example, Schwarzkopf and Rosso (1982) in Argentina developed the return period graph in Figure 22.

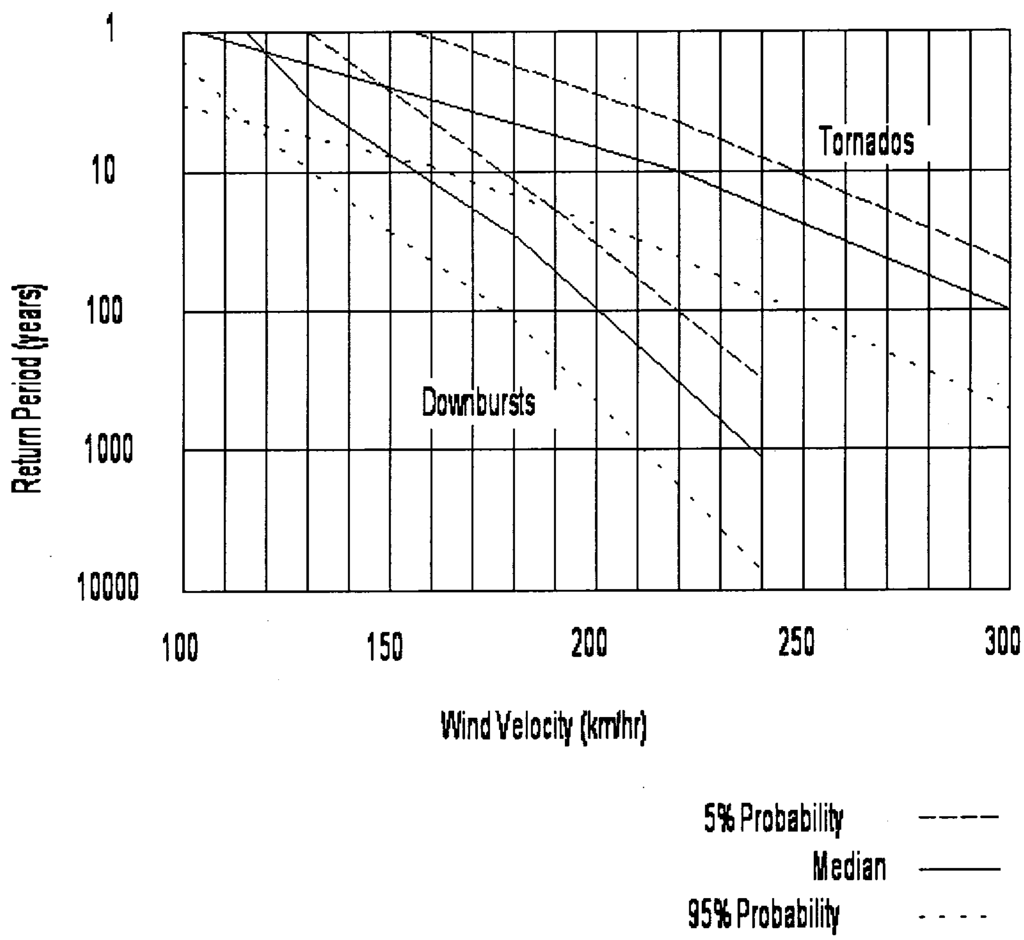

Figure 22: Return period of wind speeds for downbursts and tornadoes traversing a 650 km line section in Argentina (ASCE, 2005)

Downburst risk models are quite similar to, and in fact originate from tornado risk models. However, downbursts are generally larger in extent than tornadoes. Often, more than one span is enveloped by damaging winds and therefore, unlike for tornadoes, the wind loading on conductors is significant. For long lines not specifically designed for localized HIW and perpendicular to the normal direction of thunderstorms, risk models usually yield very low return periods.

3.3.2 Tornado Risks

Most tornadoes, and more specifically those that are expected to be survived without damage, affect a width much smaller than one line span (wind span). For example, an F2 tornado is defined by a maximum path width of about 160 m (500 ft), which is less than half the ruling span of most high voltage overhead lines supported on steel towers. Hence, risk assessment goes from looking at the probability of an event striking any point on a line, for a downburst, to the probability of an event striking any tower on a line, for a tornado. In general, tornadoes should cause damage less often than downbursts, but could possibly be more devastating due to higher wind speeds.

Tornado records are kept in most developed countries. The United States is by far the country where the largest number of tornadoes is reported with an average of 800 to 1000 each year for the contiguous states (ASCE, 1991). Shown in Figure 23 is a map of the United States with the number of tornadoes recorded during a 30-year span for each one-degree square of longitude and latitude. This map was developed by Tecson et al. (1979) and is also included in the ASCE Guidelines for Electrical Transmission Line Structural Loading (1991). In the ASCE 7-Minimum Design Loads for Buildings and Other Structures (2002), another map (Figure 24) shows the expected maximum tornadic wind speed for a theoretical 10^5-years return period.

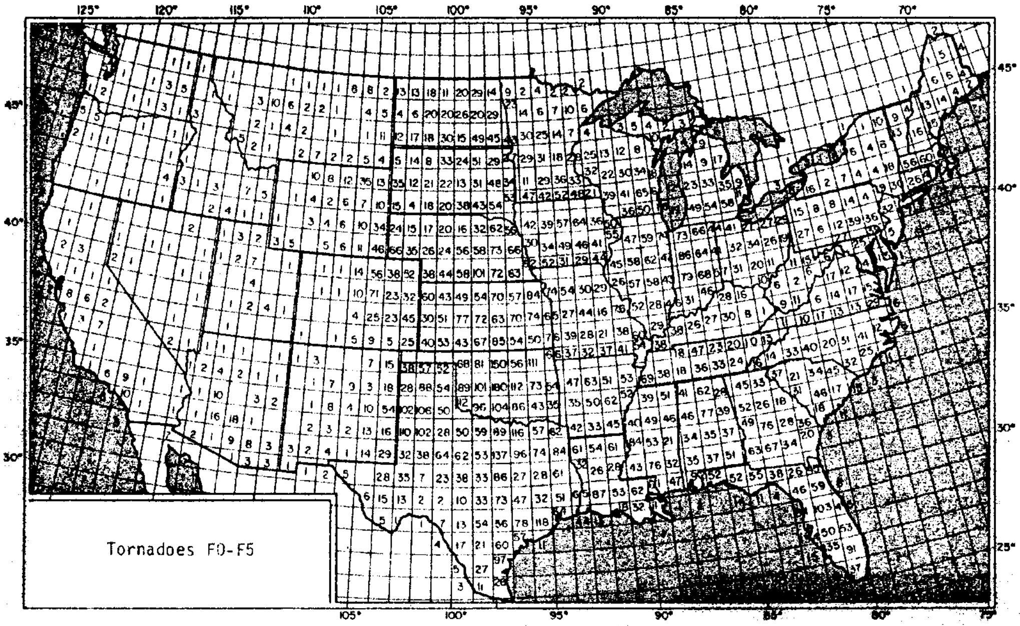

Figure 23: Total number of reported tornadoes during a 30-year period (ASCE, 1991; Tecson et al., 1979)

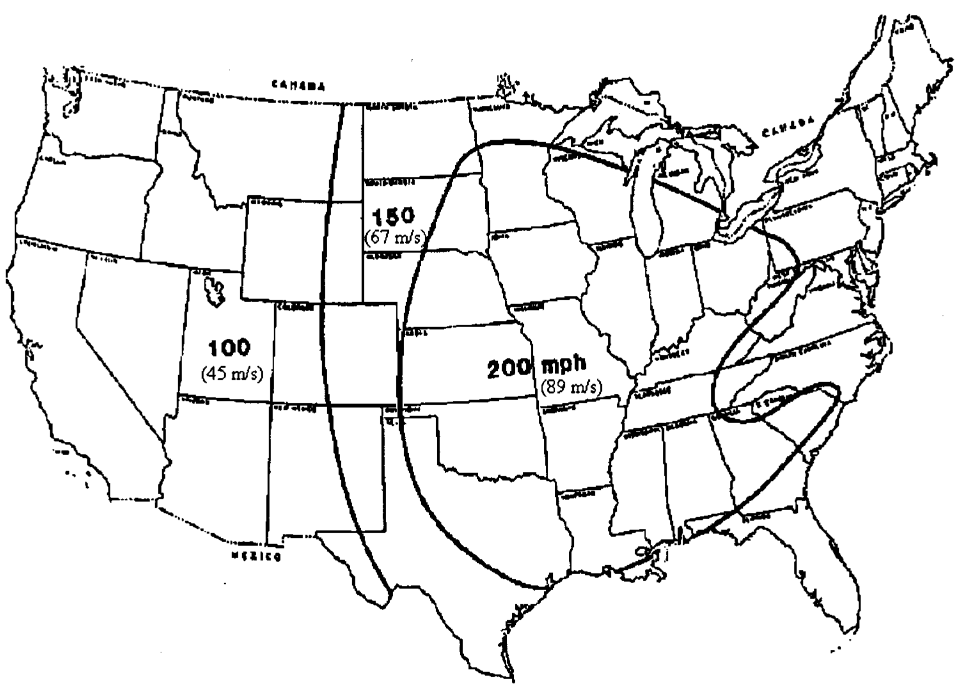

Figure 24: Tornadic gust wind speed corresponding to 100,000 year return period (ASCE, 2002)

Other authors have identified the frequency of tornadoes for South Africa (Milford & Goliger, 1994) and Argentina (Schwarzkopf & Rosso, 1982). In the early 1970s, Fujita (1973) was the first to attempt a review of tornado activity around the world . More recently Goliger and Milford (1998) performed similar work. These scientific papers identify the North American continent as being the area where most tornadoes occur. The Great Plains of the United States are, without any doubt, an area favourable to the formation of tornadoes. However, due to an increased awareness, a large portion of the tornadoes recorded are very small ones. These small tornadoes were not reported a few decades ago, and in most parts of the world, are still not reported. Therefore, the difference between the frequency of events in the United States and elsewhere is probably smaller than what is shown in the current records. For example, the recording efforts in Germany have increased the frequency from about 2 per decade before 1950, to 7 in the 1990s, to finally 20 in the year 2000 alone (Brooks et al., 2003). From the point of view of the transmission line industry, it is often more reliable to study risks looking directly at the number of failures of lines in a region. The CIGRÉ Technical Brochure 256 (CIGRÉ WG B2.16, 2004) reports estimates of the frequency of line failures for some countries. In that same report, a useful world map of wind hazard is provided.

For areas where the tornado records are reliable and statistically significant, it can be useful to derive models for the risk of tornadoes striking a line. Tornado risk models first evolved with the goal of assessing the risk of an event striking an isolated structure; many authors, including Thom (1963) and Wen and Chu (1973), have developed models of this type. Twisdale and Dunn (1983) produced a tornado wind risk model for both isolated structures and lifelines. Milford and Goliger (1997) developed a simple model for the risk of intersection of a tornado with a transmission line and provided proper values for tornado frequency to apply the model to South Africa. In a book on structural wind loading, Holmes (2001) argued that only the intersection of a tornado with a tower on a line is a critical factor for line failure. He also developed his own simple risk model based on this assumption.

The idea that all tornadoes produce extremely high and devastating winds and that nothing could be built to survive those events is no longer valid. Most records consider not only the number of tornadoes, but also their intensity. The Fujita scale, explained in Section 3.1.4, is almost always used to qualify these events. It is useful to know the percentage of low intensity tornadoes in a record because design criteria should be based on resisting most tornadoes and not all tornadoes. This percentage certainly depends on the quality of the record, but for acceptable data, the number of F0 and F1 tornadoes is very high. For the Canadian Great Lakes region, the percentage of tornadoes less than F2 is about 80 % (*Notes on meeting*, 1993). For the United States, the ASCE Manual 74 (1991) suggests that 86 % of events are F2 or smaller.

3.4 Effects of Localized HIW on Lines

3.4.1 Impact on Structures

The knowledge on the effect of localized HIW on transmission lines is limited. Research on the wind field of these events has shown that their effect is likely to be very different from the conventional boundary layer wind effect. In general, the wind loading due to tornadoes or downbursts could take any form. Therefore, the most realistic prediction for these wind loads is that they could be anything other than the synoptic wind load usually accounted for in design codes. Nevertheless, there are ways to simplify the effect of localized HIW and to economically reduce the impact of these winds on structures.

Localized Wind Loading

Based on observations of wind damage on transmission lines, Carpena and Finzi (1964) proposed an early design philosophy regarding localized HIW, and more specifically tornadoes. They wrote: "we shall then point out that by increasing the transverse strength of towers the structures may often not be safe enough against actual wind loads and that a certain longitudinal and torsional strength is required" (Carpena & Finzi, 1964, p. 2). Their view of wind loading is that a tower should be able to resist a large number of different loadings, rather than one very high transverse loading. Since most wind events do not cover a very large area, the load on conductors is rarely due to the maximum wind pressure anticipated applied on the whole wind span. Today, most design codes include a span reduction factor to account for the limited width of gust winds. To account for very narrow wind, the loading on conductors can sometimes be further reduced, while the loading on the tower is increased. Furthermore, the wind load should be expected to come from a wider range of directions. The effect on structures for this kind of loading is explained by Carpena and Finzi (1964):

> We must note that transversal loads due to wind pressure on conductors and on towers act in a different way. The former, which are applied to the crossarms, stress leg members foremost and may not stress web members appreciably; the latter, on the contrary, have their resultant applied at mid height and mainly stress web members which may have to be designed specially for these stresses (p. 19).

Hence, one way of increasing performance of lines against localized HIW would be of increasing the strength of bracing members.

A number of sources have expressed, with respect to transmission lines, the characteristics of a simplified tornado wind loading (see Section 3.5). This tornado loading consists of a very high wind pressure on the support, along with no wind pressure on the conductors. In a synoptic wind loading, the wind on conductors represents a large part of the total horizontal load on the towers. The position of the resultant transverse load is then very high on the tower, near the geometric centre of the conductors. A tower designer normally specifies, for a self-supporting tower, the intersection of the main leg slopes (identified schematically by elevations h_1 and h_2 on Figure 32 in Section 4) to coincide with this centre of effort (or with the geometric centre of the conductors). This way, the load in bracing members is reduced and failures are more likely to occur in the main legs or the foundations. In the event of a tornado affecting a tower, the wind load on conductors is likely to be small compared to the load on the structure itself. The centre of effort is therefore lowered and significant forces develop in bracing members. If buckling of one of the slender members occurs, the tower may fail in a shearing mode. This is expected in particular for panels with X-braces where the diagonal members have been designed as tension-only elements: in this case the load redistribution following the buckling of the compressed brace may yield the tensile brace. This failure mechanism is often observed for structures suffering a very narrow HIW event such as a tornado (Dempsey & White, 1996). For guyed towers, the complex wind loading patterns on guy wires and lattice sections may have various effects. For a guyed-V tower, a tornado wind loading is likely to increase the bending moments in the masts. Also, the shear distribution in the masts of guyed-Y and Delta-guyed towers can be changed (Ishac & White, 1995).

A simplified downburst loading is found in some works, but there is not yet a consensus on it. Downbursts are known to be larger than tornadoes in extent, i.e. more than one span can be affected by an event. Downburst wind loading varies greatly depending on the development stage at the moment the structure is hit. If a downburst is close to touch down, high downward vertical winds are expected. After touch down, the load is mainly horizontal (Savory et al., 2001) with possibly some upward vertical load due to the formation of a ring vortex. Based on wind tunnel simulations, Letchford and Hawes (2000) argue that since a typical downburst can create high velocity winds up to a height larger than 150 m, it can be assumed that during this type of event, towers are fully loaded over their height. In a worst-case scenario, the conductors of an entire wind span could also be fully loaded. Some authors suggested that higher span reduction factors (actually smaller load reductions) should be used for a downburst loading case (Oliver et al., 2000). This idea is based on some observations of uniform high gusts over a relatively large area (exceeding one wind span) during downburst events.

Dempsey and White (1996) express their idea on a simplified downburst loading: "At this time a patch-wind loading only on the top sections of the tower and conductors would appear to fit observations where microbursts have caused transmission line failures" (p. 40). The recommendations of the CIGRÉ Technical Brochure 256 by Working Group B2.16 (2004) support a similar idea. The wind loading below 15 m is neglected due to boundary interaction, and a strong wind is applied to the rest of the tower and the conductors. This represents well the high wind shear (high rate of change of wind speed with height) expected during downbursts but does not agree with the downburst wind profile which predicts very high winds at low altitude.

The most elaborate downburst design loading model is found in the Australian "Guidelines for Design and Maintenance of Overhead Distribution and

Transmission Lines" (ENA, 2006). The loading details are presented in Section 3.5.3. The procedure to design against downburst winds is very similar to the one for synoptic winds, except that design wind speeds are based on microburst data records and there are some restrictions to the use of span reduction factors. As for boundary layer wind effects, the structure and conductors are assumed to be fully loaded by high winds.

Finite Element Analyses

Along with the observation of line failures, the development of numerical models for wind loading and line structures is a mean to evaluate the effects of localized HIW. It was shown in Section 3.2 that a number of numerical simulation methods were developed to model a downburst or a tornado. Some of those methods were used to perform finite element analyses of towers. These analyses still need to be refined, but they give an indication of the distribution of forces in a tower due to localized HIW loadings. At least three analyses of this type were reported in recent years.

The first was done by Savory et al. (2001), who developed a model of a lattice transmission tower subjected to both a tornado and a microburst severe loading. The tornado loading created a shear failure as often observed on transmission lines. However, when the microburst wind load was applied to the structure, no non-linearity was observed. It should be noted that the model was limited to one tower and that the wind load on conductors was neglected. The fact that the model of a severe downburst affected only moderately the tower suggests that wind load on conductors should be considered for this type of wind storm.

In another study, Hoxey et al. (2003) assessed the response of a lattice and a guyed tower to a downburst. The guyed tower seemed less resistant to this type of wind load and exhibited failure of the crossarm and of the primary member above guy fixings.

Finally, Shehata et al. (2005), based on CFD work by Hangan (2002), applied a downburst loading on a lattice tower. Among other findings, they proved that "peak forces in the transmission tower members are sensitive to the downburst location with respect to the tower" (Shehata et al., 2005, p. 87). More research by these same authors is in progress at the University of Western Ontario.

Dynamic Behaviour

Localized high intensity winds usually change very rapidly with time, but their possible dynamic amplification effects on transmission line structures have rarely been raised. Many current codes, based on the concept of gust response factors (Davenport, 1967, 1979), account for the dynamic response of the line. However, for reasonably short tower height and line span, the dynamic response is believed to be very small (Holmes, 2001). Also, for high wind speeds, "dynamic response is not dominant due to high aerodynamic damping" (Matheson & Holmes, 1981, p. 109). This aerodynamic damping limits resonance that could occur in conductors due to a natural frequency often below 1 Hz, and relatively close to wind forcing frequencies. Classical lattice towers generally have larger natural frequencies (over 1 Hz) and are rarely affected by the dynamic properties of wind (Holmes, 2001).

The small number of complete time history records available makes it difficult to assess the dominant frequencies of tornadoes and downbursts. Shehata et al. (2005) evaluate that the dominant period for their numerically simulated downbursts is between 20 and 22 s, which justifies their static analysis. It is unclear whether downbursts may have a significant frequency content in the sensitivity range of line sections or individual towers.

Even if dynamic response does not seem to be a major factor in transmission line failures, not enough is known to completely eliminate possible important dynamic effects, especially in guyed towers. A study of downburst effects on tall buildings (Chen & Letchford, 2004) gives some important information about the dynamic response of transmission structures to downbursts. Looking at the time histories of some recorded and simulated downburst events, the authors identified a characterizing period of 36 s. When the response of a particular building is studied under different downburst loadings, the maximum response constantly occurs for periods around 14 s. The fundamental period of the building studied is around 5 s, and hence, the maximum dynamic response is probably not reached for tall buildings. The authors suggest that the dynamic response could be more critical for tall towers and masts of around 100 m in height due to their longer natural periods. This work by Chen and Letchford and an article by Holmes et al. (2005) are among the few documents written on the subject of dynamic structural response to localized HIW storms.

An important contributor to the advancement of wind engineering in the last decades, Alan G. Davenport, expressed at the meeting of the Task Force on High Intensity Winds on Transmission Lines in Argentina (*Notes on meeting*, 1993), concerns about the problem of structure resonant amplification: "Gust must last 30 seconds to be of concern, [and therefore] 2-3 second gusts are generally not a problem but downbursts gusts may be" (p. 8). He also added that: "High Intensity Wind flow had significant 'patchiness'. It is helpful to use influence lines to check effect of wind at different levels" (*Notes on meeting*, 1993, p. 8). The use of influence lines is briefly described in Davenport (1995) and is further developed for the application of synoptic winds on guyed telecommunication towers by Davenport and Sparling (1992).

In summary, even though it does not seem frequent, some dynamic amplification can possibly be induced in the response of transmission structures to downbursts. Very little research is available on the subject.

Topographical Effects

It is well known that local topography can influence wind speeds near the ground and that structures located on top of a hill, for example, could experience an increase in wind pressure. A discussion of the modification of wind flow due to topography is provided in Holmes (2001). It is often included in codes as a "speed-up" factor or topographic multiplier, defined as the ratio of the wind speed over a topographical feature to the wind speed at the same height in flat terrain.

Those local topographic effects have been well-studied in boundary layer wind tunnels. The application of speed-up factors to localized HIW could, however, be misleading. A few physical simulations of downbursts, including one by Letchford and Illidge (1999), showed that those multipliers are actually smaller for localized HIW than for boundary layer winds. On the other hand, this conclusion was found using stationary jet models and could be different for storms with high translational velocities. The draft revision of ASCE Manual 74 (2005) suggests speed-up factors up to 1.3. Letchford (1998) assumed that speed-up factors during a particular downburst event were about 1.2 at ground level and decreased linearly with height to a value of 1.0 at altitude 100 m.

Transverse Cascading

A major concern in the transmission line industry is the avoidance of line cascades. A cascade is defined as the progressive collapse of a large number of structures (Peabody, 2001). Most cascades are said to be longitudinal and are due to the initial failure of a structural element that maintains tension in the wires. There are sometimes also transverse cascades, which are almost exclusively initiated by localized HIW (ASCE, 2005). A tornado, damaging one or two structures, or a downburst, possibly damaging a few more, may trigger a long chain of support failures that can affect tens of structures. When a tower falls in the transverse direction, the effective span gets longer, and forces are created both in the transverse and longitudinal directions at the adjacent structures. If these towers also fail, the collapse may progress, forming a cascade (Peabody, 2001). Some properties of line systems that enhance the vulnerability to transverse cascades are: short spans, tall structures and short insulator strings (ASCE, 2005). Prevention of cascades is a critical aspect of line design and is an effective way of minimizing the potential damage due to localized HIW.

3.4.2 Reported Failures

Some documents report and sometimes analyze a number of transmission line failures due to localized high intensity winds. The purpose of this section is not to cover all failures that have occurred, but to give a summary of some case studies where the event was carefully analyzed. Unfortunately, very few of those reports can be accessed publicly.

A survey of transmission line failures was conducted by CIGRÉ (Nolasco, 1996) about 10 years ago and is currently being updated. The survey gathered information about 299 failure events involving 1731 towers in 24 countries. The data are interesting from a statistical point of view even though the survey results clearly do not cover all failures that occurred to transmission lines, nor always identify precisely the cause of failure. About 86 % of the reported failures were attributed to climatic loads such as wind, ice, or a combination of wind and ice. Other causes are, for example, broken conductors, hardware failures, and vandalism. Among failures due to climatic loads, 54 % were due to wind alone, with tornado and downburst winds often involved.

Argentina

When a first meeting of what was called the Task Force on High Intensity Winds on Transmission Lines (*Notes on meeting*, 1993) was held in Buenos Aires, Argentina, an important failure event had just occurred in that region. Three 500 kV lines were damaged from the Alicura and the El Chocon Power Stations. A total of 56 towers had failed at multiple sites, and damage was observed over a very large area of more than 150 km by 50 km. The cause of failures was attributed to 4 or 5 distinct tornadic cells.

At that same meeting, previous failures were also discussed. There had been another failure on the El Chocon 500 kV line, and one on the Rodriguez 500 kV line. Details are available in the notes of the meeting (*Notes on meeting*, 1993).

Australia and New Zealand

An important document in the domain of localized HIW is a review of failures in Australia by Hawes and Dempsey (1993). It covers some meteorological concepts, gives information on the frequency of failure events, summarizes some research on the subject, and finally, provides specific observations about some failures.

Relevant statistics given for Australia for the period 1951-1993 are:

- Total length of transmission lines between 110 kV and 500 kV: 53500 km
- Number of major failures reported: 21
- Number of structures failed: 94
- Number of failures initiated in towers: 16
- Number of failures initiated in foundations: 5
- Number of failures due to tornado: 5
- Number of failures with evidence of microburst: 10

The estimated wind gusts during the failure events range from 41 to 66 m/s and are generally between 45 and 50 m/s. Details of four different failures are reported. In most cases, there was evidence of high wind shear.

A more recent document by Letchford (1998) presents a complete study of a 275 kV line failure where 5 towers failed due to a macroburst, with possibly the presence of several microbursts within the macroburst.

In New Zealand, a report was recently completed on the loss of two pylons due to a downburst (Reid & Revell, 2006) with an estimated maximum wind speed of 43 m/s. The evaluation of damage to the vegetation surrounding the collapsed towers helped analyzing the weather elements in place.

North America

A very large cascade failure that was initiated by localized HIW was documented in the United States (Oswald et al., 1994). The failure occurred on a 345 kV wood pole line owned by the Nebraska Public Power District. Over 400 structures failed during a fast-moving storm that produced several small tornadoes and microbursts. In this report, focus is given to the inability of the system to stop the cascade.

In September 1996, Manitoba Hydro in Canada lost 19 towers following localized HIW storms. The failure occurred in a region where wind rarely causes damage without combining with ice. A report by meteorologists (McCarthy & Melsness, 1996), analyzed the weather elements that led to the failure and concluded that the event did not include tornadic winds, but was rather caused by downbursts. Following this failure, research was initiated at the University of Western Ontario (Lin et al., 2006; Shehata et al., 2005) to gain better understanding of the effects of downbursts on line structures.

3.5 Codes and Design Practices

To date, while in many regions, localized HIW storms are thought to be a larger threat to transmission lines than boundary layer winds, wind loading codes continue to be based on synoptic wind models. More and more designers, however, take into account the possibility of tornado or downburst winds hitting line systems. Guidelines for the inclusion of localized HIW risks in design are provided in Australia (ENA, 2006) and in the United States (ASCE, 1991, 2005). This section summarizes the design practices proposed.

3.5.1 IEC 60826-2003

In the standards defined in IEC 60826-2003 localized HIW are briefly mentioned. First, it is recognized that the document does not cover localized events and that those can represent a serious threat to lines due to both direct wind forces and impact of wind-carried objects (projectiles). Second, the IEC recommends that the designer perform a special study on wind extreme values before choosing a design wind speed in regions prone to localized HIW. Hence, the code suggests that localized high intensity winds need to be treated separately from synoptic winds, from a statistical point of view.

3.5.2 Tornado Loading by Behncke and White

Behncke and White (1984) have discussed the design assumptions used for Hidronor's Alicura 500 kV line in Argentina. Wind was identified as the most serious threat to the line. Due to failure experiences with the 500 kV El Chocon line, Hidronor decided to take special considerations for the risk of tornadoes. It was recognized that very severe tornadoes could probably not be resisted by transmission lines. However, it was evaluated that about 85% of tornadoes would exhibit winds equal to or less than 220-240 km/h (60-67 m/s). Static analysis was carried out on guyed-V towers subjected to a wind loading based on those wind speeds and coming from any direction. The tornado loading required only minor reinforcement to a few members near the top and the bottom of the masts. This marked the first time a special tornado loading was used in transmission line design.

Behncke et al. (1994) documented the design criteria developed for the South African utility Eskom. The tornado loading proposed consists of applying a wind speed of 250 km/h (70 m/s) to the support and neglecting wind on conductors. An analysis of the record in South Africa had shown that 90% of all tornadoes were F2 or less on the Fujita scale (see Table 3). The effect of the tornado loading was calculated for a 400 kV cross rope suspension tower: it resulted in an increase of the bending moment in the mast central portion and the reinforcement needed increased the tower total weight by 2% only. If the tower was short enough, no reinforcement was needed. According to this document, tornado loads are especially critical on guyed towers such as guyed-V and cross-rope towers.

The simplified tornado loading developed for Eskom was based on the recommendations of a previous review (CSIR, 1992) of tornado loading models.

In summary, the CSIR agrees with the ASCE Manual 74 (1991) (Section 3.5.4), except that it recommends to include the self-weight of conductors in the analysis. The ASCE suggests that due to strong vertical wind loads, the self-weight of conductors can be ignored.

Ishac and White (1995) have developed design criteria for Hydro One (formerly Ontario Hydro) to account for tornadoes. Their tornado loading model is also based on a very high (92%) proportion of small intensity tornadoes (F2 or less) recorded in the region studied. The authors suggested that the tornado wind speed applied to a line segment be proportional to its boundary layer extreme wind speed equivalent. The resulting tornado wind speed is much higher than normal extreme values, but is applied to the tower only. For example, the highest tornado wind speed used is 66.7 m/s (240 km/h) and is suggested only for segments where the extreme synoptic design wind velocity is 44.4 m/s (160 km/h). Other values for design wind speed are shown in Table 4.

Table 4: Hydro One tornado and extreme wind loading (Ishac & White, 1995)

Extreme wind speed (m/s)	22.2	26.7	35.6	40.0	44.4
Wind load on conductor (kPa)	0.29	0.39	0.77	0.96	1.15
Wind load on tower (kPa)	0.8	1.1	2.1	2.6	3.1
Tornado scale	F1		F1/F2	F2	
Tornado wind speed (m/s)	33.3	40.0	53.3	62.2	66.7
Tornado load on conductor (kPa)	0	0	0	0	0
Tornado load on tower (kPa)	1.7	2.4	4.8	6.0	6.5

Designs of two types of towers, one self-supporting latticed 4-leg tower and one guyed-V tower, were revisited while considering that new tornado load. Each tower type was redesigned for the basic and the tallest tower configurations. The basic 4-leg tower did not need any reinforcement, while the tallest configuration was adequate for overturning but needed reinforcement in shear. The total additional weight needed for the tallest configuration was limited to 2.5%. For the design of the guyed-V towers, extra bending moment and shear capacity was needed. The additional weight was also limited to 2.5% for both the basic and the tall configurations.

3.5.3 ENA C(b)1-2006

As mentioned earlier, the Australian standard ENA C(b)1-2006 specifies a design procedure for microburst loading that is very similar to the one for synoptic wind loading. The country was divided into 11 regions of microburst activity as shown in Figure 25. Table 5 provides for each region a microburst design wind speed varying with the desired line reliability level. All wind speeds in the table are based on a line length of 100 km and a microburst gust width of 500 m. Line reliability is theoretically inversely proportional to the total length of the transmission line.

Wind forces on conductors are not neglected for microbursts and span reduction factors must be not less than 0.9 for spans less than 500 m. The wind speed is further multiplied by a microburst wind direction factor that depends on the region concerned and on the critical wind direction (perpendicular to the line).

Although tornadoes are less frequent than microbursts in Australia, the ENA still recommends a tornado loading to be used where it can be an issue. For a line reliability level of 4 (400 years return period), a wind speed of 60 m/s is recommended for application on the tower only, without any wind force on the conductors.

Table 5: Microburst wind gust speeds for selected line reliability level (LR) and return period (RP) (ENA, 2006)

LR (RP Years)	1/2 (25)	1 (50)	2 (100)	3 (200)	4 (400)	5 (1000)
Regions H, I, J, K (NSW and QLD)	42.0	44.0	46.1	48.2	50.2	52.1
Region H (S-E QLD)	51.0	56.0	60.1	63.6	66.7	70.8
Region L (VIC)	46.5	48.5	50.2	52.0	54.2	56.6
Region M (VIC)	48.4	50.5	52.2	54.2	56.5	58.9
Region O (SA)	47.0	49.0	50.7	52.5	54.8	57.2
Region N(SA), P and Q(WA)	48.0	50.0	51.7	53.6	55.9	58.3

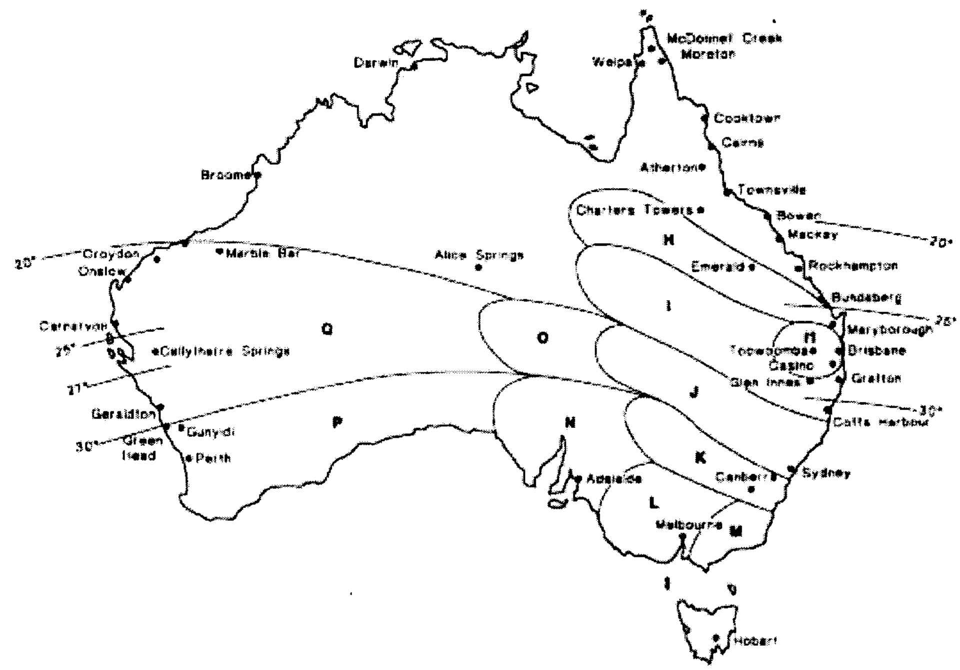

Figure 25: Microburst region boundaries (ENA, 2006)

3.5.4 ASCE Manual 74 (1991, 2005)

Along with HIW-resistant design criteria, ASCE Manual 74 (1991) and its draft revision (ASCE, 2005), provide many useful facts on the subject. This section will focus on the design criteria suggested.

The main suggestion of the document regarding tornadoes is summarized in the following quotation: "One possible 'tornado' loading is a wind loading corresponding to a moderate tornado (scale F1 or F2) applied only to the transmission structure over the full structure height from any direction" (ASCE, 2005). The wind load on conductors for this case is neglected because of the limited path size of the event and the complexity of wind force patterns. It is also suggested to consider a conductor dead load of zero as the vertical wind component in a tornado can possibly lift the conductors. Tornado winds are gust winds and therefore the gust response factor should be kept to 1.0.

The recommendation for downburst loading varies with the size of the event. For a small-scale microburst, the tornado loading specified should be used. For larger downbursts, it is suggested to use the traditional approach based on synoptic winds with gust response factors close to 1.0.

3.5.5 CIGRÉ Technical Brochure 256 (2004)

This recent CIGRÉ document (CIGRÉ WG B2.16, 2004) describes the characteristics of major types of wind events (Table 6). The report suggests designing overhead lines for a uniform F2 tornado wind on the tower only (no tornado wind on the conductors) coming from any direction, and considering torsional loads.

For downbursts, the CIGRÉ Working Group B2.16 (2004) recommends:

> Design for microburst and macroburst winds should consider the effects of surface roughness on the wind approach to the line. This has the effect of introducing high wind shears above ground that may be more onerous on the structure design. It is recommended that no wind be applied below 15 m and the full wind above this level. The wind gust will also engulf the complete wind span of conductor in this case and no reduction in span

factor should be considered. Winds gusts must be considered from any direction (p. 42).

Simplified loading for both tornadoes and downbursts are therefore proposed in this document, implying that the effects of the two phenomena are very different. A tornado striking a tower would not create any wind forces on conductors and hence, the location of the horizontal force resultant would be very low. The downburst loading, however, would produce full loading on the conductors and the top portion of the tower: that would produce a large horizontal resultant at or very near the geometric centre of the conductors.

Table 6: Characteristics of wind storm phenomena and design guidelines (CIGRÉ WG B2.16, 2004)

Wind Storm Phenomena Type	Classification	Gust Wind Velocity Range m/s (2-3 s gust)	Potential Wind Gust Width	Predominate Regional Area	Frequency of Occurrence Refer Note 5	Notes on Application to Design
Gust Front		45 - 50	10 000m	All regions	1/50	Normal Design and Span factor
Sub Tropical Thunderstorm				Subtropical Regions Refer Figure 1		
- Down Bursts		50 - 70	1,000m		1/50	Complete span over 1000m and >15m structure (Span factor 1.0) Refer Note 2
- Microbursts		70 - 80	100m		1/1000	
- Embedded tornado	F2	45 - 70	400m		1/1000	Provide for torsional loading and wind from any direction on structure only
	F3	70 - 95	300m		1/1000	Note 1
	F4	95 - 120	200m		1/4000	Note 1
	F5	> 120	100m		1/10000	Note 1
Tornado				Severe Tornado Regions		
	F2	45 - 70	1000m		1/5	Provide for torsional loading and wind from any direction on structure only Refer Note 4
	F3	70 - 95	400m		1/1000	Note 1
	F4	95 - 120	200m		1/4000	Note 1
	F5	> 120	200m		1/10000	Note 1
Cyclone / Hurricane / Typhoon				Subtropical Regions Refer Figure 1		
	2	35 - 47	20 - 50 km		1/10	
	3	48 - 63	20 - 50 km		1/100	Note 3
	4	64 - 78	20 - 50 km		1/4000	Note 1
	5	>78	20 - 50 km		1/10000	Note 1
Extratropical /Winter Storm		50 - 60	500 - 3400m	Sea coast and land masses in close proximity to polar oceans	1/1000	Note 3
Instability Depression		50 - 60		Northern polar sea coastal regions	1/50	Note 3
Katabatic /Down Slope Winds		40 - 70	1000m	Refer Figure 1	1/100	Refer local conditions

Note 1. Design consideration for wind velocities in this range is low probability and not considered viable for normal security overhead lines

Note 2. Design for Microburst and Macroburst winds should consider the effects of surface roughness on the wind approach to the line. This has the effect of introducing high wind shears above ground that may be more onerous on the structure design. It is recommended that no wind be applied below 15m and the full wind above this level. The wind gust will also engulf the complete wind span of conductor in this case and no reduction in span factor should be considered. Winds gusts must be considered from any direction.

Note 3. Cyclonic wind storms have a pronounced gustiness at maximum wind velocity that most likely will be sustained over a period of several hours. Spatial effects of this is to effectively provide some relief in wind span. A Span factor of 0.7 is recommended.

Note 4. Tornadoes generate high velocity swirling / rotational winds. Towers expected to withstand F2 tornadoes should be designed for torsional winds applied to the structure superstructure. Wind gusts >F2 do occur but are rare events.

Note 5. Frequencies provided are indicative values and may vary from region to region (Refer local Meteorology Office)

3.5.6 Direct Gust Wind Method (Behncke & White, 2006)

The recent article titled "Applying Gust Loading to Your Lines" by Behncke and White (2006), argues for a complete change of the method used to design overhead lines against high winds. According to them, the synoptic wind method should be replaced by a more direct method where 3-second gusts are applied directly to the structure and to part of the conductors as shown schematically in Figure 26. A uniform wind pressure Q_t is applied to the tower members and a uniformly distributed wind force Q_c is applied to the conductors over a distance W_G. The line designer must select proper drag factors for the calculation of wind forces and a width of gust (W_G) that is representative of the storm event. Unlike in the synoptic wind method, no adjustment for height is made and the wind pressures are not multiplied by gust response factors.

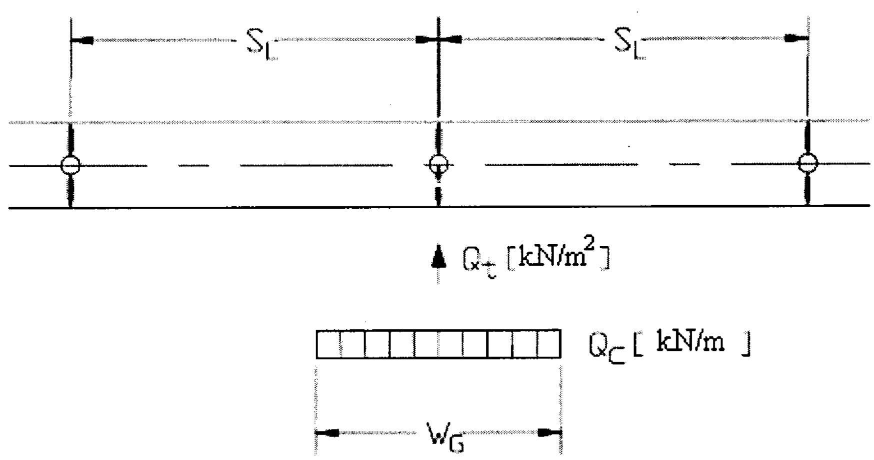

Figure 26: Direct gust wind method (Behncke & White, 2006)

4 Numerical Modeling of Overhead Lines

Using the transmission line analysis software PLS-CADD (2006), several simulations were performed to evaluate the effects of various localized HIW load cases on four self-supporting lattice towers. The lattice towers were modeled in the program TOWER (2006), also developed by Power Line Systems (PLS). All simulations are static linear elastic analyses. Because the purpose of the study is to compare the severity of different loadings cases, the linear analyses were allowed to reach high stresses in members, often beyond the failure limit. Only two-span line sections needed to be modeled and therefore, most load cases were analyzed using the limited version PLS-CADD/LITE.

Axial forces in tower members were compared for the various load cases. It is of interest to identify which load cases are critical to the type of towers examined, and which members or groups of members receive high forces under those load cases. It is noteworthy that bracing members that have been designed as tension-only elements are studied according to their tensile response only. Load cases were chosen to match previous suggestions found in the literature concerning localized HIW effects (see Section 3.5), or were based on the anticipation of worst-case loading on towers due this type of wind event. Table 7 provides a summary of the properties of each analyzed tower and more details are available in sections 4.1 and 4.2.

Table 7: Summary of properties of self-supporting lattice towers

Tower name	Peabody	Wisconsin	Can. Bridge 0°	Can. Bridge 15°
Short name	PB	WI	CB0	CB15
Source	Peabody (2004)	Peabody (2004)	Hydro-Québec	Hydro-Québec
Type of tower	suspension	suspension	suspension	dead-end
Height (m)	28.5	28.0	49.5	39.1
Span Length (m)	350	350	450	450
Insulators	I string	I string	V string	Strain
Conductors	Cardinal 54/7 ACSR	Ibis 26/7 ACSR	Bersimis 42/7 ACSR	Bersimis 42/7 ACSR
Circuit	single	double	single	single
Voltage (kV)	230	138	735	735

4.1 Modeling of the Towers

The geometry and angle shape properties were modeled in TOWER. Frame-truss models were used. Beam elements were used wherever the model needed stability in the rotational degrees of freedom. For calculating wind loads, each tower was divided into sections usually representing one tower panel. To match common practice of designers using Power Line Systems programs and to simplify the modeling process, most redundant members were not included in the models. In order to account for the presence of these members in the calculations, additional vertical dead load and equivalent drag areas were added manually. All members in the models are assumed to have a modulus of elasticity of 200 GPa.

Peabody Tower

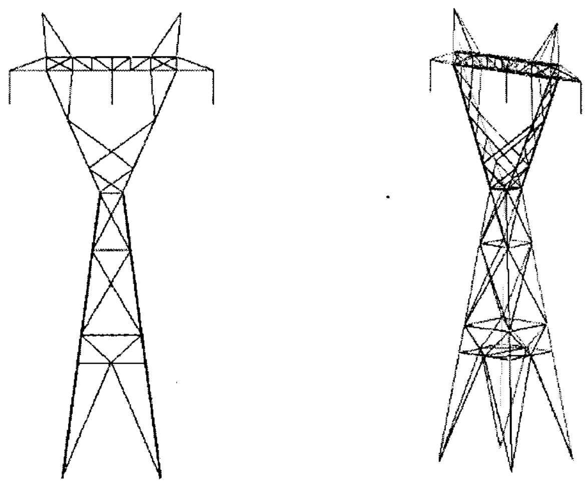

Figure 27: Peabody tower model

This single-circuit suspension tower was designed by Alan B. Peabody for the purpose of his Ph.D. work at McGill University (Peabody, 2004). The structure was meant to support a 230 kV line. Unlike the other three towers, this is only a prototype structure and it has never been built. The objective of the design process for this structure was to provide a realistic tower stiffness in the analysis of anti-cascading damping devices. The tower configuration is a typical horizontal single-circuit and it was designed to resist a maximum 1 kPa wind pressure on the tower and the conductors (weight span of 420 m). Details on the design loading cases are found in Appendix D of Peabody's thesis. It should be noted that diagonal X-braces in the tower body are designed and modeled as tension-only elements. The original model in TOWER was provided by Peabody and only the redundant members' added dead load and drag area were modified by the author. For consistency, a number of redundant members were not included for the other three models and were accounted for as additional dead load and drag area for wind force calculations. However, the Peabody model is slightly different from the other three since the details for connections are included. For each member, information is given on the type and number of bolts used, number of bolt holes, number of shear planes, eccentricity and restraint conditions, and number of connected legs. This information had no influence on the analysis results as it was used only by the component design modules. Connection details were therefore not modeled for the other three towers. The unbraced length of members, which is identified in TOWER through a ratio of the unbraced length to the total member length, was carefully modeled for all towers.

Wisconsin Tower

The second tower originates from a 138 kV line owned by Wisconsin Power and Light. Destructive tests were performed on this line section by the Electric Power Research Institute (EPRI). More details are available in Peabody (2004) and Peyrot et al. (1978). This is a classical double-circuit suspension tower (see Figure 28) and bracing members in the tower body were also designed and modeled as tension-only members, as it was common practice prior to the 1980s. The members shown in dashed lines and identified as redundant in Figure 28 are not included in the model. Connection details were not available for this tower so no eccentricity or rotational restraint is assumed at member ends. Information on the design process is unavailable to the author. Based on its location and date of construction, it can be expected that the tower was designed to resist moderate ice and wind loads derived from deterministic methods as stipulated in the American National Electric Safety Code (NESC).

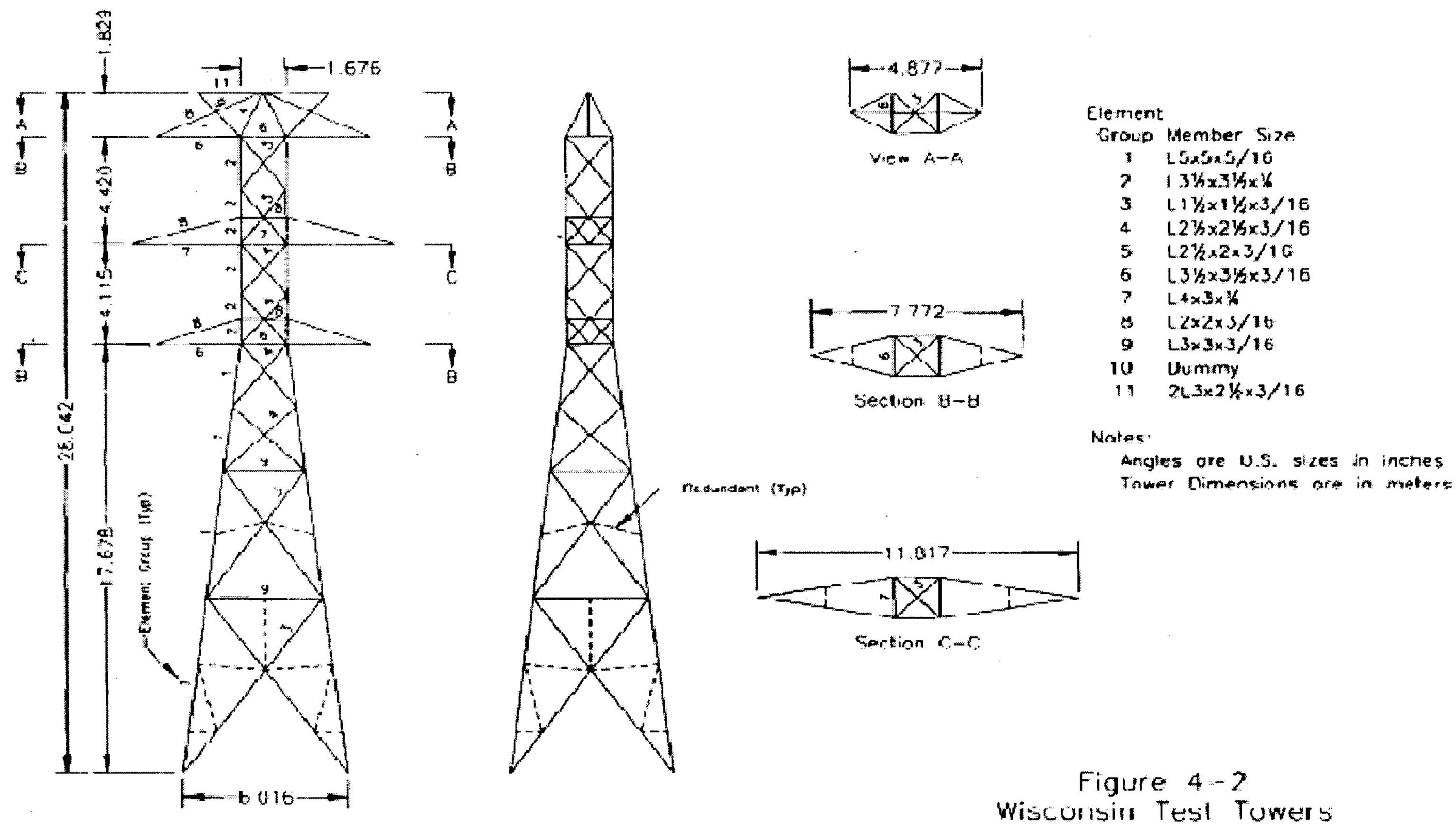

Figure 28: Wisconsin tower details (Peabody, 2004)

Canadian Bridge 0° and 15° Towers

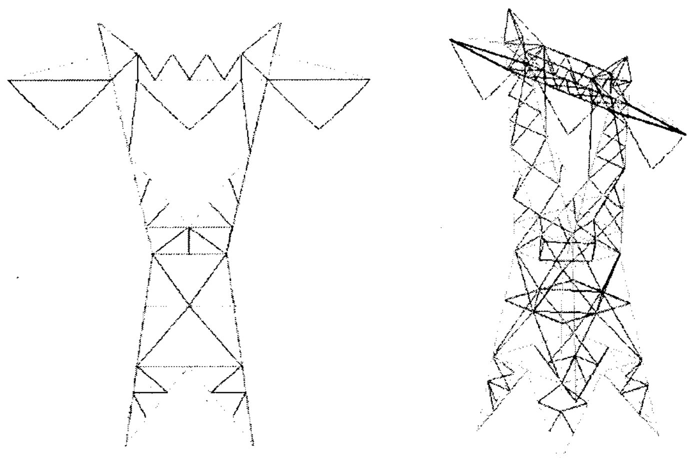

Figure 29: Canadian Bridge 0° suspension tower model

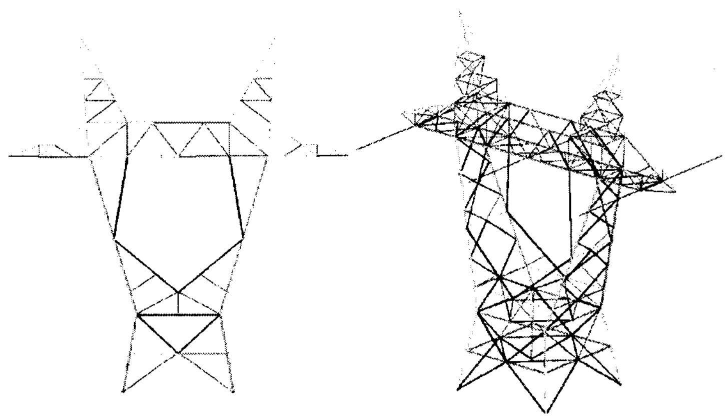

Figure 30: Canadian Bridge 15° dead-end tower model

Structural details of these two towers were obtained from Hydro-Québec and the author cannot publish them. The towers were designed in 1963 and reinforcement was recently added. The tower models are based on previous work by the author in 2004 and match the structural drawings provided by Hydro-Québec.

These single-circuit lattice towers are used on 735 kV lines in the Churchill-Manicouagan-Montreal corridor. Angles 0° and 15° refer to the horizontal line orientation change they can accommodate. The first tower is a suspension structure (Figure 29) and the second a dead-end structure (Figure 30). The other main difference between the two towers is their respective height. The suspension tower is higher by 10 m due to the inclusion in the model of a leg extension. The models are slightly different in the area of the tower truss to comply with their respective insulator types: the suspension tower requires more frame elements in this section to support the V strings.

For this numerical model, all the members were assumed with their proper axial rigidity and slenderness ratios, i.e. none of the members is modeled as tension-only elements. However, most of the diagonal X-bracing members were designed as tension-only according to industry practice at this time. Those members will require special consideration when analyzing the results. These towers were designed for a typical 0.5 in of radial ice and 8 lb/ft^2 or wind pressure.

4.2 Modeling of Conductors and Insulators

The modeling of the insulators was done in TOWER. Some insulator properties were not available and had to be approximated to the best knowledge of the author. All the parameters are shown in Table 8. The Canadian Bridge 0° V strings were modeled using the 2-part insulator option in PLS programs. The properties shown in Table 8 for this tower represent only one branch of the V string.

Table 8: Properties of insulator models

Tower name	PB	WI	CB0	CB15
Type of insulators	I string	I string	V string	Strain
Length (m)	2.1	2.1	8.5	9.8
Weight (N)	890	890	5890	17900
Transverse wind area (m^2)	0.1	0.1	0.5	0.5
Tension capacity (kN)	44.5	44.5	160.1	160.1

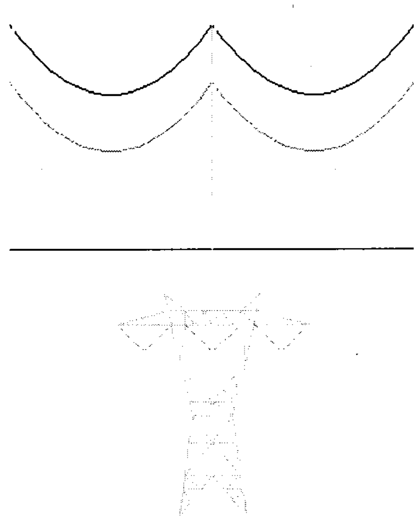

Figure 31: Example of two-span line section modeled in PLS-CADD

The version PLS-CADD/LITE used for most load cases allows to model two simple spans very rapidly (see Figure 31). Clearances were not a concern for the present simulations, and the main reason to model the conductors accurately was to transfer the correct wind forces and conductors' self-weight to the towers. All the parameters related to the sagging of conductors are shown in Table 9. The properties of the electrical conductors and the ground wires are shown in Tables 10 and 11 respectively.

Table 9: Conductor sag/tension data

Tower name	PB	WI	CB0	CB15
Span length (m)	350	350	450	450
Sagging condition	Initial	Initial	Initial	Initial
Ground wire (GW) name code	7/16 EHS	7 No. 8 CW	CDG16DP	CDG16DP
GW temperature (°C)	15	15	15	15
Number of GW in bundle	1	1	1	1
GW horizontal tension (kN)	16.0	16.0	19.6	19.6
Conductor name code	Cardinal	Ibis	Bersimis	Bersimis
Cond. stranding	54/7 ACSR	26/7 ACSR	42/7 ACSR	42/7 ACSR
Cond. temperature (°C)	75	75	75	75
Number of cables in bundle	1	1	4	4
Cond. horizontal tension (kN)	20.6	17.8	30.5	30.5

Table 10: Properties of conductors

Conductor name code	Cardinal	Ibis	Bersimis
Cross-sectional area (mm^2)	546	234	725
Outside diameter (mm)	30.4	19.9	35.1
Unit weight (N/m)	17.9	7.98	21.4
Ultimate tension (kN)	150	72.5	154
Final modulus of elasticity (GPa)	65.8	74.2	62.0
Thermal expansion coefficient ($*10^{-6}$/deg)	19.3	18.9	21.2

Table 11: Properties of ground wires

Conductor name code	7 No. 8 CW	7/16 EHS	CDG16DP
Cross-sectional area (mm^2)	59	75	152
Outside diameter (mm)	9.8	11.0	15.8
Unit weight (N/m)	4.6	5.8	11.9
Ultimate tension (kN)	20.2	93.0	160
Final modulus of elasticity (GPa)	158.6	184.1	172.4
Thermal expansion coefficient ($*10^{-6}$/deg)	13.0	13.0	12.1

4.3 Description of the Load Cases

PLS-CADD offers several wind load calculation methods, most of them in accordance with national standards. A few other general wind models such as the "wind on face" and "wind on all" methods are available for the calculation of wind loads on supports. A summary of the wind loading calculation procedure is provided here.

In general, for wind on conductors, PLS-CADD (2006) uses the following formula:

$$UH = WLF\ Q\ (W_Z)^2\ GRF_C\ CD_C\ (\cos[WA])^2\ (D + 2t_Z) \qquad \text{Equation 5}$$

where,

UH is the conductor wind load per unit length in N/m.

WLF is a weather load factor.

Q is the air density factor equal to 0.6125 kg/m^3.

W_Z is the design wind speed in m/s at height z above ground.

GRF_C is the gust response factor for conductors.

CD_C is the drag coefficient for conductors.

WA is the incidence between the wind direction and a perpendicular to the span.

D is the conductor diameter in m.

t_Z is the ice thickness in m.

For all the simulations performed, the weather load factor (WLF) is equal to 1, the drag coefficient for conductors (CD_C) is equal to 1, and the ice thickness (t_Z) is equal to 0 (only bare conditions are studied for localized HIW load effects). The user can define the wind load with an exponential profile (adjustment of wind speed W_Z with elevation above ground) or can define a uniform wind speed profile (constant with height). A number of profile adjustment models from design standards are available including the IEC 60826 (2003). The corresponding standard models are available for gust response factors (GRF_C). Another option is to specify a numerical value for GRF_C. The parameters for wind speed adjustment with height and gust response factors for conductors are directly defined as part of the weather load cases.

For the wind load on supporting structures, the formula is:

$$WF = LFW \ \ WLF \ \ Q \ \ (W_Z)^2 \ \ GRF_S \ \ CD_S \ \ A \qquad \text{Equation 6}$$

where,

WF is the wind force in N on a tower section.

LFW is the load factor for wind.

GRF_S is the gust response factor for structures.

CD_S is the drag coefficient for structures.

A is the exposed area of a tower section in m^2.

A wind force (WF) is calculated for each tower section defined in TOWER, based on its average height above ground. Values of LFW and WLF are kept to 1 in all cases for this research. The exposed area is calculated in TOWER and depends on the structure wind load model selected. For all the models, the input area A can be adjusted by a user-defined "area factor" for each tower section. The gust response factor (GRF_S) and the drag coefficient (CD_S) for the structure also depend on the wind load model selected. Three models were analyzed: the IEC 60826 model, the "wind on face" model, and the "wind on all" model. While the IEC 60826 model was described in Section 2.3, the other two models need more explanations.

"Wind on All" Model

For this wind calculation model, the wind speed is not adjusted with height and the gust response factor is equal to 1. The exposed area is calculated from the vertically projected surface of all the members defined in the tower section on a plane perpendicular to the wind direction. It is therefore assumed that no shielding effect occurs between parallel faces. The TOWER manual (2006) suggests using an overall drag coefficient of 1.6 for that model: it is defined manually as an area factor for each tower section.

"Wind on Face" Model

This model is very similar to the "wind on all" model, except that the exposed area is calculated from the members belonging to the windward faces of the section only. It is assumed that there is enough shielding effect for the other faces not to have any wind force. The drag area, which is also applied through an area factor in TOWER, is suggested to be 3.2.

Comparison of Wind Loading Models

Table 12 shows a comparison of the three models for the Peabody tower. The "wind on all" and "wind on face" models were tested at various wind speeds. Whenever those two models are used, no adjustment is made with height and no gust response factor is used for conductors. The conductor wind loads are therefore much lower than those calculated with the IEC method. In fact, as shown in the table, the total load on conductors is almost equivalent for a wind speed of 30 m/s in the IEC method and a wind speed of 45 m/s in the other two methods. For the structure loads, a wind speed of 30 m/s in the IEC method is equivalent to a wind speed of about 35 m/s for the "wind on all" model, and to a wind speed of more than 40 m/s for the "wind on face" model.

Table 12: Comparison between wind load models for the Peabody tower

Method	Drag factor	Wind speed (m/s)	Conductors load (kN)	Structure load (kN)	Total (kN)
IEC	IEC	30	45.9	36.6	82.5
All	1.6	30	22.1	25.7	47.8
All	1.6	35	30.1	35.0	65.0
All	1.6	40	39.3	45.7	84.9
All	1.6	45	49.7	57.8	108
Face	3.2	30	22.1	18.5	40.6
Face	3.2	35	30.1	25.1	55.2
Face	3.2	40	39.3	32.8	72.1
Face	3.2	45	49.7	41.5	91.3

The values for the drag coefficient were chosen as suggested by TOWER manual (2006). As explained in Section 2.3, the drag coefficient in the IEC method varies with the solidity ratio of the lattice sections. The average solidity ratios of the four towers analyzed are between 0.1 and 0.2. This would result in drag coefficients between 2.9 and 3.4. Knowing that for the IEC method, shielding is not neglected and wind forces are applied to the two windward faces only, it seems reasonable to use a value of 3.2 for the "wind on face" model.

Load Cases

A total of 28 load cases were tested on the self-supporting towers. They can be divided into four categories: synoptic wind, tornado wind, downburst wind, and direct gust wind. All load cases are described in Table 13. The IEC standard method, as described in Section 2.3, was used for synoptic wind cases assuming a terrain category B and reference conditions of temperature and pressure. The "wind on all" and the "wind on face" were judged to be equivalent for the purpose of this study and the "wind on all" was used to simulate all non-synoptic load cases. The tower drag coefficient of 1.6 used in the "wind on all" method is difficult to verify, but it seems acceptable considering that the wind speeds selected for the comparison are arbitrary values. Ideally this coefficient would be selected for each tower based on validated models or wind tunnel tests.

A gust wind speed of 70 m/s was used for all tornado loadings to match the upper limit of an F2 tornado (see Table 3). On the other hand, the gust wind velocity for downburst loading is 50 m/s based on design wind speeds in the Australian standard (ENA, 2006). Unless otherwise specified, the wind pressures obtained for these load cases were not adjusted with height and a gust response factor of 1 was applied. For the downburst load cases, the wind pressure is also uniformly applied to the conductors. It is important to note that these load cases were selected to explore some possible reasonable approaches to design overhead lines against localized HIW. It is recommended that for the study of an actual line, specific wind speeds be chosen based on field observations, whenever available. Considering that current knowledge is limited on localized HIW effects on overhead lines, the "wind on all" method is deemed adequate as the reduced number of multiplying factors allows for a rational choice of the design wind speed. Hopefully, in a near future, a better localized HIW loading model and relevant wind speed data will become available. It will then be possible to improve the simplified load cases discussed herein.

The "Synoptic 30" load case represents a typical synoptic wind load: the wind speed of 30 m/s in this case is a 10-minute average value. Other simulations at wind speeds of 35 m/s and 40 m/s were performed to be used as controls. The transverse direction (wind perpendicular to conductors) is used by default because it is the basic case and sometimes the only direction considered by designers for synoptic wind loading.

All the tornado load cases studied neglect the wind forces on conductors as suggested by some authors (ASCE, 1991; Behncke & White, 1984; Behncke et al., 1994; Ishac & White, 1995). The "Tornado below h_1" load case is suggested to obtain the worst effect in the bracing members of self-supporting towers located below the centroid of the conductor loads. The height h_1 is determined by the projected intersection of the main legs as shown in Figure 32. All the towers used in the simulations have only one bend line and therefore there is no value for h_2. For the Canadian Bridge 0° tower, this load case does not exist since the projected leg intersection is located above the tower top. Load cases "Tornado 15°" to "Tornado 90°" are the same as "Tornado full", except that they are applied in different directions. These variable directions were also tested for downburst winds.

Table 13: Summary of wind load cases

Load case no.	Name	Structure wind model	Conductor GRF	Adjustment with height	Wind on conductor	Wind on support	Wind speed (m/s)	Wind direction
1	Synoptic 30	IEC	IEC	IEC	full span	full height	30	0° (transverse)
2	Synoptic 35	IEC	IEC	IEC	full span	full height	35	0° (transverse)
3	Synoptic 40	IEC	IEC	IEC	full span	full height	40	0° (transverse)
4	Tornado full	Wind on all	1	none	none	full height	70	0° (transverse)
5	Tornado below h_1	Wind on all	1	none	none	below h_1	70	0° (transverse)
6	Tornado 15°	Wind on all	1	none	none	full height	70	15°
7	Tornado 30°	Wind on all	1	none	none	full height	70	30°
8	Tornado 45°	Wind on all	1	none	none	full height	70	45°
9	Tornado 60°	Wind on all	1	none	none	full height	70	60°
10	Tornado 75°	Wind on all	1	none	none	full height	70	75°
11	Tornado 90°	Wind on all	1	none	none	full height	70	90° (longitudinal)
12	Downburst full	Wind on all	1	none	full span	full height	50	0° (transverse)
13	Downburst above 15m	Wind on all	1	none	full span	above 15 m	50	0° (transverse)
14	Downburst above h_1	Wind on all	1	none	full span	above h_1	50	0° (transverse)
15	Downburst 15°	Wind on all	1	none	full span	full height	50	15°
16	Downburst 30°	Wind on all	1	none	full span	full height	50	30°
17	Downburst 45°	Wind on all	1	none	full span	full height	50	45°
18	Downburst 60°	Wind on all	1	none	full span	full height	50	60°
19	Downburst 75°	Wind on all	1	none	full span	full height	50	75°
20	Downburst 90°	Wind on all	1	none	full span	full height	50	90° (longitudinal)
21	Tornado lift	Wind on all	1	none	none	full height	70	0° (transverse)
22	Tornado BL profile	Wind on all	1	boundary layer	none	full height	varies	0° (transverse)
23	Tornado Wen profile	Wind on all	1	Wen's model	none	full height	varies	0° (transverse)
24	Downburst BL profile	Wind on all	1	boundary layer	full span	full height	varies	0° (transverse)
25	Downburst Wood profile	Wind on all	1	Wood's formula	full span	full height	varies	0° (transverse)
26	Synoptic above 15 m	IEC	IEC	IEC	full span	above 15 m	30	0° (transverse)
27	Synoptic above h_1	IEC	IEC	IEC	full span	above h_1	30	0° (transverse)
28	Direct gust	Wind on all	1	none	up to 80 m	full height	70	0° (transverse)

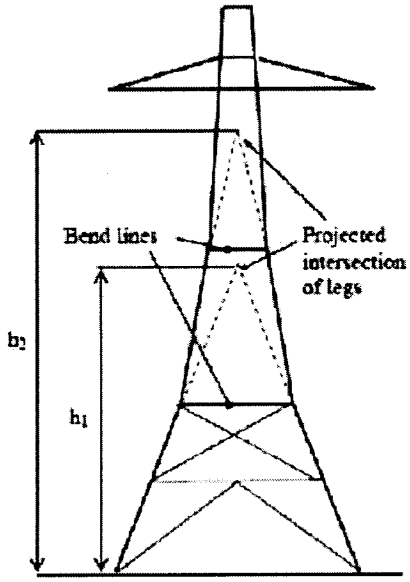

Tower	h_1 (m)	Total height (m)
PB	22.0	28.5
WI	24.0	28.0
CB0	larger than 49.5	49.5
CB15	34.3	39.1

Figure 32: Determination of h_1 for load cases "Tornado below h_1" and "Downburst above h_1"

Downburst load cases are more similar to synoptic load cases than tornado cases because wind is applied to both the supports and the conductors. "Downburst above 15 m" matches a suggestion made in CIGRÉ TB 256 (2004). "Downburst above h_1" is similar, but the wind on structure is only applied to the part above the projected intersection of the main legs. This is the complement of the "Tornado below h_1" load case. "Synoptic above 15 m" and "Synoptic above h_1" were also created in order to compare the synoptic wind method to the "wind on all" approach for this type of loading.

Additional load cases were defined to verify some of the assumptions made in the tornado and downburst loadings. First, load case "Tornado lift" verifies the suggestion made in the ASCE Manual 74 (1991) that upward vertical winds during a tornado could be strong enough to lift conductors and therefore, the self-weight of conductors should be neglected for tornado loadings. The "Tornado lift" loading is a strong uniform wind applied over the full height of the structure, but no wind nor gravity load are coming from the conductors.

Second, the assumption of not adjusting wind pressure with height for all tornado and downburst load cases was verified. For tornadoes, two profiles were used: the boundary layer 1/7 power law described in Section 2.2 (Tornado BL profile), and a profile taken from the model by Wen (1975) (Tornado Wen profile) assuming a boundary layer thickness of 200 m. Wen's model is partially described in Appendix B. The profile derived from this model cannot be assumed to be typical of tornadoes as it is only one possibility among others. In effect, the profile varies greatly with the boundary layer thickness value, and with the location of the tower with respect to the centre of the tornado. In order to be able to compare the "Tornado BL profile" and the "Tornado Wen profile" with the "Tornado full" load case, the design wind speeds were selected such that the total wind force applied to the structure was the same for the three load cases. The three profiles are as shown in Figure 33. For downbursts, the same boundary layer profile was used, as well as a profile given by Wood's formula (Wood et al., 2001) assuming that the maximum wind speed occurs at an altitude of 50 m. Wood's formula is described in Appendix A. Figure 34 shows the profiles for the "Downburst BL profile" and the "Downburst Wood profile" load cases. These profiles cannot be specified directly in PLS-CADD. Therefore, the area factor of each section was adjusted in TOWER to simulate their statically equivalent effects on the tower.

Whenever needed, the conductor gust response factor was also adjusted in PLS-CADD to make sure that the total wind force resultant was the same for all the load cases compared.

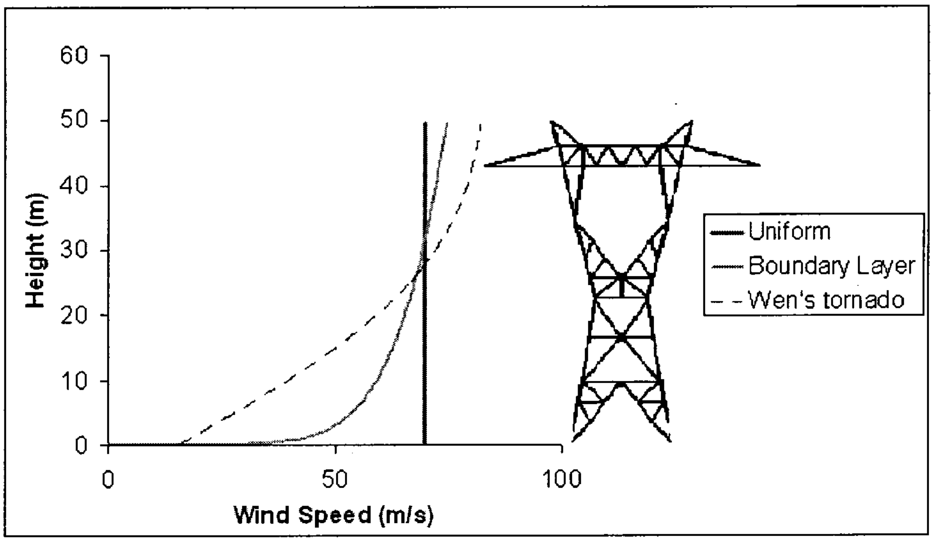

Figure 33: Horizontal tornado wind profiles for the CB0 tower

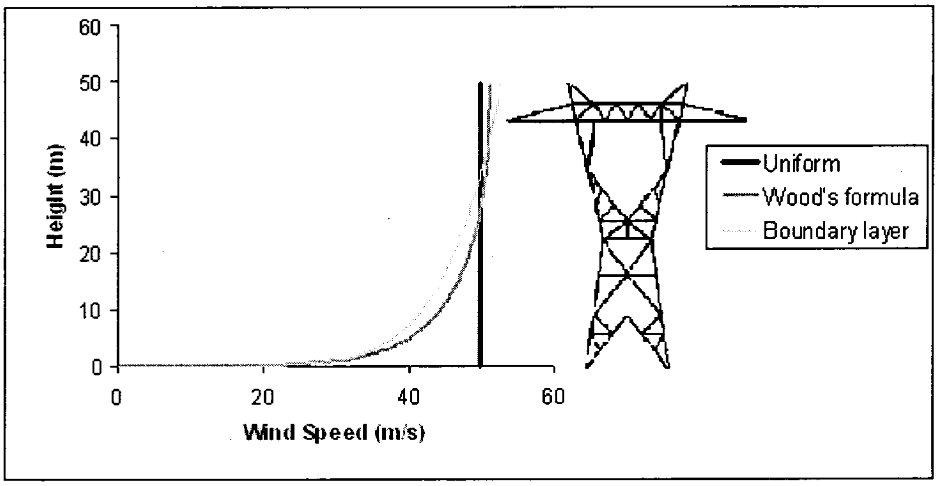

Figure 34: Horizontal downburst wind profiles for the CB0 tower

The last load case in Table 13 is the "Direct gust" loading. This case is based on the suggestion by Behncke and White (2006) as summarized in Section 3.5.6. For this loading, wind pressure is applied to the support and to part of the conductors (see Figure 35). The LITE version of PLS-CADD does not allow for partial loading of conductors and therefore, this load case was analyzed in the regular version of the program. Wind load on conductors is defined using fictitious icing accumulations on conductor sections which provide increased projected area exposed to wind. More details on the procedure follow to guide the reader who may want to apply it. Firstly, a partial span icing load is created in the window "concentrated load properties". To simulate an adequate drag area, the fictitious ice thickness must be equal to half the diameter of the conductor. The density of ice is set close to 0. Next, load points are defined in the "wire lengths and attachment stiffness" window (see Figure 36) to delimit the span sections with wind loading. Each load point indicates the beginning of the section where a partial fictitious icing is applied. To simulate the conditions shown in Figure 35, the following data are specified. For the first span (lines 1 and 2 in Figure 36), the partial load called "partialwind1" is applied in the last (right) portion of the span (from a 0.771 fraction into the span until the end). For the second span (lines 3 and 4), the same partial load is applied from the beginning (left) of the span (from a 0.001 fraction into the span) and a second load point needs to be defined to identify where the partial load stops (in this example from a fraction of 0.229 in to the span). The "concentrated load file" called "noload" in Figure 36 must have a zero ice thickness to reset the bare conditions in the second span after the 0.229

fraction. This procedure to represent the "Direct gust" load case is applied to model the effects of an F2 tornado on both the conductors and the tower directly hit by the tornado. Hence, the wind speed is 70 m/s and the width of the gust is 160 m (80 m on each side of the support) as defined using the Fujita-Pearson scale (Table 3).

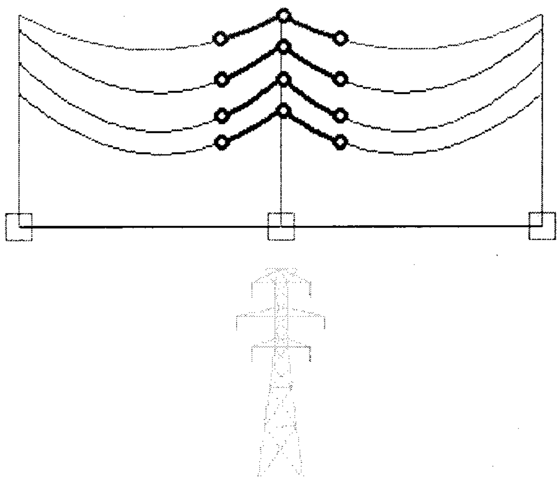

Figure 35: "Direct gust" load case on the Wisconsin tower

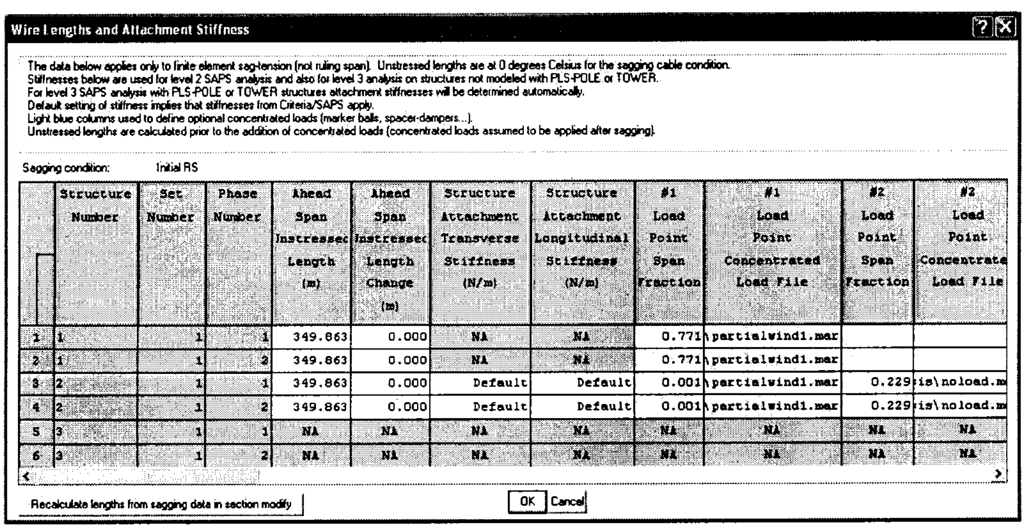

Wire Lengths and Attachment Stiffness

The data below applies only to finite element sag-tension (not ruling span). Unstressed lengths are at 0 degrees Celsius for the sagging cable condition.
Stiffnesses below are used for level 2 SAPS analysis and also for level 3 analysis on structures not modeled with PLS-POLE or TOWER.
For level 3 SAPS analysis with PLS-POLE or TOWER structures attachment stiffnesses will be determined automatically.
Default setting of stiffness implies that stiffnesses from Criteria/SAPS apply.
Light blue columns used to define optional concentrated loads (marker balls, spacer-dampers...).
Unstressed lengths are calculated prior to the addition of concentrated loads (concentrated loads assumed to be applied after sagging).

Sagging condition: Initial RS

	Structure Number	Set Number	Phase Number	Ahead Span Unstressed Length (m)	Ahead Span Unstressed Length Change (m)	Structure Attachment Transverse Stiffness (N/m)	Structure Attachment Longitudinal Stiffness (N/m)	#1 Load Point Span Fraction	#1 Load Point Concentrated Load File	#2 Load Point Span Fraction	#2 Load Point Concentrated Load File
1	1	1	1	349.863	0.000	NA	NA	0.771	\partialwind1.mar		
2	1	1	2	349.863	0.000	NA	NA	0.771	\partialwind1.mar		
3	2	1	1	349.863	0.000	Default	Default	0.001	\partialwind1.mar	0.229	is\noload.m
4	2	1	2	349.863	0.000	Default	Default	0.001	\partialwind1.mar	0.229	is\noload.m
5	3	1	1	NA	NA	NA	NA	NA	NA	NA	NA
6	3	1	2	NA	NA	NA	NA	NA	NA	NA	NA

Recalculate lengths from sagging data in section modify | OK | Cancel

Figure 36: "Wire lengths and attachment stiffness" window in PLS-CADD

5 Results and Discussion

This section shows and analyzes the effects of the various wind loadings described in Section 4 on the member forces in the four towers modeled. Although insulators and conductors were modeled adequately, their sensitivity to localized HIW loadings was not assessed during these static numerical simulations. The variation of axial forces in the tower members for the various load cases is the focus of this discussion.

5.1 Results

To facilitate the analysis of results, all the tower members were classified into 12 groups according to their location and function:

LL are the main leg members below the waist.

UL are the main leg members above the waist.

BTX are the transversal diagonal bracing members below the waist.

BLX are the longitudinal diagonal bracing members below the waist.

WTX are the transversal diagonal bracing members above the waist.

WLX are the longitudinal diagonal bracing members above the waist.

HT are the transversal horizontal members.

HL are the longitudinal horizontal members.

HX are the horizontal bracing members.

TC are the upper and lower chord members in the tower truss.

TX are all the members in the tower truss that are not TC members.

P are all the members of the ground-wire peaks and the crossarms.

Tables 14 to 21 show the maximum value of usage (in %) in compression or in tension of the various groups for the four towers and all the load cases. The percentage of usage (or use factor) is equal to the axial force in the member divided by the member capacity. In compression, the capacity is equal to the design compression stress defined by ASCE 10 standard formulas multiplied by the member gross cross section area. The design compression stress decreases with the slenderness ratio of members. The capacity in tension is defined as the design tension stress (equal to the steel yield stress F_y) times the net cross section area. For the Peabody tower, the net area is calculated directly because the number and size of bolts are defined. For the other towers, the net area is an approximation calculated by the software. Table 22 presents the total horizontal wind forces in kN applied to the towers for each load case.

For most load cases, the 100% level of usage is reached in some of the members: this is expected since the localized HIW loads studied represent extreme loading conditions. Therefore, one must be careful in interpreting these results. Transmission towers are complex structures, and the internal load paths in towers that have failed could be significantly different than what is shown in these tables. The author insists that the results are to be studied on a comparative basis among the 28 loading cases. To perform nonlinear analyses to assess the collapse load and detailed failure sequence of towers was beyond the scope of this study.

Table 14: Maximum usage (%) in compression for the Peabody tower

No.	Name	LL	UL	BTX	BLX	WTX	WLX	HT	HL	TC	TX	P
1	S 30	81.9	61.4	0.0	0.0	91.5	21.3	95.3	70.2	56.1	96.6	21.0
2	S 35	110	82.0	0.0	0.0	124	28.2	133	97.7	75.6	136	29.0
3	S 40	142	106	0.0	0.0	161	36.0	177	129	98.1	182	38.1
4	T full	93.4	45.3	0.0	0.0	69.9	15.9	141	58.6	32.3	51.1	13.8
5	T below h_1	57.2	10.4	0.0	0.0	15.6	3.3	156	31.0	7.7	8.2	13.5
6	T 15°	109	67.5	56.2	0.0	81.5	41.1	159	56.4	32.9	51.7	15.5
7	T 30°	127	79.6	0.0	0.0	79.7	63.1	146	47.3	29.4	49.7	15.8
8	T 45°	135	88.1	0.0	0.0	74.4	81.4	139	56.0	27.3	44.8	17.9
9	T 60°	134	90.6	0.0	0.0	63.8	94.1	145	73.3	26.8	36.0	22.7
10	T 75°	126	86.8	0.0	35.9	48.3	100	154	84.2	24.6	25.0	25.3
11	T 90°	114	76.0	0.0	4.0	27.8	99.8	148	87.5	21.2	22.4	23.6
12	D full	123	91.7	0.0	0.0	140	31.5	156	113	83.0	152	30.3
13	D above 15 m	123	91.8	0.0	0.0	140	31.6	153	112	83.1	152	30.3
14	D above h_1	119	89.2	0.0	0.0	134	30.6	131	100	83.3	152	30.3
15	D 15°	128	96.8	0.0	0.0	137	41.5	146	106	78.2	142	29.7
16	D 30°	118	90.9	0.0	0.0	117	48.9	120	87.7	65.8	117	28.1
17	D 45°	104	78.4	0.0	0.0	88.3	52.7	91.3	59.6	48.1	80.1	23.5
18	D 60°	87.1	65.2	23.2	0.0	59.6	54.2	83.7	32.9	28.2	44.4	17.5
19	D 75°	70.4	52.4	25.1	68.6	34.5	53.4	81.5	40.2	14.5	17.6	15.8
20	D 90°	61.6	41.0	0.0	2.1	15.2	51.3	78.8	41.7	10.3	13.1	14.5
21	T lift	90.4	42.0	0.0	0.0	70.0	15.1	141	61.6	29.3	60.4	6.5
22	T BL profile	97.6	49.4	0.0	0.0	76.6	17.4	133	64.8	35.5	57.9	13.8
23	T Wen profile	108	60.8	0.0	0.0	94.9	21.4	116	81.6	44.6	77.0	14.0
24	D BL profile	127	94.7	0.0	0.0	144	32.5	162	117	85.7	157	31.2
25	D Wood profile	127	94.5	0.0	0.0	144	32.4	161	117	85.5	157	31.1
26	S above 15 m	84.6	63.5	0.0	0.0	94.7	22.0	96.7	71.7	58.1	101	21.9
27	S above h_1	80.1	60.3	0.0	0.0	88.9	20.8	82.6	63.8	56.2	96.8	21.0
28	Direct gust	144	96.4	0.0	0.0	149	33.2	174	127	82.7	153	27.7

Table 15: Maximum usage (%) in tension for the Peabody tower

No.	Name	LL	UL	BTX	BLX	WTX	WLX	HT	HL	TC	TX	P
1	S 30	50.0	53.2	27.1	52.2	81.4	7.8	3.0	0.0	40.2	63.4	13.7
2	S 35	69.5	74.1	36.8	72.9	110	10.5	4.1	0.0	55.2	84.2	13.6
3	S 40	92.1	98.2	48.1	96.8	143	13.5	5.3	0.0	72.7	108	17.7
4	T full	42.1	36.4	144	44.8	58.1	5.9	10.5	0.0	21.7	36.6	14.1
5	T below h_1	8.2	1.2	157	9.0	9.9	1.3	10.1	0.0	5.9	5.6	14.1
6	T 15°	63.0	48.4	162	60.6	68.4	15.4	24.7	3.2	25.3	36.4	16.1
7	T 30°	77.9	62.7	150	96.9	67.5	23.3	45.5	5.9	23.7	33.9	16.7
8	T 45°	84.1	71.0	129	127	63.6	30.3	63.6	8.0	23.8	30.3	17.3
9	T 60°	82.5	74.2	100	149	55.1	35.3	76.9	9.5	23.0	25.1	17.7
10	T 75°	74.0	72.5	72.4	159	42.5	38.7	84.4	10.2	20.5	20.2	17.8
11	T 90°	60.2	67.7	63.6	140	24.9	39.7	86.9	10.6	16.5	17.4	17.1
12	D full	80.2	83.8	44.4	85.0	123	11.8	4.0	0.0	60.8	91.7	14.3
13	D above 15 m	80.1	83.8	25.9	82.9	123	11.8	0.0	0.0	60.9	91.7	14.3
14	D above h_1	74.0	81.3	41.3	72.8	120	11.4	0.0	0.0	60.8	91.7	14.3
15	D 15°	86.3	86.4	64.2	83.5	121	15.9	4.1	2.4	58.6	86.8	15.7
16	D 30°	83.1	81.5	64.1	73.6	103	18.4	20.1	3.3	48.6	73.8	14.7
17	D 45°	71.5	69.3	59.1	71.8	77.5	19.7	33.3	4.0	34.5	54.7	15.2
18	D 60°	56.3	52.3	48.3	79.9	52.5	20.0	39.1	4.4	20.6	33.2	16.0
19	D 75°	40.6	37.9	34.9	83.4	30.6	19.7	41.1	4.7	13.3	16.3	16.3
20	D 90°	28.4	32.2	30.0	71.4	13.6	19.8	42.6	4.8	9.2	11.5	15.6
21	T lift	44.3	39.4	144	47.1	58.3	5.6	10.4	0.0	23.7	32.6	3.0
22	T BL profile	46.5	40.6	135	49.4	63.8	6.4	9.4	0.0	24.2	40.0	14.1
23	T Wen profile	60.4	52.1	108	62.0	79.5	7.9	6.4	0.0	31.4	49.5	14.1
24	D BL profile	83.5	86.8	38.0	87.9	127	12.1	3.2	0.0	62.9	94.5	14.7
25	D Wood profile	83.2	86.5	38.6	87.7	127	12.1	3.3	0.0	62.7	94.2	14.6
26	S above 15 m	51.8	55.3	19.8	52.6	84.3	8.1	0.0	0.0	41.7	65.5	13.6
27	S above h_1	47.2	52.0	27.6	46.0	80.0	7.7	0.0	0.0	40.2	63.4	13.7
28	Direct gust	90.7	88.5	121	96.4	129	12.4	10.0	0.0	60.8	90.9	13.3

Table 16: Maximum usage (%) in compression for the Wisconsin tower

No.	Name	LL	UL	BTX	BLX	WTX	WLX	HT	HL	HX	P
1	S 30	57.8	43.0	11.8	8.9	22.8	5.6	23.7	31.4	3.7	31.8
2	S 35	76.9	56.9	15.6	11.9	30.9	7.5	32.1	43.8	3.9	35.2
3	S 40	98.9	72.9	20.0	15.3	40.4	9.6	41.9	58.2	4.1	39.0
4	T full	69.7	32.6	20.8	7.0	22.6	5.0	58.9	31.8	3.9	25.0
5	T below h_1	54.9	12.7	22.6	2.8	14.0	2.8	60.7	20.2	3.8	25.0
6	T 15°	84.7	43.9	25.5	14.2	26.1	15.1	60.6	30.7	13.0	31.5
7	T 30°	96.5	51.2	25.9	20.6	26.1	22.7	55.9	36.2	15.6	37.4
8	T 45°	102	55.0	24.0	25.4	24.1	28.4	47.0	49.3	16.4	42.3
9	T 60°	102	55.4	20.5	28.5	20.4	32.3	36.5	59.0	16.3	46.0
10	T 75°	95.2	51.8	15.3	28.8	14.8	33.4	41.1	63.9	13.7	48.1
11	T 90°	84.8	43.7	11.0	24.6	6.5	30.7	42.6	62.1	4.0	48.6
12	D full	87.4	61.5	19.3	13.0	34.9	8.3	39.5	50.1	4.0	36.8
13	D above 15 m	74.8	61.5	17.0	13.1	34.9	8.3	14.3	46.7	3.9	36.8
14	D above h_1	62.6	57.8	10.8	11.9	28.1	7.1	8.9	38.7	3.9	36.4
15	D 15°	90.3	65.3	22.7	15.5	36.3	14.1	41.4	47.1	12.5	39.3
16	D 30°	87.3	61.2	21.1	17.1	31.9	16.8	37.2	38.9	13.2	40.1
17	D 45°	78.0	52.5	17.8	17.5	25.1	18.4	30.3	27.3	13.5	39.5
18	D 60°	66.0	41.6	13.1	16.8	16.9	18.5	21.1	31.1	11.8	38.3
19	D 75°	54.1	31.8	8.3	15.3	9.4	17.7	19.5	33.2	9.3	37.1
20	D 90°	45.8	24.5	6.3	12.5	3.4	15.8	20.3	31.9	3.8	36.4
21	T lift	67.9	30.3	21.4	6.8	22.5	4.9	58.9	33.1	1.7	9.6
22	T BL profile	72.9	35.7	21.7	7.7	24.7	5.5	57.8	34.6	3.9	25.1
23	T Wen profile	80.9	44.2	23.4	9.6	30.5	6.7	53.6	41.9	4.0	25.5
24	D BL profile	89.3	63.6	19.7	13.4	36.3	8.6	38.6	51.9	4.0	37.1
25	D Wood profile	89.2	63.4	19.8	13.4	36.1	8.6	38.7	51.7	4.0	37.1
26	S above 15 m	50.4	43.0	10.7	9.0	22.7	5.6	8.6	29.4	3.6	31.8
27	S above h_1	44.9	41.3	8.0	8.4	19.6	5.0	6.3	25.8	3.6	31.6
28	Direct gust	108	65.5	27.8	14.0	40.5	9.3	65.9	59.0	4.1	33.9

Table 17: Maximum usage (%) in tension for the Wisconsin tower

No.	Name	LL	UL	BTX	BLX	WTX	WLX	HT	HL	HX	P
1	S 30	16.8	20.6	16.2	10.4	10.0	2.3	5.8	2.7	0.0	6.0
2	S 35	23.6	28.8	22.0	14.6	13.7	3.2	5.7	3.5	0.0	6.0
3	S 40	31.4	38.2	28.8	19.4	17.9	4.3	5.6	4.5	0.0	5.9
4	T full	17.9	15.8	43.5	11.1	10.0	2.0	6.2	2.1	0.0	6.5
5	T below h_1	11.9	4.9	44.6	7.4	6.1	1.1	6.2	1.2	0.0	6.5
6	T 15°	26.3	18.9	44.1	17.6	10.0	5.9	6.4	2.1	1.2	6.7
7	T 30°	31.7	22.3	40.3	25.3	9.7	8.9	6.5	1.9	1.7	6.8
8	T 45°	34.1	24.3	33.7	34.9	9.0	11.2	6.6	1.5	1.9	7.0
9	T 60°	34.0	24.7	24.9	42.0	7.6	12.7	6.7	1.2	1.9	7.1
10	T 75°	30.3	23.7	20.9	45.8	5.5	13.6	6.8	1.0	1.3	7.1
11	T 90°	23.7	22.9	14.7	45.2	2.9	13.5	6.8	0.9	0.0	7.1
12	D full	27.1	31.9	26.9	16.8	15.5	3.6	6.1	3.9	0.0	6.4
13	D above 15 m	25.7	31.9	10.4	15.3	15.5	3.6	6.1	3.8	0.0	6.4
14	D above h_1	21.7	28.6	6.2	12.5	12.6	3.0	6.1	3.5	0.0	6.4
15	D 15°	30.5	30.6	27.8	19.7	15.3	5.4	6.2	3.7	1.0	6.5
16	D 30°	30.0	27.9	25.0	19.9	13.3	6.5	6.3	3.1	1.2	6.6
17	D 45°	27.0	22.8	20.4	18.4	10.3	7.2	6.4	2.4	1.3	6.7
18	D 60°	21.6	17.3	14.2	21.8	6.8	7.2	6.5	1.5	1.0	6.8
19	D 75°	16.0	12.6	10.3	23.5	3.6	7.0	6.5	1.0	0.4	6.8
20	D 90°	11.1	10.7	6.9	23.1	1.4	6.8	6.5	0.9	0.0	6.8
21	T lift	18.5	16.7	43.5	11.5	10.0	2.1	2.2	1.7	0.0	2.3
22	T BL profile	19.4	17.7	41.8	12.0	10.9	2.3	6.2	2.3	0.0	6.5
23	T Wen profile	23.2	22.9	36.6	14.4	13.5	2.9	6.2	2.7	0.0	6.5
24	D BL profile	28.0	33.1	25.7	17.3	16.1	3.8	6.1	4.0	0.0	6.4
25	D Wood profile	27.9	33.0	25.9	17.3	16.0	3.7	6.1	3.9	0.0	6.4
26	S above 15 m	16.3	20.6	6.2	9.5	10.0	2.3	5.8	2.7	0.0	6.0
27	S above h_1	14.4	19.1	4.4	8.3	8.8	2.1	5.8	2.6	0.0	6.0
28	Direct gust	32.5	34.9	47.1	20.1	18.0	4.1	6.0	4.0	0.0	6.2

Table 18: Maximum usage (%) in compression for the Canadian Bridge 0° tower

No.	Name	LL	UL	BTX	BLX	WTX	WLX	HT	HL	HX	TC	TX	P
1	S 30	46.2	30.6	117	158	69.1	36.2	14.2	49.7	14.2	54.3	108	27.4
2	S 35	60.7	40.4	143	211	95.8	47.1	20.5	74.1	17.7	87.1	156	30.2
3	S 40	77.6	51.7	172	271	127	62.7	27.8	102	20.5	125	211	33.3
4	T full	45.8	25.8	166	153	64.3	77.6	33.3	31.2	58.8	27.3	77.2	15.2
5	T below h_1	N/A	N/A	N/A	N/A	N/A	N/A	N/A	N/A	N/A	N/A	N/A	N/A
6	T 15°	58.0	35.0	213	209	63.3	174	40.1	31.8	62.5	23.5	75.2	17.4
7	T 30°	66.9	42.8	249	251	55.8	257	43.4	31.3	64.4	21.6	68.2	19.5
8	T 45°	71.8	48.4	270	277	43.9	325	43.3	37.7	64.8	21.7	56.6	21.1
9	T 60°	72.4	51.1	274	284	29.3	370	39.9	40.9	63.3	20.5	41.5	22.3
10	T 75°	68.6	50.9	260	273	16.9	392	33.8	41.2	60.5	18.6	45.3	22.9
11	T 90°	60.9	47.6	230	245	9.1	394	25.5	39.3	57.0	18.2	45.7	23.0
12	D full	63.6	41.4	153	220	102	56.8	24.2	76.8	31.0	85.2	161	31.1
13	D above 15 m	63.6	41.4	147	218	102	57.5	16.0	79.2	23.0	85.2	161	31.1
14	D above h_1	45.4	32.6	85.4	161	71.7	38.7	4.9	52.5	3.4	61.2	125	31.0
15	D 15°	67.1	44.2	173	238	96.7	105	27.4	71.8	34.0	76.7	150	31.7
16	D 30°	64.5	42.9	183	233	80.0	144	28.0	57.7	36.3	53.7	120	30.9
17	D 45°	57.5	38.7	182	212	56.9	173	26.2	38.4	37.8	24.2	79.0	28.7
18	D 60°	49.5	34.7	168	187	34.4	193	22.0	23.5	37.8	16.2	46.2	24.0
19	D 75°	41.7	30.7	150	161	15.4	202	16.9	22.6	35.9	13.2	23.1	20.2
20	D 90°	35.6	27.5	131	141	5.5	206	11.8	21.4	31.9	13.2	23.8	18.7
21	T lift	42.9	22.9	155	144	61.2	77.2	35.2	35.7	58.7	44.0	77.2	6.0
22	T BL profile	49.0	27.8	171	161	70.1	82.8	32.3	38.1	57.5	32.9	86.0	15.3
23	T Wen profile	55.6	32.0	181	180	82.3	95.0	30.1	51.2	53.4	43.9	103	15.5
24	D BL profile	65.9	43.0	155	228	106	59.2	23.5	81.5	29.6	90.5	169	31.4
25	D Wood profile	65.4	42.6	155	226	105	58.9	23.7	80.4	30.3	89.1	167	31.4
26	S above 15 m	46.1	30.6	112	158	69.1	36.5	9.3	50.6	8.9	54.3	108	27.4
27	S above h_1	36.8	26.4	77.1	129	53.8	31.5	3.1	36.2	2.5	44.7	93.5	27.4
28	Direct gust	50.4	28.2	168	170	74.5	79.6	36.4	46.1	58.7	55.1	101	11.5

Table 19: Maximum usage (%) in tension for the Canadian Bridge 0° tower

No.	Name	LL	UL	BTX	BLX	WTX	WLX	HT	HL	HX	TC	TX	P
1	S 30	24.5	13.4	8.8	11.1	24.9	3.8	6.7	18.0	0.4	15.4	35.0	16.3
2	S 35	37.4	22.2	11.8	16.8	34.6	5.2	8.4	24.5	0.5	19.7	45.6	16.4
3	S 40	52.2	32.5	15.3	23.3	45.8	6.6	10.3	32.1	0.6	26.0	57.9	16.4
4	T full	24.3	10.3	18.2	8.8	19.8	6.4	12.0	20.4	2.2	12.0	18.7	9.9
5	T below h_1	N/A	N/A	N/A	N/A	N/A	N/A	N/A	N/A	N/A	N/A	N/A	N/A
6	T 15°	34.8	17.9	17.9	14.7	20.6	13.9	14.4	20.4	3.1	12.1	18.4	10.6
7	T 30°	42.5	23.6	21.2	19.5	20.4	20.3	16.0	19.0	3.7	12.4	16.3	11.2
8	T 45°	46.8	27.2	22.6	23.0	19.0	25.1	16.6	16.3	3.9	12.2	14.9	11.7
9	T 60°	47.3	28.6	22.1	24.7	16.0	28.1	16.0	13.2	3.7	11.4	14.7	12.0
10	T 75°	44.2	27.7	20.0	24.4	11.8	31.2	14.3	13.0	3.0	9.9	15.6	12.1
11	T 90°	37.5	24.6	16.5	22.2	6.5	32.9	11.7	12.1	2.0	9.3	15.5	12.1
12	D full	39.8	23.8	13.4	17.8	36.0	6.2	9.4	26.4	1.0	21.5	44.6	17.6
13	D above 15 m	39.8	23.8	10.3	18.3	36.0	6.3	7.0	26.1	0.7	21.5	44.6	17.6
14	D above h_1	23.8	15.6	4.1	11.6	29.1	4.3	4.0	17.3	0.0	17.5	42.9	17.6
15	D 15°	43.0	25.9	13.4	19.7	33.9	10.0	10.4	25.3	1.5	20.5	42.2	17.9
16	D 30°	40.6	24.0	14.3	19.2	27.7	12.6	10.8	21.5	1.8	17.3	34.9	18.2
17	D 45°	34.5	19.9	13.8	17.0	19.5	14.3	10.5	16.0	1.9	15.6	25.5	17.6
18	D 60°	27.5	16.0	11.9	14.4	12.3	15.2	9.4	10.8	1.7	12.4	19.6	14.4
19	D 75°	20.6	12.3	9.5	11.8	6.1	16.1	8.0	7.3	1.5	9.9	15.4	11.8
20	D 90°	15.2	9.6	7.2	9.9	2.0	16.4	6.5	6.6	1.1	9.0	13.6	10.8
21	T lift	26.8	12.8	18.2	9.8	20.8	6.3	11.5	19.3	2.2	10.2	17.1	3.9
22	T BL profile	27.1	12.1	17.5	10.5	21.8	6.9	11.7	21.6	2.1	13.0	20.6	10.0
23	T Wen profile	32.8	15.8	16.1	13.8	26.0	8.0	11.2	24.4	1.9	14.9	24.3	10.1
24	D BL profile	41.9	25.3	13.0	18.9	37.6	6.5	9.1	27.4	1.0	22.4	46.4	17.6
25	D Wood profile	41.4	24.9	13.1	18.6	37.2	6.4	9.2	27.1	1.0	22.2	46.0	17.6
26	S above 15 m	24.4	13.4	6.1	11.3	24.9	3.8	5.3	17.9	0.2	15.4	35.0	16.3
27	S above h_1	16.3	9.6	3.3	8.0	22.1	3.3	3.6	13.9	0.0	15.5	34.9	16.4
28	Direct gust	31.9	16.0	19.0	12.1	24.8	6.8	12.1	22.5	2.2	12.9	23.9	7.4

Table 20: Maximum usage (%) in compression for the Canadian Bridge 15° tower

No.	Name	LL	UL	BTX	BLX	WTX	WLX	HT	HL	HX	TC	TX	P
1	S 30	19.5	19.2	17.6	42.8	65.7	8.5	8.4	5.3	1.5	19.3	100	16.5
2	S 35	24.7	23.8	21.4	53.7	88.9	9.9	10.6	7.5	1.9	29.2	117	20.8
3	S 40	30.7	29.2	25.9	66.2	118	11.4	13.2	10.1	2.3	40.7	136	25.9
4	T full	23.0	21.2	26.9	52.4	78.2	10.2	21.4	8.0	6.4	22.7	93.1	74.5
5	T below h_1	21.3	19.5	26.8	48.9	71.2	10.2	22.8	7.3	6.4	18.1	86.1	59.4
6	T 15°	27.6	25.4	33.2	73.1	72.4	32.6	20.0	14.6	7.1	19.7	100	72.7
7	T 30°	30.4	34.8	44.7	82.4	123	65.7	199	22.0	7.8	38.2	162	65.1
8	T 45°	31.5	35.1	46.6	95.3	106	89.7	171	29.1	8.0	34.3	155	79.7
9	T 60°	31.1	33.6	45.2	103	79.5	107	117	35.2	7.5	27.6	134	95.4
10	T 75°	28.9	31.1	41.5	104	49.5	117	45.6	39.5	6.8	20.5	105	104
11	T 90°	24.7	27.7	36.9	97.1	25.3	122	23.7	40.0	6.1	16.4	95.5	106
12	D full	28.6	27.2	24.5	62.5	107	7.7	9.5	9.8	3.7	37.7	100	39.3
13	D above 15 m	27.4	27.0	18.8	58.5	105	14.0	9.1	9.2	0.8	37.7	100	39.3
14	D above h_1	20.5	20.8	14.1	44.3	76.4	10.0	5.0	6.1	0.7	25.3	75.8	17.7
15	D 15°	30.1	28.3	26.9	71.0	101	20.2	9.3	9.2	3.9	34.7	98.8	38.3
16	D 30°	28.9	27.5	28.0	73.9	87.2	35.8	9.0	13.2	4.0	26.3	94.4	35.1
17	D 45°	25.4	30.4	33.9	66.3	114	52.6	136	15.5	4.6	33.8	136	39.9
18	D 60°	22.3	25.0	29.1	64.6	70.5	60.0	79.5	18.6	3.8	21.7	94.2	47.7
19	D 75°	18.2	19.7	25.2	60.7	33.9	63.7	22.1	20.6	3.8	12.5	65.3	52.1
20	D 90°	15.1	16.9	21.9	55.7	14.4	64.7	14.3	21.1	3.5	8.8	57.8	52.9
21	T lift	21.8	19.4	25.2	50.1	78.8	9.6	22.3	8.3	6.4	26.3	89.3	74.7
22	T BL profile	24.3	22.5	27.0	54.8	84.2	9.5	17.7	8.4	5.5	25.4	99.4	82.5
23	T Wen profile	27.1	25.4	26.6	60.0	98.9	7.4	9.2	9.2	3.7	32.0	114	102
24	D BL profile	29.3	27.9	24.6	63.8	111	7.5	8.0	10.1	3.2	39.3	104	43.2
25	D Wood profile	29.3	27.9	24.6	63.7	110	7.6	8.1	10.1	3.3	39.1	103	42.1
26	S above 15 m	18.8	19.0	14.6	41.1	65.7	10.9	4.6	5.2	0.5	19.3	100	16.5
27	S above h_1	16.3	16.8	12.7	36.1	56.2	7.9	4.7	4.0	0.5	15.1	85.7	11.9
28	Direct gust	31.5	29.0	31.4	70.2	120	11.0	17.7	11.9	6.5	40.4	117	73.8

Table 21: Maximum usage (%) in tension for the Canadian Bridge 15° tower

No.	Name	LL	UL	BTX	BLX	WTX	WLX	HT	HL	HX	TC	TX	P
1	S 30	8.4	4.7	0.9	2.8	22.5	1.8	1.3	4.5	0.1	20.8	19.0	11.7
2	S 35	12.9	8.1	2.2	4.3	30.1	1.8	1.4	5.9	0.1	26.6	24.7	11.7
3	S 40	18.2	12.0	3.8	5.9	38.9	2.4	1.6	7.6	0.2	33.3	31.3	14.0
4	T full	11.5	6.3	5.5	3.8	28.4	2.6	3.2	3.9	0.7	21.5	20.6	11.0
5	T below h_1	10.0	5.0	5.5	3.4	26.2	2.6	3.2	3.5	0.7	18.8	18.0	11.0
6	T 15°	15.4	8.8	7.8	6.8	29.5	6.1	3.3	4.1	1.0	22.4	20.0	11.0
7	T 30°	18.2	20.5	6.8	10.3	57.0	8.6	2.9	3.5	1.1	44.4	33.1	11.1
8	T 45°	19.4	20.5	8.2	11.6	48.9	11.9	2.6	4.7	1.1	38.3	28.2	11.1
9	T 60°	18.8	18.6	8.7	12.1	36.5	14.4	2.3	5.5	1.1	29.5	20.6	11.0
10	T 75°	16.6	15.8	8.3	11.7	22.5	15.9	1.9	5.8	0.9	19.9	12.5	11.0
11	T 90°	13.3	13.6	6.6	10.6	11.7	16.3	1.3	5.7	0.7	12.9	14.6	11.0
12	D full	16.3	10.6	3.6	5.5	36.0	2.3	1.6	6.2	0.4	30.1	29.0	11.6
13	D above 15 m	15.2	10.3	1.5	5.2	33.9	2.3	2.5	6.7	0.0	30.2	29.0	11.6
14	D above h_1	9.2	5.8	0.4	3.3	23.9	2.3	1.5	4.7	0.0	22.8	21.8	11.5
15	D 15°	17.4	11.3	4.6	6.8	35.2	3.2	1.6	6.1	0.5	29.1	27.6	11.1
16	D 30°	16.5	10.3	5.0	7.3	31.1	4.8	1.7	5.3	0.6	26.1	23.7	10.9
17	D 45°	14.4	17.3	2.4	7.9	49.1	6.8	1.5	3.4	0.5	40.2	30.6	11.0
18	D 60°	10.5	11.4	2.7	7.0	30.0	7.3	1.5	2.9	0.6	26.0	17.2	11.0
19	D 75°	7.3	6.9	2.6	5.8	14.9	8.1	1.4	2.9	0.5	14.5	7.9	10.9
20	D 90°	4.8	4.8	1.7	4.9	7.5	8.4	1.1	2.8	0.3	10.0	9.1	10.9
21	T lift	12.5	7.6	6.2	4.1	28.1	2.6	3.2	3.7	0.7	19.3	19.1	12.1
22	T BL profile	12.6	7.2	5.2	4.2	30.2	2.5	3.0	4.4	0.6	23.1	22.2	11.0
23	T Wen profile	15.0	9.2	4.2	5.0	34.2	2.4	2.4	5.5	0.4	27.0	26.0	11.0
24	D BL profile	16.9	11.1	3.4	5.7	37.0	2.3	1.5	6.5	0.3	31.0	29.9	11.6
25	D Wood profile	16.8	11.0	3.4	5.7	36.9	2.3	1.5	6.4	0.3	30.9	29.8	11.7
26	S above 15 m	7.8	4.6	0.2	2.6	21.3	1.8	1.9	4.5	0.0	20.8	19.0	11.7
27	S above h_1	5.6	2.9	0.0	1.9	17.6	1.8	1.5	3.7	0.0	18.3	16.6	11.7
28	Direct gust	19.0	12.1	6.9	6.2	40.6	2.7	2.9	6.2	0.7	31.7	30.6	10.7

Table 22: Total horizontal wind force (kN) in longitudinal and transverse directions

		PB		WI		CB0		CB15	
No.	Name	Long.	Trans.	Long.	Trans.	Long.	Trans.	Long.	Trans.
1	S 30	0.0	82.5	0.0	97.3	0.0	435	0.0	380
2	S 35	0.0	112	0.0	132	0.0	592	0.0	518
3	S 40	0.0	147	0.0	173	0.0	774	0.0	677
4	T full	0.0	141	0.0	155	0.0	655	0.0	633
5	T below h_1	0.0	106	0.0	135	N/A	N/A	0.0	606
6	T 15°	41.7	136	46.1	150	202	632	188	612
7	T 30°	80.6	122	89.0	134	390	567	364	549
8	T 45°	114	99.5	126	109	551	463	514	448
9	T 60°	140	70.4	154	77.4	675	327	630	317
10	T 75°	156	36.4	172	40.1	753	169	703	164
11	T 90°	161	0.0	178	0.0	779	0.0	727	0.0
12	D full	0.0	133	0.0	154	0.0	648	0.0	637
13	D above 15m	0.0	98.3	0.0	106	0.0	539	0.0	492
14	D above h_1	0.0	78.9	0.0	85.6	0.0	318	0.0	332
15	D 15°	21.3	126	23.5	146	103	615	96.1	605
16	D 30°	41.2	108	45.4	124	199	524	186	515
17	D 45°	58.2	81.2	64.2	93.2	281	393	262	385
18	D 60°	71.3	51.1	78.7	58.2	344	245	321	240
19	D 75°	79.5	22.7	87.7	25.4	384	107	358	105
20	D 90°	82.3	0.0	90.8	0.0	398	0.0	371	0.0
21	T lift	0.0	141	0.0	155	0.0	655	0.0	633
22	T BL profile	0.0	141	0.0	155	0.0	655	0.0	633
23	T Wen profile	0.0	141	0.0	156	0.0	655	0.0	633
24	D BL profile	0.0	133	0.0	154	0.0	649	0.0	638
25	D Wood profile	0.0	133	0.0	154	0.0	649	0.0	638
26	S above 15 m	0.0	62.9	0.0	68.4	0.0	368	0.0	303
27	S above h_1	0.0	51.6	0.0	59.4	0.0	249	0.0	242
28	Direct gust	0.0	188	0.0	212	0.0	713	0.0	820

5.2 Comparison of Tower Response to Load Cases and Discussion

Dividing tower members into groups allowed rapid identification of the critical load cases. Also, it was necessary to look at the axial forces on each individual member to see which member of each group was actually critical. Each of the following subsections discusses the results of a small number of load cases. For a particular load case, a member is defined as critical if its percentage of usage is significantly higher than for the other load cases, or if its percentage of usage is above 100%.

One general observation from Tables 14 to 21 is that for the BTX members, the PB and WI towers have higher use factors in tension, while the CB0 and CB15 towers have higher use factors in compression. This result is expected since the tension-only modeling assumption for the BTX members in PB and WI actually removes the possibility for these members to take up any compressive load even below their buckling capacity. For CB0 and CB15, the compression diagonals are allowed to take up loads. The results shown in Table 18 for the compression use factors of the CB0 tower indicate that the diagonal bracing members below the waist (BTX and BLX) have been designed as tension-only. Therefore, for the lower bracing members, the usage in compression for the CB0 tower cannot be compared to the usage in compression for the PB and WI towers.

5.2.1 Synoptic Loading Versus Tornado Loading

This first group of load cases discussed is composed of "Synoptic 30", "Tornado full", and "Tornado below h_l". Despite their different wind speeds and loading models, it is interesting to compare results of the tornado load cases and the traditional synoptic load case to identify which members might need to be reinforced to sustain such tornado loadings.

Compared to "Synoptic 30", "Tornado full", which applies a much higher total force on the system, creates similar forces in the main legs (including the main members above the tower waist). The most significant increase for the main leg members is seen in the lower portion of the Peabody tower where the usage in compression increases from 82% to 93%. As expected, for "Tornado below h_l", the forces in the main leg members drop significantly. Most critical members for the tornado load cases are diagonal and horizontal bracings located in the lower portion of the towers. Some of them undergo very large increases in axial force and would certainly need to be changed to resist localized HIW effects. Figure 37 shows use factors in some critical members of the Peabody tower. Note that the use factors shown in this figure are for the specific members identified and do not necessarily match the values shown in Tables 14 to 21 which represent extreme values obtained for each member group.

PB

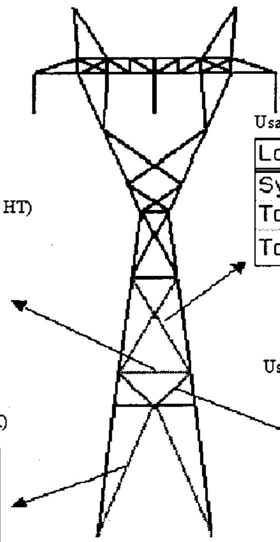

Usage in compression of member H2T (group HT)

Load case	% usage
Synoptic 30	28.5
Tornado Full	141
Tornado below h_1	156

Usage in tension of member LDT (group BTX)

Load case	% usage
Synoptic 30	27.1
Tornado Full	144
Tornado below h_1	157

Usage in tension of member X1T (group BTX)

Load case	% usage
Synoptic 30	10.7
Tornado Full	42.8
Tornado below h_1	57.9

Usage in tension of member VT (group BTX)

Load case	% usage
Synoptic 30	18.7
Tornado Full	116
Tornado below h_1	129

Figure 37: Critical members under tornado loadings for the Peabody tower

It is seen in Figure 37 that for the Peabody tower, "Tornado below h_l" is more critical than "Tornado full". However, for the other three towers, the "Tornado full" load case yields higher forces. For example, in the CB15 tower, not a single member has a significantly higher axial force for "Tornado below h_l". For this tower, critical members under "tornado full" are not limited to transversal bracing. They include diagonal members in the ground-wire peak, horizontal X-bracing in the tower truss, and transversal bracing above the tower waist. Of the members that have a larger load under "Tornado full", none reach the 100% usage limit.

In all, the tower forces under tornado loading were as expected. These load cases affect mostly the bracing members in the bottom part of the tower because the location of the resultant wind force applied to the system is lower than for the loadings where wind on conductors is considered. Even for a very high wind speed of 70 m/s, almost all the members would resist the tornado load case in the transverse direction, and only a few members would need reinforcement. With such a high wind speed, it could be necessary to verify if redundant members could support the bending moments associated with high wind pressures in the windward face. "Tornado below h_l" is not critical enough to justify a change of the basic tornado loading. Also, this type of loading is unlikely to occur during a tornado event. "Tornado full" loading highlights the need for stronger bracing systems in classical self-supporting towers. The tension-only assumption in the design of bracing members should be avoided in order to increase tower resistance against tornadoes and any other type of non-synoptic wind events.

5.2.2 Varying Direction of Tornado Loading

This section compares axial forces for tornado loadings over the full height of the structure applied in various directions. The "Tornado full" load case, which is in the transverse direction, and six other load cases varying from 15° to 90° with respect to the transverse axis of the tower are analyzed to identify the critical directions for tornado loadings.

A first observation from Table 22 is that the total wind force on the structure is highest for the longitudinal load case (90°) since there is more drag area in the longitudinal faces of all the towers studied. This is typical of self-supporting towers. For tornado loadings, the drag area of conductors, which is maximum in the transverse direction, does not affect the total wind force. However, the difference in total wind force for longitudinal and transverse loadings is small, and the longitudinal load case is not critical for all members.

The critical wind direction for a given member mostly depends on the member position in the tower. For example, as shown in Figure 38, the loading is critical at an angle of 45° for the main legs. In lean towers such as the Peabody model, where the main leg members almost reach their capacity limit under a moderate synoptic wind, those leg members will be too weak to resist a tornado load of 70 m/s at an angle of 45° on the structure only. These towers are typically found in regions where atmospheric icing of conductors is not a design consideration. In that case, structural changes required to make the tower HIW-resistant would be very costly. Similarly, if changes are required to the foundations due to the very high tornado total wind force, the consideration of this loading could also be very costly. It should be emphasized that the tornado wind speed of 70 m/s selected for these simulations is very high: in most regions, a lower tornado design wind speed is appropriate. In this context, increasing the overall reliability of towers at low cost will be possible if the necessary design changes are limited to diagonal bracing members. However, the simplified tornado loading suggested only covers for the situation where an extremely narrow horizontal wind force is applied to the structure. The decision to consider severe tornado loads in design must be justified either by a history of tornado-related line failures in the region, or by successful tornado-resistant design practices in other regions with similar climates.

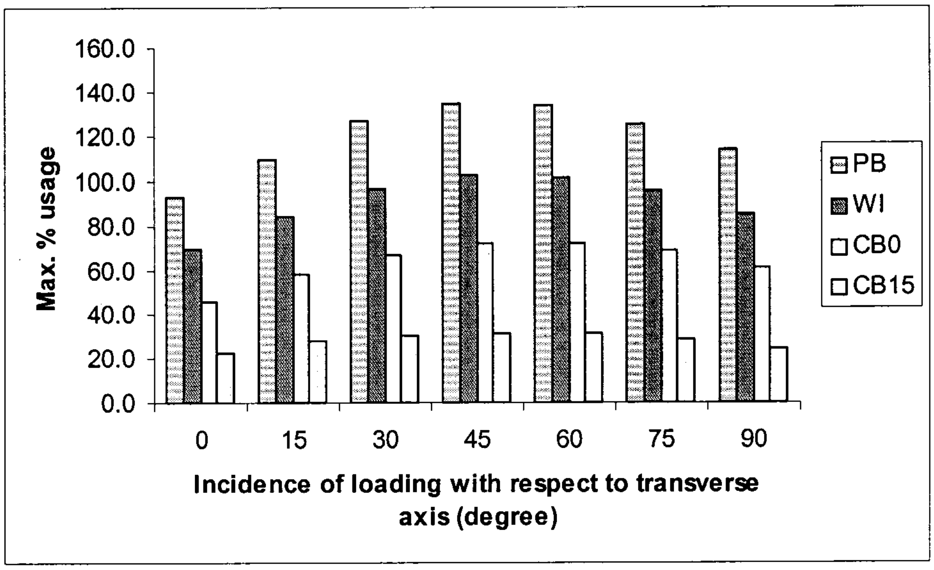

Figure 38: Maximum usage in compression in the main legs below the waist for various tornado loading directions

As expected, transverse bracing members take generally higher wind forces when the wind is applied transversally, whereas longitudinal bracing members are often critical for wind applied longitudinally. This can be seen in Tables 14 to 21 where maximum usage in the transversal members is highest for the transverse (Tornado full) and the 15° load cases. On the other hand, maximum usage for the longitudinal members is in general highest for the load cases "Tornado 75°" and "Tornado 90°". It is therefore crucial to apply the tornado load case in a number of directions. Based on the towers studied, it would seem reasonable for example to apply a tornado load case in three different directions: transversally, at 45°, and longitudinally. This should cover critical loads for all the members.

5.2.3 Synoptic Loading Versus Downburst Loading

This section compares synoptic loadings of 30, 35 and 40 m/s to the following three downburst load cases: "Downburst full", "Downburst above 15 m", and "Downburst above h_l". Both the synoptic and downburst loadings are applied to the conductors and the supports. The fundamental difference between the proposed downburst loadings and the synoptic wind loadings is that the design wind speed for downbursts is converted to horizontal pressures without the application of gust response factors and height adjustment associated with boundary layer winds. This section also includes comments on the "Synoptic above 15 m" and "Synoptic above h_l" load cases, which allow direct comparison with the "Synoptic 30" load case.

Table 23: Maximum usage (%) under synoptic and downburst loadings for the Wisconsin tower

No.	Name	LL	UL	BTX (*)	BLX (*)	WTX	WLX	HT	HL
1	S 30	57.8	43.0	16.2	10.4	22.8	5.6	23.7	31.4
2	S 35	76.9	56.9	22.0	14.6	30.9	7.5	32.1	43.8
3	S 40	98.9	72.9	28.8	19.4	40.4	9.6	41.9	58.2
12	D full	87.4	61.5	26.9	16.8	34.9	8.3	39.5	50.1
13	D above 15m	74.8	61.5	10.4	15.3	34.9	8.3	14.3	46.7
14	D above h_1	62.6	57.8	6.2	12.5	28.1	7.1	8.9	38.7
26	S above 15 m	50.4	43.0	6.2	9.5	22.7	5.6	8.6	29.4
27	S above h_1	44.9	41.3	4.4	8.3	19.6	5.0	6.3	25.8

(*) Use factor for tension in BTX and BLX. Results for all other member groups are for compression

Table 23 shows the maximum usage (in %) in compression (in tension for BTX and BLX) for some groups of members of the Wisconsin tower. The "Downburst full" load case is nearly equivalent to a severe synoptic load case in terms of the distribution of axial forces. In Table 23, the maximum percentage of usage is slightly lower for "Downburst full" compared to "Synoptic 40" in all the member groups compared. Among the three downburst loadings studied, "Downburst full" yields higher loads in most members for all four towers. For the "Downburst above 15 m" load case, the load is often similar to the "Downburst full" load case, especially in member groups located in the upper portion of towers such as UL, WTX, and WLX. In most of the members located below the tower waist, the axial forces are significantly higher for "Downburst full". Similarly, the "Synoptic 30" load case is more critical than "Synoptic above 15 m" and "Synoptic above h_l" for most of the members in the WI and CB0 towers. For the PB and CB15 towers, the percentage of usage is generally higher by less than 5% for "Synoptic above 15 m" compared to "Synoptic 30".

"Downburst above h_l" loads only a small portion of the structures, and most members take lower axial forces than for the other downburst load cases. However, since the load paths are different, a few members are critical for this loading. In the Peabody tower, a few horizontal and diagonal bracings near the waist in the transverse face receive high loads under "Downburst above h_l". The CB15 tower has a large number of members taking higher loads under this same load case. As shown in Figure 39, the load in three members increases very significantly and reaches 100% usage. The first two members are X-braces in the truss and bracing members just below the truss. Those have limited capacity in compression and, due to their elevated position in the tower, are greatly affected by wind applied only in the top portion of the structure and on the conductors.

The other critical member is a horizontal member located just above the waist that becomes loaded in compression under "Downburst above h_l". Under synoptic loading, this member usually takes tension forces: its very low compression capacity results in a very high percentage of usage for the "Downburst above h_l" loading.

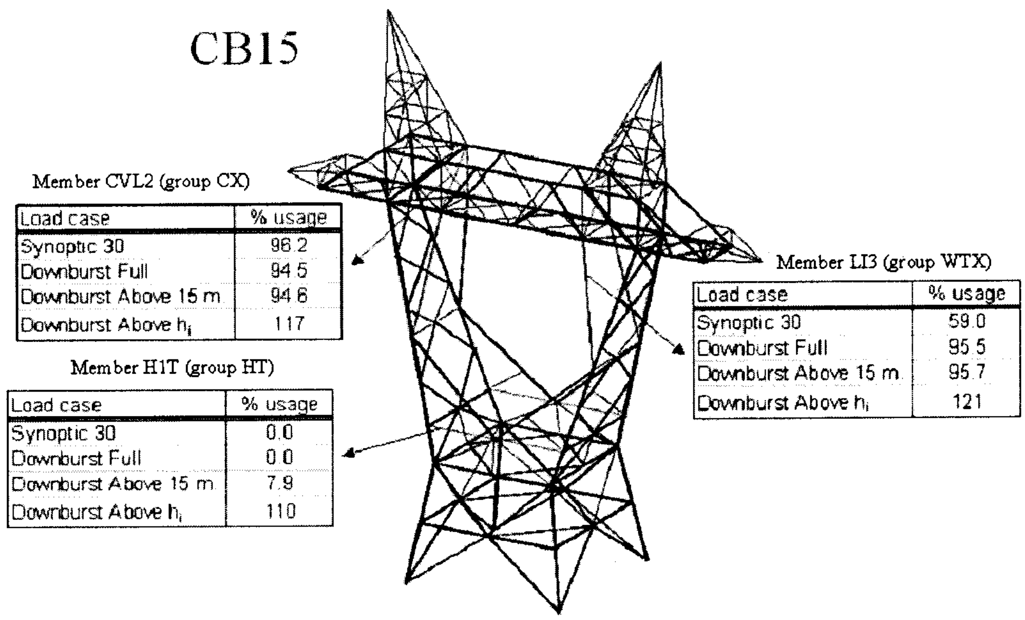

Figure 39: Critical members (in compression) of the Canadian Bridge 15° tower under the "Downburst above h_l" loading case

The critical members in CB15 illustrate the vulnerability of some towers under loads different from the traditional synoptic loading. In the following sections, the same members with low compression capacity will be mentioned since they are also critical under other types of non-conventional loads. Tower designers need to be aware that extreme wind loading events vary significantly, and that members with low capacity in compression can rapidly become critical under non-synoptic wind events.

The "Downburst above 15 m" does not change axial forces enough to be considered as a design load case. The "Downburst above h_l" affects severely only a few weak members. If slender members with low compression capacity are avoided, this load case will not be critical. This load case can still be useful to designers since it is very different from conventional wind loadings. Also, it might be critical for guyed towers. Applying wind on the full structure for downbursts seems more reasonable knowing the physical characteristics of downbursts. However, the load path is the same for the "Downburst full" and synoptic loadings. Hence, "Downburst full" might not be relevant since synoptic load cases are already applied to the tower. A valid option is to use a similar procedure for downburst winds and synoptic winds, as suggested in the Australian standards (ENA, 2006), while using design wind speeds from separate statistical databases. The disadvantage of this approach is that most of the factors derived for the synoptic wind procedure do not apply to downburst winds. Also, for codes such as the IEC 60826 (2003), where the averaging period of wind speeds is 10 minutes, it is difficult for the designer to select rationally a downburst design wind speed. In most instances, only a few downburst records or damage analyses are available, even for regions where downbursts frequently occur. Until more knowledge is available on the effect of downbursts on overhead lines, the

"Downburst full" load case is deemed adequate to complement the synoptic wind loading.

5.2.4 Varying Direction of Downburst Loading

The "Downburst full" load case was compared to equivalent loads applied at angles varying from 15° to 90° with respect to the transverse axis. From Tables 14 to 21, it is observed that the usage of members decreases with increasing angles for most groups of members. This is due to the wind force on the conductors which is very high for transverse wind, but negligible for longitudinal wind. Hence, the "Downburst full" and the "Downburst 15°" load cases govern for a large majority of the members in all four towers. However, as shown in Table 24 for the CB0 tower, a number of bracing members in the longitudinal face are critical under "Downburst 90°". All the members shown in the table are longitudinal X-bracings between the waist and the tower truss. WX1LP is closer to the truss and WX7LP is closer to the waist. Members closer to the waist are particularly critical. The three other towers have similar but less critical response under longitudinal loading. These results indicate that for downburst loadings, the assumption that transverse wind is the governing load case is not always valid. The same warning could be made for synoptic wind loading, especially for suspension towers with low longitudinal strength.

Table 24: Percentage of usage in compression of longitudinal bracing members in the CB0 tower under downburst loadings

Member name	S30	D full	D 15°	D 30°	D 45°	D 60°	D 75°	D 90°
WX1LP	20.4	30.0	46.3	58.3	65.8	69.3	70.1	69.6
WX2LP	8.2	1.5	0.0	15.6	37.5	56.1	69.0	73.7
WX3LP	18.9	30.8	48.5	62.2	71.3	76.1	77.6	77.7
WX4LP	12.6	0.8	0.0	30.3	61.6	88.9	108	116
WX5LP	22.0	1.7	42.2	79.8	112	136	152	157
WX6LP	12.9	28.0	57.4	81.8	100	113	120	122
WX7LP	36.2	53.8	70.3	118	157	185	201	206

The CB15 tower is a dead-end structure and the effect of longitudinal wind on this tower is limited. Dead-end structures have larger longitudinal strength since they are designed to resist the load of conductors from each side of the tower independently. However, a dozen members reach their peak axial force when the downburst loading is at an angle 45° with the transverse axis. Among those are the three members described in Figure 39. Those are once again very critical under this particular load case due to very low compression capacity.

Overall, even though the downburst loading applied transversally is critical for most members, the direction of this load case should still be varied. As proposed for tornado loading, the downburst loading can be applied at 0°, 45° and 90° to ensure all members can resist such conditions.

5.2.5 Neglecting the Self-Weight of Conductors in Tornado Loading

The "Tornado full" load case was compared to "Tornado lift" to investigate the effect of neglecting the self-weight of conductors in tornado loadings. This test was based on the suggestion made in the ASCE Manual 74 (1991) that conductors could be lifted due to large upward wind forces produced in tornadoes. For a Cardinal conductor with a length of 175 m (half the wind span of the Peabody tower), this uplift represents a vertical wind force of more than 3 kN. The tornado wind field model and the parameters for a severe tornado (F3) presented by Wen (1975) were used to perform simple calculations of upward forces during tornadoes. Assuming the tornado is centred at the support, the wind force over 175 m for that particular event is lower than 2 kN. Therefore, it is unlikely that the upward forces during a tornado are large enough to compensate for the whole self-weight of conductors. Moreover, the simulations indicate that most members have slightly higher loads under the "Tornado full" load case where the weight of conductors is not neglected than for the "Tornado lift" load case. This is observed in Tables 14 to 21. Only a few members of each tower are more severely loaded under "Tornado lift", but none reaches the 100% usage level. Generally, those members are part of the top portion of the towers or longitudinal bracings. For example, in the Peabody tower, the X-bracing members from the transverse face in the tower truss see an increase in their usage by up to 10% when neglecting the self-weight of conductors. In all, the "Tornado lift" load case does not need to be applied since conductors are unlikely to be completely lifted, and it is not more critical than the "Tornado full" load case for self-supporting towers.

5.2.6 Varying Wind Profile of Tornado Loading

The "Tornado full" loading was compared to the "Tornado BL profile" and "Tornado Wen profile" load cases to verify whether the assumption of a uniform wind profile is adequate for tornado loadings. As shown previously in Figure 33, the comparison is relevant since the total wind force is equivalent for these three load cases. The most severe case for the top portion of the towers is the "Tornado Wen profile". This load case is probably not representative of all tornado events, but the results are still useful to assess the effect of wind profile changes on the axial forces within tower members.

For most members, the "Tornado Wen profile" load case produces larger forces in the tower members. However, as shown in Tables 14 to 21, some bracing members have higher forces under the "Tornado full" load case. For example, in the BTX group of the PB tower, the use factor is 144% in tension for "Tornado full" and 108% for "Tornado Wen" (see Figure 15).This is particularly true for the bracing members in the bottom part of the towers. This illustrates the same concept mentioned in Section 5.2.1 where synoptic and tornado loadings are compared: when the resultant wind force on the tower is located at a lower height, the lower bracing components receive larger loads and the main members receive smaller loads. Therefore, applying a uniform tornado wind pressure with height underestimates the forces in the main leg members and overestimates the forces in the bracing members. This may turn out to be a good design compromise as the main leg members are likely to be governed by other loads than tornadoes.

To obtain the same total wind force for the "Tornado Wen profile" as for the "Tornado full" load case, a very high wind speed was applied at the top of the tower (over 80 m/s for the CB0 tower). This wind speed could only be produced in very severe tornadoes and hence, the importance of underestimating the main member forces in "Tornado full" is limited. Therefore, unless better load modeling is possible with the availability of detailed tornado parameters for a region, the uniform profile of wind is adequate for tornado loadings.

5.2.7 Varying Wind Profile of Downburst Loading

In this section, the effects of changing the wind profile for downburst loadings were studied. As for profile changes in tornado loadings (see previous section), the average forces in the main leg members and the bracings depend on the location of the resultant wind force. The profile from Wood et al. (2001) is similar to the boundary layer profile, but has slightly more wind pressure at low altitude as shown in Figure 34. Hence, axial forces are higher in the main leg members for the "Downburst BL profile" load case and are higher in the transverse bracing members below the waist for the "Downburst full" load case. The results in Tables 14 to 21 also indicate that the choice of the wind profile has less impact on the percentages of usage for downburst loadings than for tornado loadings.

From these results, a uniform profile of wind seems adequate for downburst loadings. The profile suggested by Wood et al. (2001) could be interesting after further validation. However, the main characteristic of this profile is its high wind speed at low altitude, and therefore a simpler uniform profile can produce realistic results.

5.2.8 Direct Gust Wind Loading

This last HIW load case is very severe because the 70 m/s wind speed of the tornado load cases is applied not only to the structure but also to part of the conductors over a width of 160m. These values of wind speed and path width correspond to the upper limits of the F2 tornado. Because of its high wind speed, this is a very severe loading.

In terms of the loading paths, the "Direct gust" load case is an intermediate between a severe synoptic wind load case (S40) and a tornado loading (T full). An important advantage of the "Direct gust" wind loading method as proposed in Behncke & White (2006) is that the designer can make a rational decision for the wind speed to apply to the system. This approach eliminates the problem of extrapolating from incomplete statistical data and does not rely on complex wind models that might not apply to the type of gust winds encountered in the region of the line. However, with this method, one could easily apply unrealistically large forces to the system if the wind speeds are too large. The most difficult parameter to evaluate is the path width of the wind storm.

6 Conclusions

A number of simplified load cases to account for localized HIW on overhead transmission lines were discussed. The tornado loading proposed by some authors (ASCE, 1991, 2005; Behncke & White, 1984; Behncke et al., 1994; Ishac & White, 1995) and consisting of applying a strong uniform horizontal wind pressure on the full height of the tower and no pressure on the conductors is critical for the bracing system of self-supporting towers. The loading needs to be applied in a number of different directions including the transverse and longitudinal directions in order to identify the critical members. The suggestion of the ASCE Manual 74 to neglect the self-weight of conductors for this loading has little effect on the axial forces for the four towers studied and its implementation is not recommended. Therefore, the author's final recommendation for the tornado loading cases is to consider a uniform horizontal wind speed profile in at least three orientations (longitudinal, transverse, and oblique at 45°) with conductor self-weight and tension. The wind is considered on the tower only and the resulting pressure load is calculated with a drag factor appropriate to the tower geometry. Wind speeds corresponding to an F2 tornado (maximum wind speed between 50 and 70 m/s) are appropriate for this tornado loading in the regions affected by this type of storm. This load case needs further validation through analysis of tower failures under tornadoes.

Severe downbursts apply high wind pressures to both the line supports and the conductors. The approach of the Australian standards (ENA 2006) is deemed adequate in the absence of validated loading models specific to downbursts. It consists of using the conventional wind loading calculation procedure with design wind speeds based on specific statistical analysis of downbursts rather than derived from synoptic wind observations. Another possible option is to use a uniform horizontal wind speed applied to both the conductors and the support, without adjustment with height: this allows the designer to make a rational decision on the downburst design wind speed in the case that limited information on previous downburst events is available. Like tornado loadings, downburst loadings should also be applied in several directions to identify critical members.

Applying non-conventional load cases on transmission lines highlighted the vulnerability of slender members with very low compression capacity: the tension-only assumption used sometimes for the design of bracing members should be avoided. Load paths in the tower can vary considerably for what appear as only slightly different load cases. Also, extreme wind loadings certainly differ from one storm to another and the design challenge is to ensure that all the members resist safely a large number of very diverse wind loading conditions.

The scope of the study had to be limited and the analysis was restricted to self-supporting towers. It would also be interesting to study the effect of HIW loadings on guyed towers of various geometries where the lattice masts always actively participate in the resistance to lateral loads, unlike the main legs in lattice towers.

Another important limitation in the project was that the knowledge available on the wind flow during downbursts is still limited compared to the knowledge on tornadoes or synoptic winds. As mentioned earlier, the linear analyses performed in this study do not represent accurately the behaviour of towers under failure conditions. Nonlinear analyses could give more details on the effect of HIW on transmission structures. More importantly, future work should include the participation of utilities. The load cases need to be applied on specific towers in a particular region. Only the utilities can judge on how useful HIW load cases can be for their structures.

For transmission line engineers, the first step towards dealing properly with localized HIW effects is to recognize that present design codes and their traditional wind loading methods do not cover such localized storms. Next, it is important that the statistical analysis of downburst, tornado, and synoptic wind events be done separately for a rational reliability-based design approach. In the absence of statistically significant observations, deterministic values of wind speeds may be selected which reflect the vulnerability of the area to a credible extreme storm. Changes to wind design practices may become necessary only if a genuine hazard of localized HIW storms is identified. Otherwise, the traditional synoptic wind design approach is sufficient. Extensive and costly mitigation on existing overhead line supports may be difficult to justify considering the many uncertainties and limited knowledge on the effects of localized HIW storms, whereas design of new lines can more easily integrate HIW-resistant load cases.

When the hazard is real and its mitigation impractical, security measures can be implemented in order to reduce the risk of cascading failures following the collapse of a support and to ensure rapid recovery of the network.

References

American Society of Civil Engineers. (1991). *Guidelines for electrical transmission line structural loading* (No. 74). New York.

American Society of Civil Engineers. (2002). *Minimum design loads for buildings and other structures* (No. 7). Reston, VA.

American Society of Civil Engineers. (2005). *Guidelines for electrical transmission line structural loading, draft revision* (No. 74). New York.

Battan, L. J. (1984). *Fundamentals of meteorology*. Englewood Cliffs, NJ: Prentice-Hall.

Behncke, R. H., & White, H. B. (1984). Alicura 500 kV transmission system. *Proceedings of the International Conference on Large High Voltage Electric Systems (CIGRÉ), 22-02*, Paris, France.

Behncke, R. H., & White, H. B. (2006, March). Applying gust loading to your lines. *Proceedings of the 9th International Conference on Overhead Lines*, Fort Collins, CO.

Behncke, R. H., White, H. B., & Milford, R. V. (1994). High intensity wind and relative reliability based loads for transmission line design. *Proceedings of the International Conference on Large High Voltage Electric Systems (CIGRÉ), 22-205*, Paris, France.

Brooks, H., Doswell, C., III, Dowell, D., Holle, R., Johns, B., Jorgenson, D., et al. (2003). Severe thunderstorms and tornadoes. In T. D. Potter & B. R. Colman (Eds.), *Handbook of weather, climate, and water: Dynamics,* *climate, physical meteorology, weather systems, and measurements* (pp. 575-619). New York: John Wiley & Sons.

Carpena, A., & Finzi, M. (1964). Wind damage on transmission lines. *Proceedings of the International Conference on Large High Voltage Electric Systems (CIGRÉ)*, *229*, Paris, France.

Chay, M. T., Albermani, F., & Wilson, R. (2006). Numerical and analytical simulation of downburst wind loads. *Engineering Structures, 28*(2), 240-254.

Chen, L., & Letchford, C. W. (2004). Parametric study on the along-wind response of the CAARC building to downbursts in the time domain. *Journal of Wind Engineering and Industrial Aerodynamics, 92*(9), 703-724.

Church, C. R., Snow, J. T., Baker, G. L., & Agee, E. M. (1979). Characteristics of tornado-like vortices as a function of swirl ratio: A laboratory investigation. *Journal of the Atmospheric Sciences, 36*(9), 1755-1776.

CIGRÉ WG B2.16. (2004). *Report on current practices regarding frequencies and magnitude of high intensity winds* (TB 256). Paris: CIGRÉ.

Council for Scientific and Industrial Research. (1992). *Transmission line loading due to narrow winds* (No. 550 23121). Johannesburg, South Africa: Eskom.

Davenport, A. G. (1967). Gust loading factors. *ASCE Journal of the Structural Division, 93*(ST3), 11-34.

Davenport, A. G. (1979, July). *Gust response factors for transmission line loading.* Paper presented at the 5th International Conference on Wind Engineering, Fort Collins, CO.

Davenport, A. G. (1995). How can we simplify and generalize wind loads?. *Journal of Wind Engineering and Industrial Aerodynamics, 54/55*, 657-669.

Davenport, A. G., & Sparling, B. F. (1992). Dynamic gust response factors for guyed towers. *Journal of Wind Engineering and Industrial Aerodynamics, 43*(pt 3), 2237-2248.

Davies-Jones, R. (1976). Laboratory simulation of tornadoes. In R. E. Peterson (Ed.), *Symposium on tornadoes: Assessment of knowledge and implications for man* (pp. 151-174). Lubbock: Texas Tech University.

Dempsey, D., & White, H. B. (1996). Wind wreak havoc on lines: The cause of most transmission structure outages in many areas of the world is high intensity wind. *Transmission and Distribution World*, 32-42.

Energy Networks Association (2006). *Guidelines for design and maintenance of overhead distribution and transmission lines* (ENA C(b)1-2006).

Fujita, T. T. (1973). Tornadoes around the world. *Weatherwise, 26*, 56-62 & 78-83.

Fujita, T. T. (1981). Tornadoes and downbursts in the context of generalized planetary scales. *Journal of the Atmospheric Sciences, 38*(8), 1511-1534.

Fujita, T. T. (1990). Downbursts: Meteorological features and wind field characteristics. *Journal of Wind Engineering and Industrial Aerodynamics, 36*(pt 1), 75-86.

Goliger, A. M., & Milford, R. V. (1998). Review of worldwide occurrence of tornadoes. *Journal of Wind Engineering and Industrial Aerodynamics, 74-76*, 111-121.

Gomes, L., & Vickery, B. J. (1976). On thunderstorm wind gusts in Australia. *Australian Civil Engineering Transactions, CE18*(2), 33-39.

Gomes, L., & Vickery, B. J. (1978). Extreme wind speeds in mixed wind climates. *Journal of Industrial Aerodynamics, 2*(4), 331-344.

Hangan, H. (2002). Numerical simulations of high intensity winds. Downburst simulations. Retrieved January 5, 2006, from http://www.iclr.org/pdf/Hangan%20report%20-%20downburst%20simulations.pdf

Hawes, H., & Dempsey, D. (1993, April). *Review of recent Australian transmission line failures due to high intensity winds.* Paper presented at the Task Force on High Intensity Winds on Transmission Lines, Buenos Aires, Argentina.

Hjelmfelt, M. R. (1988). Structure and life cycle of microburst outflows observed in Colorado. *Journal of Applied Meteorology, 27*, 900-927.

Holmes, J. D. (1999, June). Modeling of extreme thunderstorm winds for wind loading of structures and risk assessment. *Proceedings of the 10th International Conference on Wind engineering*, Copenhagen, Denmark.

Holmes, J. D. (2001). *Wind loading of structures.* New York: Spon Press.

Holmes, J. D., Forristall, G., & McConochie, J. (2005, June). *Dynamic response of structures to thunderstorm winds.* Paper presented at the 10th Americas Conference on Wind Engineering, Baton Rouge, LA.

Holmes, J. D., & Oliver, S. E. (2000). Empirical model of a downburst. *Engineering Structures, 22*(9), 1167-1172.

Hoxey, R., Robertson, A., Toy, N., Parke, G. A. R., & Disney, P. (2003). Design of an experimental arrangement to study the wind loads on transmission towers due to downbursts. *Advances in Fluid Mechanics, Fluid Structure Interaction II, 36*, 395-404.

Hydro-Québec (1982). *Vocabulaire illustré des lignes aériennes de transport et de distribution d'électricité, fascicule 1: les supports* [Illustrated vocabulary of overhead electric transmission and distribution lines, part 1: supports]. Bibliothèque nationale du Québec.

International Electrotechnical Commission (2003). *Design criteria of overhead transmission lines* (International Standard IEC 60826-2003, 3rd ed.). Geneva, Switzerland.

Ishac, M. F., & White, H. B. (1995). Effect of tornado loads on transmission lines. *IEEE Transactions on Power Delivery, 10*(1), 445-451.

Jischke, M. C., & Light, B. D. (1983). Laboratory simulation of tornadic wind loads on a rectangular model structure. *Journal of Wind Engineering and Industrial Aerodynamics, 13*, 371-382.

Kuo, H. L. (1971). Axisymmetric flows in the boundary layer of a maintained vortex. *Journal of the Atmospheric Sciences, 28*(1), 20-41.

Lafrenière, M. (2004, April). *Amélioration de la robustesse des lignes de transport, étude sur le soulèvement des fondations et les vents forts: Calcul des pressions de vent* [Strength improvement of transmission lines, study on the uplift of foundations and high winds: Wind pressure calculation]. Hydro-Québec.

Langlois, S. (2006). *Effect of high intensity winds on overhead transmission lines.* Structural Engineering Series No. 2006-02, McGill University, Montréal, Canada. http://digital.library.mcgill.ca/pse/docs/CER_pdfs/Structural/CER_no_06-2.pdf

Letchford, C. W. (1998). *Wind environment experienced by Tarong-Mt England transmission line at Harlin during the thunderstorm on 18 March 1998* (No. 10764). Powerlink.

Letchford, C. W., & Hawes, H. (2000). Risk assessment to improve reliability of transmission facilities exposed to sub-tropical high wind storm events. *Proceedings of the International Conference on Large High Voltage Electric Systems (CIGRÉ), 22-104*, Paris, France.

Letchford, C. W., & Illidge, G. (1999, June). Turbulence and topographic effects in simulated thunderstorm downdrafts by wind tunnel jet. *Proceedings of the 10th International Conference on Wind Engineering*, Copenhagen, Denmark.

Letchford, C. W., Mans, C., & Chay, M. T. (2002). Thunderstorms: Their importance in wind engineering (a case for the next generation wind tunnel). *Journal of Wind Engineering and Industrial Aerodynamics, 90*(12-15), 1415-1433.

Li, C. Q. (2000). Stochastic model of severe thunderstorms for transmission line design. *Probabilistic Engineering Mechanics, 15*(4), 359-364.

Li, C. Q., & Holmes, J. D. (1995). Failure prediction of transmission line structural systems under severe thunderstorms. *Australian Civil Engineering Transactions, CE37*(4), 309-314.

Lin, W.E, Novacco, C. and Savory, E. (2006, May). Transient simulation of a microburst outflow: Review and proposed new approach [CD-ROM]. *Proceedings of Canadian Society of Mechanical Engineers (CSME) Forum 2006,* Kananaskis, Canada.

Liu, H. (1991). *Wind engineering: A handbook for structural engineers.* Englewood Cliffs, NJ: Prentice-Hall.

Lutgens, F. K., & Tarbuck, E. J. (2001). *The atmosphere: An introduction to meteorology* (8^{th} ed.). Upper Saddle River, NJ: Prentice Hall.

Mason, M. S., Letchford, C. W., & James, D. L. (2005). Pulsed wall jet simulation of a stationary thunderstorm downburst, Part A: Physical structure and flow field characterization. *Journal of Wind Engineering and Industrial Aerodynamics, 93*(7), 557-580.

Matheson, M. J., & Holmes, J. D. (1981). Simulation of the dynamic response of transmission lines in strong winds. *Engineering Structures, 3*(2), 105-110.

McCarthy, P., & Melsness, M. (1996). *Severe weather elements associated with September 5, 1996 hydro tower failures near Grosse Isle, Manitoba, Canada.* Winnipeg, Canada: Manitoba Environmental Services Centre - Environment Canada.

McCaul, E. W., Jr. (1987). Observations of the hurricane "Danny" tornado outbreak of 16 August 1985. *Monthly Weather Review, 115*(6), 1206-1223.

Milford, R. V., & Goliger, A. M. (1994). Tornado activity in South Africa. *Journal of the South African Institution of Civil Engineers, 36*(1), 17-23.

Milford, R. V., & Goliger, A. M. (1997). Tornado risk model for transmission line design. *Journal of Wind Engineering and Industrial Aerodynamics, 72*(1-3), 469-478.

Minor, J. E., McDonald, J. R., & Mehta, K. C. (1993). *The tornado: An engineering perspective* (No. NWS SR-147). Fort Worth, TX: National Oceanic and Atmospheric Administration.

National Research Council (U.S.) - Committee on Atmospheric Sciences. (1973). *Weather & climate modification: Problems and progress*. Washington, D.C.: National Academy of Sciences.

Nolasco, J. F. (1996). Analysis of recent transmission line failures. In CIGRÉ WG 22.06 (Ed.), *Review of IEC 826: Loading and strength of overhead lines* (pp. 87-98). Paris: CIGRÉ.

Notes on meeting. (1993, April). Paper presented at the Task Force on High Intensity Winds on Transmission Lines, Buenos Aires, Argentina.

Oliver, S. E., Moriarty, W. W., & Holmes, J. D. (2000). Risk model for design of transmission line systems against thunderstorm downburst winds. *Engineering Structures, 22*(9), 1173-1179.

Oswald, B., Schroeder, D., Catchpole, P., Carrington, R., & Eisinger, B. (1994). Investigative summary of the July 1993 Nebraska public power district Grand Island: Moore 345 kV transmission line failure. *Proceedings of the IEEE Power Engineering Society Transmission and Distribution Conference*, Chicago, IL.

Peabody, A. B. (2001). *Transmission line longitudinal loads, a review of design philosophy.* Structural Engineering Series No. 2001-02, McGill University, Montréal, Canada.

Peabody, A. B. (2004). *Applying shock damping to the problem of transmission line cascades.* Ph.D. Thesis, Department of Civil Engineering and Applied Mechanics, McGill University, Montréal, Canada.

Peyrot, A. H., Kluge, R. O., & Lee, J. W. (1978). *Longitudinal loading tests on a transmission line* (EPRI EL-905). Palo Alto, CA: Electric Power Research Institute.

PLS-CADD (Version 7.62+). (2006). Madison, WI: Power Line Systems.

Reid, S., & Revell, M. (2006). *Winds near Kawerau on 25 March 2005 and transmission line damage* (No. WLG2005-24). Wellington, New Zealand: National Institute of Water & Atmospheric Research.

Savory, E., Parke, G. A. R., Zeinoddini, M., Toy, N., & Disney, P. (2001). Modelling of tornado and microburst-induced wind loading and failure of a lattice transmission tower. *Engineering Structures, 23*(4), 365-375.

Schwarzkopf, M. L. A., & Rosso, L. C. (1982). Severe storms and tornadoes in Argentina. *Proceedings of the Conference on Severe Local Storms*, San Antonio, TX.

Selvam, R. P., & Holmes, J. D. (1992). Numerical simulation of thunderstorm downdrafts. *Journal of Wind Engineering and Industrial Aerodynamics, 44*(1-3), 2817-2825.

Shehata, A. Y., El Damatty, A. A., & Savory, E. (2005). Finite element modeling of transmission line under downburst wind loading. *Finite Elements in Analysis and Design, 42*(1), 71-89.

Tecson, J. J., Fujita, T. T., & Abbey, R. F., Jr. (1979, October). Statistics of U.S. tornadoes based on the DAPPLE tornado tape. *Proceedings of the 11th Conference on Severe Local Storms*, Kansas City, MO.

Thom, H. C. S. (1963). Tornado probabilities. *Monthly Weather Review, 91*, 730-736.

TOWER (Version 7.61). (2006). Madison, WI: Power Line Systems.

Twisdale, L. A. (1982). Wind-loading underestimate in transmission line design. *Transmission & Distribution, 34*(13), 40-46.

Twisdale, L. A., & Dunn, W. L. (1983). Probabilistic analysis of tornado wind risks. *ASCE Journal of Structural Engineering, 109*, 468-488.

Twisdale, L. A., & Vickery, P. J. (1992). Research on thunderstorm wind design parameters. *Journal of Wind Engineering and Industrial Aerodynamics, 41*(1-3), 545-556.

Ward, N. B. (1972). The exploration of certain features of tornado dynamics using a laboratory model. *Journal of the Atmospheric Sciences, 29*(6), 1194-1204.

Wen, Y.-K. (1975). Dynamic tornadic wind loads on tall buildings. *ASCE Journal of the Structural Division, 101*(ST1), 169-185.

Wen, Y.-K., & Chu, S.-L. (1973). Tornado risks and design wind speed. *ASCE Journal of the Structural Division, 99*(ST12), 2409-2421.

Wood, G. S., Kwok, K. C. S., Motteram, N. A., & Fletcher, D. F. (2001). Physical and numerical modelling of thunderstorm downbursts. *Journal of Wind Engineering and Industrial Aerodynamics, 89*(6), 535-552.

Zhu, S., & Etkin, B. (1985). Model of the wind field in a downburst. *Journal of Aircraft, 22*(7), 595-601.

Appendix A

Wood's empirical formula (Wood et al., 2001)

Wood's formula was obtained from mean velocity measurements at various distances of a jet of air impinging on a vertical surface. The wind velocity profile (see Figures 17 and 34) resulting from this formula is normalized with respect to the peak mean velocity, whereas the height is normalized with respect to the height where the velocity is equal to half its maximum value.

$$V/V_{max} = 1.55\,(z/\delta)^{1/6}\,[1 - \mathrm{erf}(0.70\,z/\delta)],$$

where

V is the mean velocity (m/s) at height above ground z (m).

V_{max} is the peak mean velocity in m/s.

δ is the height where the velocity is equal to half its maximum value (m).

erf is the error function.

For the numerical study reported in Sections 4 and 5, δ is equal to 270 m, resulting in a peak mean velocity located at 50 m above ground. The value of V_{max} was chosen to make the total wind force resultant of the "Downburst Wood profile" and "Downburst full" load cases equal (see Section 4.3). V_{max} ranges between 51.3 and 52.2 m/s for the various towers.

Appendix B

Wen's model (Wen, 1975)

Wen's model divides the tornado wind speed into tangential, radial, and vertical components (see Figure 18). For the purpose of our study, only the tangential component (T) was used.

Above boundary layer:

$T = 1.4\ V_{max} / r\ [\ 1 - \exp\ (-1.259\ r^2\ )]$

Within boundary layer:

$T = 1.4\ V_{max} / r\ [\ 1 - \exp\ (-1.259\ r^2\ )] * [\ 1 - \exp\ (-\pi n\ )] * \cos\ (\ 2b\pi n\ )$

$r = r' / r_{max}$

$n = z / \delta$

$\delta = \delta_0\ [\ 1 - \exp\ (\ -0.5r^2\ )\ ]$

$b = 1.2\ \exp\ (\ 0.8r^4\ )$

where

T is the tangential velocity (m/s) at a given height above ground z (m) and distance from the centre of the tornado vortex r' (m).

V_{max} is the maximum tangential velocity above the boundary layer in m/s.

r_{max} is the core radius of the tornado vortex in m.

δ_0 is the boundary layer thickness in m.

The profile shown in Figure 33 would be located at r' equals r_{max} and considers some translational velocity of the tornado. The boundary layer thickness, δ_0, is equal to 200 m, r_{max} is equal to 30 m, and V_{max} was originally taken as 45 m/s. After adding a translation velocity of about 10 m/s to the tangential velocity calculated, the profile was scaled to make the total wind force resultant of the "Tornado Wen profile" and "Tornado full" load cases equal.

The choice of the parameters may influence the profile. For this study, they were chosen to the best knowledge of the author to match an F2 or F3 tornado. Therefore, the profile shown is only one possible profile among others. It was beyond the scope of this project to develop accurate tornado profiles.